

Investigation of low temperature soil removal from cotton fibers

Dissertation

zur Erlangung des

Doktorgrades der Naturwissenschaften

(Dr. rer. nat.)

der Fakultät für Chemie und Pharmazie

der Universität Regensburg



vorgelegt von

Susanne Dengler

aus Willmannsried

Regensburg 2014

Official Registration:

18.03.2014

Defense:

02.05.2014

Ph. D. Supervisor:

Prof. Dr. W. Kunz

Adjudicators:

Prof. Dr. W. Kunz

Prof. Dr. H. Motschmann

Prof. Dr. A. Pfitzner

Chair:

Prof. Dr. J. Daub

***Für meine Eltern
und Andreas***

Preface

This PHD thesis was carried out at the Institute of Physical and Theoretical Chemistry, Faculty of Natural Science IV, University of Regensburg, between October 2010 and January 2014, under the supervision of Prof. Dr. Werner Kunz. The realization of this work would not have been possible without the support and help of various people to whom I want to express my honest thanks.

First of all I want to thank my supervisor Prof. Dr. Werner Kunz, who gave me the opportunity to carry out this thesis at his institute and for kindly granting me financial support. Of course I also want to thank him for the time he spent on several discussions to promote my work.

Parts of this work could not have been realized without the close collaboration with Bernhard von Vacanao, Regina Klein and Sebastian Koltzenburg (Employees of BASF, Ludwigshafen). Thank you very much for the many ideas and the long and fruitful discussions.

Beyond that I want to thank BASF, Ludwigshafen for the financial support.

This collaboration with the BASF would not have been possible without the SKH GmbH, Ortenburg. They employed me and enabled me the collaboration. Thank you very much.

I am likewise grateful to Prof. Dr. G. J. Tiddy (School of Chemical Engineering and Science, University of Manchester) for long and fruitful discussions on NMR.

Additionally, I want to thank PD Dr. Rainer Müller (from the Institute of Physical and Theoretical Chemistry, University of Regensburg) for providing access to his DSC equipment and his support whenever I had problems with the device.

Furthermore, I want to thank Prof. Dr. Arno Pfitzner (from the Institute of Inorganic Chemistry, University of Regensburg) for giving me the opportunity to measure DSC and X-ray powder diffraction. I also want to thank Ulrike Schießl and Manuel Avola

(both from Institute of Inorganic Chemistry, University of Regensburg) for performing the DSC measurements.

For measuring X-Ray powder diffraction I have to thank earnestly Dr. Martina Andratschke (Institute of Inorganic Chemistry, University of Regensburg).

I also would like to express my gratitude to Dr. Thomas Burgemeister and Dr. Ilya Shenderovich (both of the Chemical Analysis, University of Regensburg) for providing the NMR equipment. Special thanks go to Fritz Kastner, Annette Schramm and Georgine Stühler (all from the Chemical Analysis, University of Regensburg) for performing my countless NMR measurements.

Additionally, I would like to express my thank to Dr. Michael Bodensteiner (Chemical Analysis, University of Regensburg) for introducing me in X-Ray powder diffraction measurements and for discussing the results with me.

I am also very grateful to M.Sc. Tobias Graßl (Institute of Inorganic Chemistry, University of Regensburg) for plotting my XRD results.

I would like to express my gratitude to Damian Brock, Alexandre Delangue, B.Sc. Theresa Hoess and B.Sc. Lydia Zahnweh, the students who helped me with some experiments during my thesis. I would like to thank specially Lydia, she will continue working on the investigation of washing process and was a great support for the last experiments of my thesis.

I also want to thank Franziska Wolf (from the Institute of Physical and Theoretical Chemistry, University of Regensburg) who shared the laboratories with me and ordered everything without any delay.

Special thanks go to Andreas Eiberweiser, Veronika Fischer, Auriane Freyburger, Michael Klossek, Andreass Nazeth, Julien Marcus, Oliver Masur, Tobias Premke and Eva-Maria Schön for the amusing lunchtime every day in the cafeteria, the activities beside the University and being good friends.

In addition I want to thank the members of the Kafferunde, Georg Berger, Richard Buchner, Andreas Eiberweiser, Veronika Fischer, Auriane Freyburger, Michael Klossek, Andreas Nazeth, Roland Neueder, Julien Marcus, Eva Müller and Thomas Sonnleitner. I really enjoyed the funny and often senseless discussions with you.

Furthermore I want to thank Andreas Eiberweiser, Andreas Nazet and Veronika Fischer for critical reading parts of this manuscript.

I specially want to thank Eva Müller. We shared our office since I started my master thesis. I always could count on your support also beside scientific questions. I really enjoyed the many hours we discussed about chemistry and about god and the world.

My honest thanks go to my parents Maria and Josef and my brothers Tobias and David. I always could trust on your mental and financial support. You never questioned my decisions. Unfortunately, I could not convince you that chemistry is not boring.

Last but not least I want to thank cordially Andreas Eiberweiser. During the first time of my thesis you became a very good friend to me. We spent so much time on discussing about everything in the world. During this time you grow dear to my heart. And I hope you will accompany me for the rest of my life.

Susanne Dengler

Table of Contents

Chapter 1 Introduction.....	1
Chapter 2 Fundamentals	5
2.1 Soil removal	6
2.1.1 General Aspects	6
2.1.2 Soil Release Mechanism.....	11
2.1.3 Commercial Washing agents	16
2.2 Triglyceride	17
2.2.1 General Aspects	17
2.2.2 Structure	18
2.2.3 Blended fats.....	19
2.3 Surfactants.....	21
2.3.1 General Aspects	21
2.3.2 Lyotropic Liquid Crystals	23
2.3.3 Solubility	25
2.4 Cosolutes	27
2.4.1 Hydrotropes	27
2.4.2 Cosurfactants	28
2.5 Microemulsion.....	29
2.6 Hansen Solubility Parameters.....	32
2.7 Hofmeister Series and Collins Concept	36
2.8 Characterization Methods	38
2.8.1 Ternary Phase Diagram.....	38
2.8.2 Differential Scanning Calorimetry	39
2.8.3 NMR	41
2.8.4 Colorimetry	48
Chapter 3 Experimentals	51
3.1 Materials	52
3.2 Methods	54
3.2.1 Differential Scanning Calorimetry	54

3.2.2	Microscopy.....	55
3.2.3	X-Ray powder diffraction.....	55
3.2.4	COSMO <i>therm</i>	55
3.2.5	Determination of triglyceride solubility.....	56
3.2.6	Washing test.....	56
3.2.7	Krafft temperature determination.....	59
3.2.8	Nuclear Molecular Resonance	60
3.2.9	Karl Fischer titration.....	61
Chapter 4	Results and Discussion	63
4.1	Investigation of triglycerides and binary mixtures with surfactants	64
4.1.1	Introduction.....	64
4.1.2	Results.....	65
4.1.3	Conclusion.....	73
4.2	Solubilisation of triglycerides in organic solvents	74
4.2.1	Introduction.....	74
4.2.2	Results.....	74
4.2.3	Conclusion.....	83
4.3	Washing tests.....	84
4.3.1	Introduction.....	84
4.3.2	Results.....	85
4.3.3	Conclusion.....	108
4.4	The influence of osmolytes on the Krafft temperature	110
4.4.1	Introduction.....	110
4.4.2	Results.....	116
4.4.3	Conclusion.....	120
4.5	NMR studies.....	124
4.5.1	Introduction.....	124
4.5.2	Results.....	129
4.5.3	Conclusion.....	144
Summary	145
Zusammenfassung	151
Bibliography	157

Appendix	177
List of figures	178
List of tables	185
Supplementary	188
List of publications	192
Eidesstattliche Erklärung	193

Chapter 1

Introduction

1. Introduction

Laundry has a long tradition [1]. The first documents about washing with soaps date from 2500 B.C. and origin from Mesopotamia [2]. The washing process has changed through the last centuries. In the beginnings the laundry was washed in the rivers and paddles were used to improve the washing results whereas the Romans washed in barrels and stamped on the laundry. In the 19th century the paddles were replaced by wash boards. Over time wash houses were built, for which the principal setting is given in figure 1.1 [3].

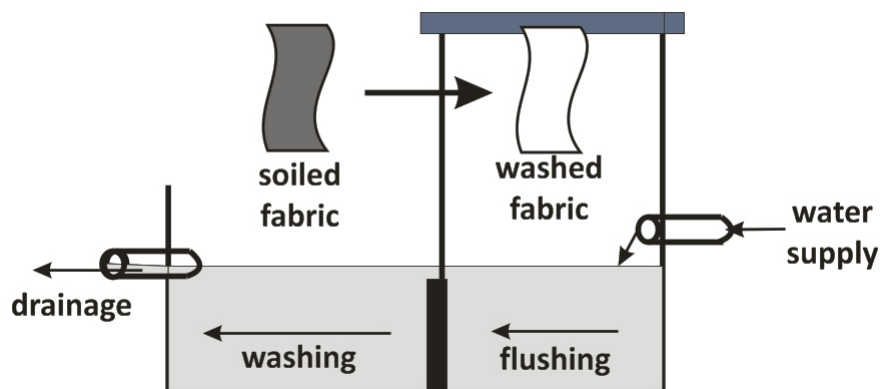


Figure 1.1: Schematic drawing of a wash house. The direction of washing is reversed to the water flow direction.

The flushing basin was supplied with fresh water from the river and the washing basin was supplied by the flushing water. In some wash houses the water was heated by chimneys which facilitated the washing. The precursor of the modern washing machine is the Bugadier, developed by the shepherd. It is a simple box with several chambers. The first chamber is filled with washing agent and the chambers below are filled with laundry. The water is filled in the top of the box, runs through the chambers and is collected at the bottom. The same washing liquor was used several times [3]. The first electrical washing machine was invented in 1901. However, it took until the seventies of the 20th century until the drum-type washing machines found their way into the German household [2].

But also the detergents have undergone changes. In the beginning, additionally to washing agents originated from excrement and urine, the most important detergents were soaps and wood ash. The soaps were produced from animal fat and wood ash. Later on the soap quality was increased by replacing the animal fat by herbal oils and the wood ash by alkali. The suds produced from wood ash and water contain softening components like phosphates and cleaning agents like alkali- and earth alkali compounds which become soap like by heating in the

presence of fat from the laundry. The composition of a suds produced by suspending 1 kg wood ash in 10 l water is given in table 1.1 [3].

Table 1.1: Average composition of a sud produced by suspending 1 kg wood ash in 10 l water.

<i>Ingredient</i>	<i>Averaged content [%]</i>	<i>Content [g] / 10 l</i>	<i>Source</i>
P ₂ O ₅	5	50	Ash
K ₂ CO ₃	65	65	Ash
CaO	34	34	Ash
CaO		3	Water (30° dH)

In water P₂O₅ becomes H₃PO₄ and CaO becomes Ca(OH)₂. The phosphate and the carbonate precipitate as calcium phosphate and calcium carbonate. Calcium hydroxide and potassium hydroxide, which remain in the suds, are casual for the washing activity by cleaving fatty soil.

The use of these washing agents was still common in the 20th century. The first self-actuating detergent was developed in 1907 by Fritz Henkel which is today still known as Persil. It is an abbreviation for the ingredients sodium **per**borate and **sil**icate [4]. Since the introduction of this first detergent the composition was refined to improve washing results, to reduce the required amount and to reduce the environmental impact [3, 4]. For example, magnesium silicate and complex phosphate were added to Persil in 1934 causing water softening and thus avoiding calcium deposition on the laundry. Until the end of the fifties the washing active agent was soap before it was replaced by less water hardness sensitive synthetic surfactants. The initially used surfactants were poorly water-degradable and were replaced by more environmentally friendly, easily degradable ones. A key step for the protection of the environment was done by avoiding the use of phosphates. Phosphates reduce the water hardness but in bodies of water it induces eutrophication. Today, Sasil (**sodium-aluminium-silicate**) is used instead of phosphates in Persil [3, 4].

Nowadays, the improvement of detergents is still an important industrial field. The main aims are the reduction of washing temperature and of environmental impact. In 1961 a law (Detergenziengesetz) was passed in Germany which regulates the use of surfactants in detergents. Surfactants used in detergents have to be biodegradable to at least 80% [5]. In subsequent acts (WMRG in 1998, amendment in 2007, EU- Detergenziengesetz in 2005) the requirements on biodegradability

1. Introduction

were tightened and the petrochemical based surfactants are replaced more and more by the oleochemical based ones from renewable resources [6, 7].

For efficient washing at low temperatures a sufficient solubility of the surfactants is required. Therefore, the reduction of the solubility temperature by adding additives like osmolytes is investigated within this work. In a NMR study the interaction between surfactant and ions is investigated. Depending on the nature of the ion and concentration different binding situations are observed. This illustrates the role of additives on the solubility temperature.

Most knowledge about washing is empirical. To improve the washing process the role of the surfactants and the washing conditions have to be understood. Consequently, the aim of this work is to figure out the influencing factors on the washing efficiency in order to give advice how to improve detergents. Therefore, the impact of surfactants and solvents on triglycerides is investigated. Additionally, washing liquors with varied chemical and physical properties are tested.

Chapter 2

Fundamentals

2.1 Soil removal

2.1.1 General Aspects

Laundry is an old, well studied process with most of our knowledge stemming from empirical studies [8]. Nowadays, the interest in the deeper understanding of the molecular processes increases in order to improve the washing process. A further aim is to reduce the washing temperature without losing washing power to save energy and make the detergency more environmentally friendly [9].

The mechanism and efficiency of soil removal depends strongly on the nature of the soiled fabric [9]. In normal household laundry hydrophilic cotton textiles as well as hydrophobic polyester fabrics and mixtures of polyester and cotton fibres are common [10]. Agents being very good for polyester fibers may be ineffective for the soil release from cotton [11]. Therefore, commercial laundry detergents are mixtures of different surfactants and additives. Detergent formulations containing twelve and more components are not unusual [10]. Beside the surface properties of the fabric, the type and concentration of the detergent, the washing temperature, mechanical processes during laundry, the soiling condition as well as the aging of the soil impact the washing power [9, 10, 12]. As the washing process is very complex, it is ambitious to mention all contributing factors. Therefore the following disquisition is restricted to the soil removal from cotton fibres.

Cotton Fibres

For a better understanding of the soil removal from cotton textiles it is insightful to envision the structure of the cotton thread. A single twine consists of countless billions of twisted cotton hairs, which are composed of layers: the cuticle, the primary wall, the winding layer, the secondary wall and the lumen (Fig. 2.1 a) [13-15]. Due to this, there are various sized porous and capillary spaces and the fibre can be described as a microscopic sponge with a complex porous structure. The main components of the fibre are [16]:

- 80-90 % cellulose
- 6-8 % water
- 4-6 % hemicellulose and pectins

- 1-1.8 % ash
- 0.5-1 % waxes and fats
- 0-0.15 % proteins

Before spinning the fibres they are treated with caustic soda (sourcing) to saponify the natural waxes and fats and to release the pectins and other impurities. Afterwards, they get bleached and mercerized for a better luster and better sorption properties. The dried fibres consist of 99 % cellulose and the fibres are twisted, crumpled and wrinkled (Fig. 2.1 b) [13, 17, 18].

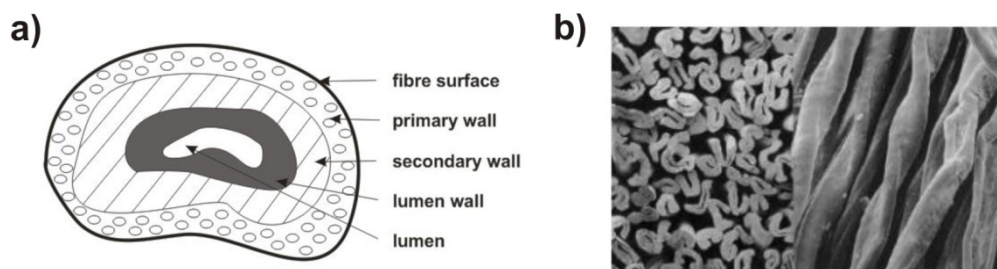


Figure 2.1: Schematic presentation of the cross section through a cotton fibre [18].

When cotton fabric becomes soiled, the oily soil covers the fibre surface, forming a peripheral coating and incorporates between the fibres [9]. Due to the structural characteristic of cotton fibres, they are very hydrophilic and can adsorb 32 % water of its own weight [19]. The associated swelling enables the diffusion of water into and between the soiled cotton fibres, which is the first step of soil release [20, 21]. Therefore, soil release from pure cotton is quite easy. However, common fabrics are processed to reduce the swelling and slipping, which hinders the washing [8, 22, 23].

Nature of Soil

Venkatesh et al. investigated the composition of common household laundry soil [8]. They found, that the soil originates from two sources, the human body and the environment. Soil secreted from the skin contains primarily fatty substances (Tab. 2.1) [24-27].

2. Fundamentals

Table 2.1: Composition of fatty soil secreted from the human body.

Component	% Content
Free fatty acids	22-27
Triglyceride	25-35
Wax and sterol ester	20-22
Squalene	10-15
Diglyceride	6-10
Sterol	2-5
Paraffin	0.5-1.5

Soil originated from the environment is either fatty or particulate. Particulate soil are mainly clay minerals (Tab. 2.2) [8, 24, 28]. Additionally, the wash liquor itself soils the fabric by redeposition and wet soiling during laundering [24, 29]. However, this soiling source is almost entirely eliminated by the addition of anti-redeposition additives like polymers to the washing agent. In summary, normal household laundry is soiled with fluid and particulate components.

Table 2.2: Average composition of soil originated from the environment.

Component	% Content
Ash containing	50-55
SiO ₂	23-26
Organic substances (fats, fibres, soot, etc.)	20-25
Water soluble components	10-15
Fe ₂ O ₂	10-12
Ether soluble components	8-12
CaO	7-9
Moisture	2-5
MgO	1-2

Soiling condition

The forces of the soiling mechanism depend on the state of soil matter. It was shown that an approaching particle adsorbs easier on fabrics already polluted with liquid dirt [10]. The reversed phenomenon was not observed. Particulate and fluid

soil behave different for soiling and release, therefore both have to be discussed as two types of pollution [10].

Fabric can be contaminated mechanically by direct contact with another soiled surface, by the interaction with a solution containing soil or by soil distributed in the air [8, 30-32]. The dirt retains on the substrate due to Van der Waals forces, mechanical and electrostatic forces and oil bonding [8, 10, 33].

Beside the forces which have to be broken during laundry also the location of the impurity within the scrim has to be mentioned. Dirt penetrates by mechanical entrapment, occlusion and repeated flexing the inter-fiber and inter-yarn spaces, the irregularities of the fiber surface and the crevices and pores of the fibers [8, 10, 33-36]. For oily soil the wetting or relative surface energy has to be considered. Additionally, wetting is supported by the oils attempt to minimize the oil-air contact area and the capillary forces which facilitates the distribution of the oil within the fibres (equation 2.1) [8, 37].

$$p = \frac{2\gamma_{OS} \cos\Theta}{r} \quad (2.1)$$

The capillary pressure p is given by the interfacial tension γ_{OS} of the oil-fiber interface, the contact angle Θ of the oil on the surface and the factor r , which describes the air filled core within the fibre [8, 38]. If the surface energy of the oil is lower than of the substrate, the contact angle is lower 90° , p is greater zero and the substrate will be wetted and the oil will penetrate the core [8, 39].

The simplified treatment of the soiled surface as plane enables the consideration of the environment for the soil droplet shape. For liquid soil the contact angle Θ between substrate surface and soil is given by the interplay of the interfacial tensions between surrounding environment/substrate surface (γ_{ES}), oil/substrate surface (γ_{OS}) and oil/surrounding environment (γ_{OE}) and can be calculated by Young's equation (equation 2.2) [8, 40].

$$\cos\Theta = \frac{\gamma_{ES} - \gamma_{OS}}{\gamma_{OE}} \quad (2.2)$$

Therefore, changes in the contact area and the droplet shape result from changes of the interfacial tensions. Hence, the transformation of the oily soil/fibre system in

2. Fundamentals

another environment results in a changed droplet shape. In contrast, the droplet shape of the particulate soil varies barely for a changed environment (Fig. 2.2) [10]. The release of solid soil should be easier due to the smaller contact area. However, the situation changes completely when electrical interactions contribute. The adhesion and release of particulate soil from a plane surface can be approached by the DLVO theory for colloids which describes the coagulation of a colloidal dispersion.

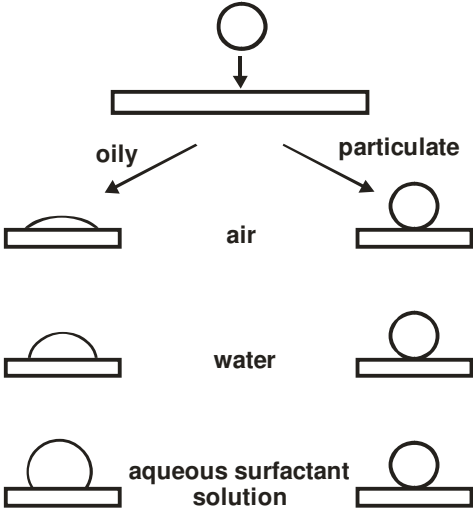


Figure 2.2: Contact area and angle between substrate and soil depending on the state of soil matter and the environment.

2.1.2 Soil Release Mechanism

As mentioned above, cotton fibres are porous structures and the soil is not restricted to the surface. Therefore, diffusion and penetration of water and detergent into the textile are often rate limiting steps. Kissa was able to show that the removal rate of soil decreases with increasing soiling time and intensity of mechanical action during soiling [41]. Apart from that, it was shown that the soil release from cotton fibres is similar to the washing of hard surfaces [40, 42]. This facilitates the description of the washing process and it was investigated and described in detail by Bäckström and Engström [43]. The fundamental washing process can be separated into two primary processes [11],

- 1) Diffusion of water and detergent
- 2) Mechanical dislodgement and transport of soil

With the soil release mechanism depending on the state of soil matter [8, 10, 11]. In the following section the soil release mechanism for the two contrary states is described. However, this description is only theoretical because normal household soil is normally a mixture of liquid and particulate soil.

Oily soil removal

For oily soil removal from cotton fabric the detergency process can be separated in three subsequent periods [11, 41].

- 1) **Induction period:** Diffusion of water and washing agent to the soiled surface.
- 2) **Soil removal period:** Interaction between cleaning agent and soil, forming water soluble or at least removable aggregates.
- 3) **Final period:** Transport of the aggregates into the aqueous phase.

The induction period is composed of a fast movement of soil release agent in the aqueous solution and the slow diffusion into the pores. Within this period the soil removal is slow and insignificant. During the subsequent soil removal period, the main important mechanism for soil removal is the roll-up mechanism [40]. Further contributing, but of lesser importance are the mechanisms of emulsification,

2. Fundamentals

solubilisation and penetration [11, 44-47]. Within the second period nearly the complete removal takes place [47].

For the sake of the completeness it should be mentioned that the main soil release mechanisms for fabrics containing a high amount of hydrophobic fibres (like polyester and other synthetic fibres) are the solubilisation and emulsification mechanism [48-50].

The amount of removed soil can be enhanced by agitation, which affects the following steps resulting in an improved detergency [11, 43]:

- Increases the surfactant transport (induction period)
- Accelerates the roll-up mechanism (soil removal period)
- Speeds up the displacement process (soil removal period)
- Increases the transport of aggregates into the aqueous phase (final period)

Bäckström and Engström also investigated the influence of the temperature [43].

They found that increasing the washing temperature results in:

- Particulate soil might melt when the temperature is increased enough (→roll-up mechanism).
- Viscosity of oily soil decreases, which facilitates the roll-up mechanism.
- Diffusion rate of surfactant (induction period) and aggregates (final period) increases (increases soil removal).
- Dielectric constant of water decreases, thus becoming more hydrophobic (better solvent for hydrophobic soil).

The roll up mechanism is caused by the interplay of the interfacial tensions between oil on fiber surface γ_{OS} , water on fiber γ_{WS} and oil on water γ_{OW} (equation 2.3) [45].

$$R = \gamma_{OS} - \gamma_{WS} + \gamma_{OW} \cos \Theta \quad (2.3)$$

The oily droplet rolls up as long as the resulting R is positive. During the roll-up mechanism the contact angle increases and becomes 180 ° for the finished roll-up (Fig. 2.3a) [40]. R can be increased by decreasing γ_{WS} and by increasing γ_{OS} . The addition of surfactants promotes the hydrophilic character of the fiber surface and

facilitates the roll-up mechanism. Additionally, for cotton the soil removal is enhanced by swelling of the fabric. Water and detergent solution wet the fiber (swelling of the cotton), increasing the hydrophilic character of the fiber surface and decreasing the interfacial tension γ_{WS} between water and fiber [40, 51].

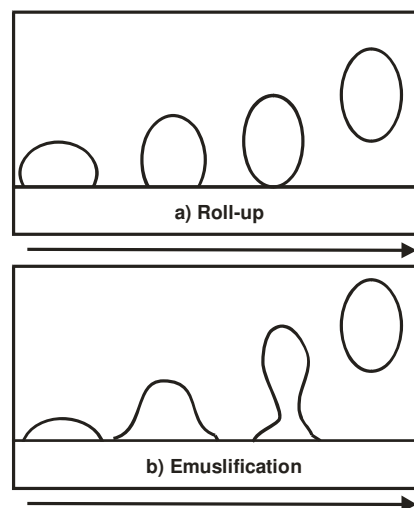


Figure 2.3: Schematic representation of liquid soil release by (a) roll-up mechanism and (b) emulsification.

For very hydrophobic fiber surfaces the washing liquor cannot adsorb to the fiber surface. The soil is removed in small droplets formed by undercutting the oil surface (Fig. 2.3b) [40, 42, 51, 52]. The efficiency can be enhanced by reducing the interfacial tension between oil and water, which facilitates the droplet formation.

For soils with a high content of polar groups a third mechanism was proposed, the formation of liquid crystals. The surfactant in the washing liquor interacts with the polar groups in the soil, forming the intermediate phase, which becomes broken by agitation and emulsified into the aqueous solution [40, 53, 54].

The direct solubilisation of the oil in surfactant micelles is only observed for high content of surfactant. However, it was shown that the soil removal rate is enhanced when surfactant rich phases are present in the washing liquor which promote direct solubilisation and formation of intermediate phases [40].

Particulate soil removal

While the most important factor for oily soil release is the hydrophilicity of the cotton fiber, this is of less importance for the solid soil removal [11]. For particulate soil removal the attractive, mainly van der Waals forces, have to be overcome and

2. Fundamentals

the separated fiber surface and soil have to be wetted afterwards (Fig. 2.4) [47]. The required energy depends primarily on the contact area.

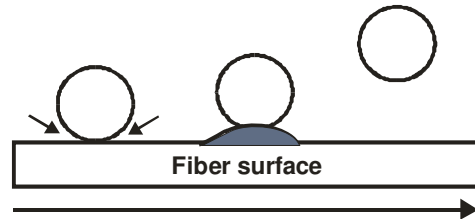


Figure 2.4: Two-step particulate soil removal from fiber in aqueous washing liquid.

The two main mechanisms inducing soil removal are:

- Wetting of the fibre and the particulate soil.
- Adsorption of surfactant and other washing liquor components at the fiber/water and the soil/water interface.

The wetting of the fiber reduces the Van der Waals forces between soil and fiber, diminishing the adhesion of particulates to the textile [55]. Furthermore, the presence of water enables the formation of an electrical double layer at the fiber/water and soil/water interface which normally repel each other resulting in a reduced net adhesion of the soil. The adsorption of detergent on the fiber/water and the soil/water interface has two soil removal improving effects. It reduces the attractive interactions between fiber and soil and for ionic detergents it also increases the charge on the particle and fabric surface, resulting in increased electrostatic repulsion. The repulsive forces can be described by the DLVO theory for forces between double layers [55]. The coagulation of colloidal particles is comparable with the adhesion of solid soil to the fiber surface. The difference of the two systems is that for soiled fabric, one of the two particles is of infinite size and the coagulation is a heterocoagulation because the soil is composed of different components [10]. The classical DLVO theory states that the long-ranged interparticle interactions control the colloidal stability. Two potentials contribute to the total interaction potential $V(tot)$: the Van der Waals potential $V(vdW)$ and the potential of the electric double layer $V(elec)$ (equation 2.4) [10, 56].

$$V(tot) = V(elec) + V(vdW) \quad (2.4)$$

Normally the Van der Waals forces are attractive, but for dissimilar particles in presence of a third medium they can be repulsive. Also, the potential of the double layer, normally repulsive, gets attractive for two particles with unequal charge density [10, 57].

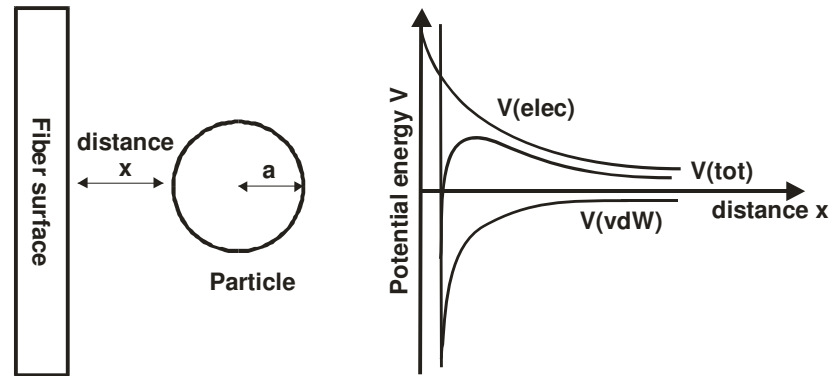


Figure 2.5: Sphere-plate model representing the geometry on the left side and the trend of the potential energies on the right side.

The system of soiled textile can be represented as a spherical particle (solid soil) approaching to a plane surface (fibre) (Fig. 2.5) [10]. Lange has shown that this geometry can be described similar to two interacting spheres leading to the development of equations to calculate $V(\text{tot})$ and $V(\text{vdW})$ [58-61]. This approximations predict an increase of $V(\text{elec})$ for electrolyte addition and an increase of both potentials with increasing particle size a .

2.1.3 Commercial Washing agents

As already mentioned above, commercial washing agents are composed of various components. The main ingredients are [4]:

- Surfactants
- Softening agents
- Bleaching agents and bleach activators
- Enzymes
- Optical brighteners
- Dye transfer inhibitors
- Fragrances
- Filling material

In detergents, mixtures of nonionic and anionic surfactants are crucial for the washing activity. The addition of nonionic surfactants increases the washing results for decreased temperature. Cationic surfactants are the main component of fabric softener. They have no cleaning efficiency but show an impact on the fiber surface and make the laundry softer.

Typically used softening agents are zeolithes and polycarboxylates. They are added to avoid calcium deposition on clothing and on the heating rod grooves in the washing machine. Bleaching agents, like sodium perborate, bleach organic stains by chemical oxidation. For a higher bleaching efficiency at low temperatures bleach activators like Tetraacetylenediamine are added. The addition of enzymes like amylases and lipases facilitates the removal of amylaceous and albuminous soils. Optical brighteners are compounds which remain on the fiber and reflect blue light. The fabric thus appears whiter to the human eye. Dye transfer inhibitors avoid the deposition of dissolved pigments in the washing liquor and fragrances are only cosmetical. The addition of filling materials improves the pourability and facilitates the dosing [4].

2.2 Triglyceride

2.2.1 General Aspects

Triglycerides are the main component in vegetable oils and animal fats [62-64]. In living organism they store and provide energy, deliver essential fatty acids and serve as carrier of oil soluble vitamins [65]. They find application in food industry, as raw materials in pharmaceutical and cosmetic products, in industrial processes and as renewable material for biodiesel production [66-71].

Triglycerides are triesters of glycerol with three fatty acids which might be identical or up to three different ones (Fig. 2.6) [64, 72, 73].

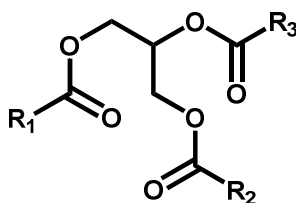


Figure 2.6: Schematic structure of a triglyceride composed of glycerol and three different fatty acids.

Those can differ in the alkyl chain length and the degree of saturation. Three classes of fatty acids are distinguished: the saturated, the mono unsaturated and the polyunsaturated ones. Natural fatty acids are normally unbranched and have an even number of carbon atoms; the most common alkyl chain lengths are 16, 18 and 20 [74-77]. The structure of the fatty acids determines the physical properties of the triglycerides. With increasing degree of unsaturation the melting point of the triglyceride decreases, due to unfavoured packing of the chains, and the fat becomes more hydrophobic [64].

The shortcut for fatty acid nomenclature is C_x:_y, x giving the number of carbon atoms and y giving the number of unsaturation. The most common fatty acids derived from natural resources are palmitic acid (C₁₆:0), stearic acid (C₁₈:0), oleic acid (C₁₈:1), linoleic acid (C₁₈:2) and linolenic acid (C₁₈:3) (Fig. 2.7) [65]. Additionally, for personal care products like soaps and washing agents, capric acid (C₁₀:0), lauric acid (C₁₂:0) and myristic acid (C₁₄:0) are very important [65].

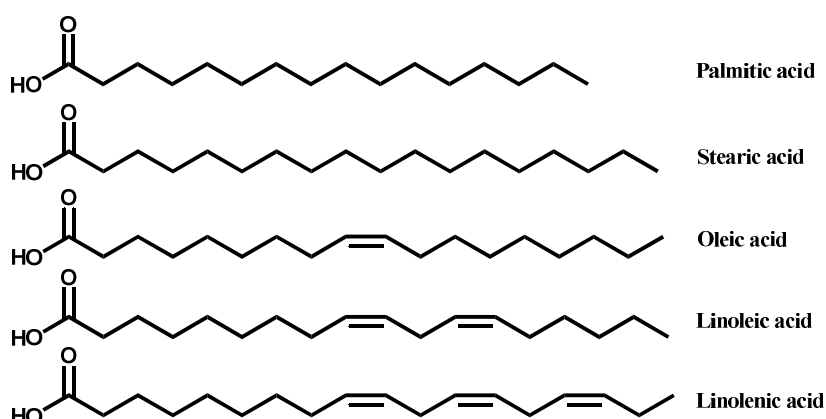


Figure 2.7: Structure of the most common natural fatty acids.

Due to the bulky polar head group and the three long alkyl chains, triglycerides are very difficult to emulsify compared to hydrocarbons or alkyl monoesters. However, great effort was made investigating the impact of the structure of triglycerides on the interaction with water and surfactant [64, 78-83]. This enables a deeper insight in triglyceride microemulsions, which are still today not well understood and are very important for daily life applications [64, 78-83].

2.2.2 Structure

Crystalline fats are present in crystal networks with specific polymorphic crystalline structures [66, 84]. The most common morphologies are named α , β' and β in the order of increasing melting temperature [85, 86]. They are characterised by the packing of the chains in the subcell: The subcell structure is hexagonal for α (H), orthorhombic-perpendicular for β' (O_{\perp}) and triclinic parallel for β (T_{\parallel}) (Fig. 2.8) [66].

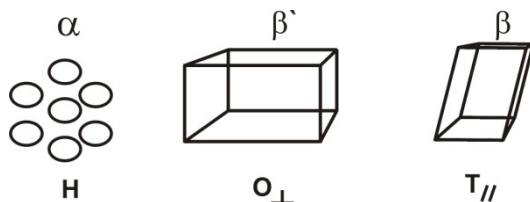


Figure 2.8: Polymorphic structures of triglyceride subcells in the order of increasing melting temperature.

The kinetically favoured morphology is the α subcell, but the thermodynamically stable one is the β morphology. This morphology tends to form large plates which

are disadvantageous for many applications like in margarine, which should stay soft over a long time. Therefore, the formation of the β morphology is avoided in these applications. In contrast, for chocolate the crystallisation of cacao butter in the β morphology is desired. However, the appearance and the relative stability of the morphologies depends on the fatty acids the triglyceride is composed of. For triglycerides with three identical fatty acids the series mentioned above is correct. It was found that the β morphology becomes the most stable one when one fatty acid is replaced by another one [66, 84, 87, 88].

Furthermore, the crystalline structure of triglycerides is determined by the chain length packing (Fig. 2.9). The triple chain length packing is typically formed by triglycerides consisting of three structural very different fatty acids [66].

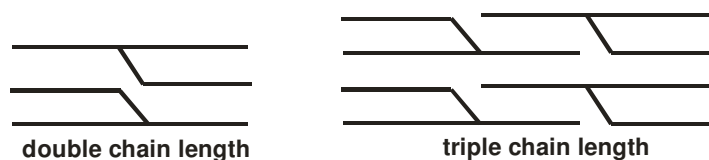


Figure 2.9: Double and triple chain length packing of triglycerides.

Depending on the morphology and the packing, the physical properties of the triglycerides differ [66]. Therefore, a deeper understanding of the structure-function relationship and the systematic molecular design as well as the investigation of the influence of the presence of other triglycerides on the structure is essential for applications.

2.2.3 Blended fats

Fats, which are used in industrial applications, are typically mixtures of various triglycerides, influencing the melting, crystallisation, transformation behaviour and crystal morphologies of each other [66, 89]. Depending on the chain length structure, blending of different triglycerides results in the formation of molecular compounds or segregation during solidification or after a long storage or formation of non miscible mixtures [66]. For binary mixtures of triglycerides the melting point of the minor component is altered in the direction of the major one and the melting point of the major one is depressed. This is probably due to the formation of

2. Fundamentals

eutectic mixtures or the solubilisation of the minor one in the major triglyceride [90, 91]. Additionally, on this account and because of disruption of the chain packing, the enthalpy of fusion of the minor component is decreased.

2.3 Surfactants

2.3.1 General Aspects

Surfactants are surface active and amphiphilic molecules. Amphiphilic derives from the two Greek words “amphi” (both sides) and “philia” (loves), describing the affinity towards oil and water. These properties are the result of the hydrophobic head group and the hydrophobic tail, the two characteristic parts of a surfactant (Fig. 2.10).

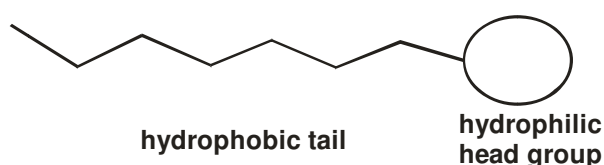


Figure 2.10: Schematic surfactant monomer molecule.

Typically, surfactants are classified by the charge of their head group. Surfactants with a charged head group are either anionic, cationic or zwitterionic. Surfactants without a charge at the head group are called nonionic surfactants (Tab. 2.3) [56, 92, 93].

Table 2.3: Classification of surfactants.

Classification	Head group	Example
anionic		Alkylcarboxylates, Alkylsulfonates
cationic		Alkyltrimethylammonium chloride
zwitterionic		Alkybetaines
nonionic		Alkylpolyethyleneglycols

2. Fundamentals

When surfactants are dissolved in water, the hydrophobic chain disrupts the hydrogen bonding structure of water, yielding an increased free energy of the system. Therefore, surfactants adsorb to the air/water surface and align the head group into the water and the tail towards the air to minimize the contact area with the water, resulting in a reduced free energy of the system [56]. After exceeding a well defined concentration, the critical micellar concentration (cmc), the surfactant starts to self-assemble into micelles. Self-assembling and micellization are primarily entropy driven processes [94-96]. However, the assembling of the surfactants accompanies with a loss of freedom and for ionic surfactants electrostatic repulsion of approximated similarly charged head groups increases, resulting in an increase of the free energy of the system and opposing the micellization. Hence, the cmc depends on the balance between forces, favouring the micellization (van der Waals and hydrophobic forces) and the opposing forces (kinetic energy of the molecules and electrostatic repulsion) [97]. This particular concentration can be determined from the kink of the plot of physical properties of the solution as a function of the surfactant concentration (Fig. 2.11) [56, 92, 94, 98]. Above the cmc the physical properties (except the solubility) change only slightly with increasing surfactant concentration because the added surfactant monomers are consumed in the micelle formation.

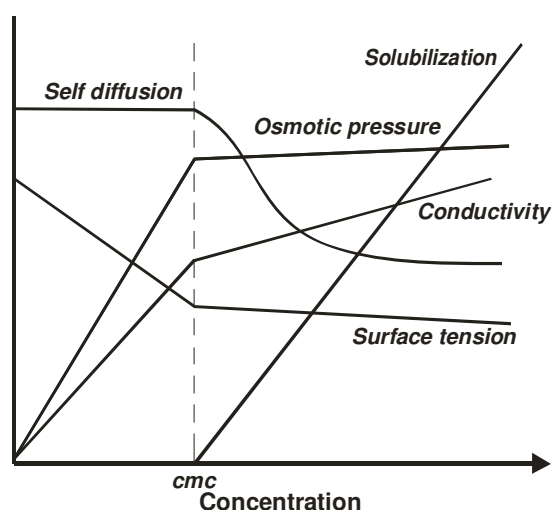


Figure 2.11: Schematic representation of the development of concentration dependent physical properties of an amphiphile dissolved in water.

The cmc depends strongly on the charge on the surfactant head group, the chain length, the degree of alkyl chain branching, the temperature, the valency of the counterions and the presence of cosolutes like electrolytes or alcohols [94, 98-103]. The shape of the formed micelles also depends strongly on the geometry of the surfactant monomers (Tab. 2.4) [56]. The packing parameter P enables an estimation of the micelle shape (equation 2.5). It depends on the volume ν of the single surfactant hydrocarbon chain, the cross-sectional area a of the head group and the length l of the fully extended hydrocarbon chain [56, 92, 93, 98, 104, 105].

$$P = \frac{\nu}{a * l} \quad (2.5)$$

The values ν and l can be estimated by the approximations made by Tanford depending on the number of carbon atoms, n_C (equations 2.6, 2.7) [106].

$$\nu = 27.4 + 26.9n_C \quad (2.6)$$

$$l = 1.5 + 1.265n_C \quad (2.7)$$

Table 2.4: Correlation between packing parameter P and the shape of the formed micelle.

<i>Packing parameter</i>	<i>Micelle shape</i>
$P = 1/3$	spherical
$P = 1/2$	rod
$P = 1$	disc

2.3.2 Lyotropic Liquid Crystals

If the surfactant is sufficiently soluble, the formation of liquid crystal phases occurs with increasing surfactant concentration [92, 94]. Depending on the micelle shape, which depends on the surfactant structure, different liquid crystalline phases can be observed (Tab. 2.5).

2. Fundamentals

Table 2.5: Correlation of micellar shape and type of formed liquid crystal by increasing the surfactant concentration.

<i>Micelle shape</i>	<i>Liquid crystal</i>
spherical	cubic
rod	hexagonal
disc	lamellar

Lyotropic liquid crystals consist of an amphiphile and a solvent and combine characteristics of liquids and crystals [95]. They have a certain order which can reach from atomic scale to longer length scales and are less viscose than crystals. Some liquid crystals are optically anisotropic, like for example the hexagonal and the lamellar one, the most important ones in applications [92, 95]. Therefore, both are showing a characteristic texture under the polarizing optical microscope [107-110].

The lamellar mesophase is built up by surfactants arranged in double layers which are separated by a water phase (Fig. 2.12a). The alkyl chains and the water phases are in a liquid like disordered state [95, 111-113]. In the hexagonal mesophase the amphiphiles are assembled in parallel cylindric micelles which are packed in a hexagonal order (Fig. 2.12b). For the hexagonal mesophase two alternative types are distinguished, the normal (H_1) and the reversed one (H_2). In the normal one the water is the continuous phase and in the reversed one the alkylchains are the continuous phase. The hexagonal phases have a higher viscosity than the lamellar phase [92, 95, 109, 110, 112, 113].

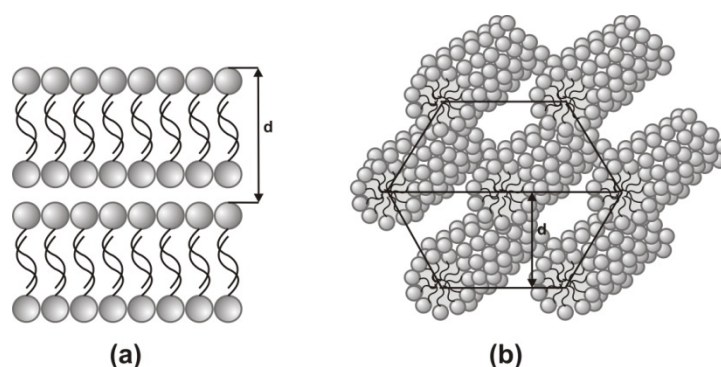


Figure 2.12: Schematic illustration of (a) a lamellar liquid crystalline phase and (b) a normal hexagonal liquid crystalline phase.

2.3.3 Solubility

The solubility of ionic surfactants depends strongly on temperature. For low temperatures the solubility of surfactant is low and increases with increasing temperature. At a certain temperature the solubility increases abruptly. At this point the solubility curve and the cmc curve are equal, it is called the Krafft temperature (Fig. 2.13) [56, 92, 93, 95]. The Krafft temperature is determined by the energetic relationship between the solid crystalline state (melting point) and the heat of hydration of the system [114].

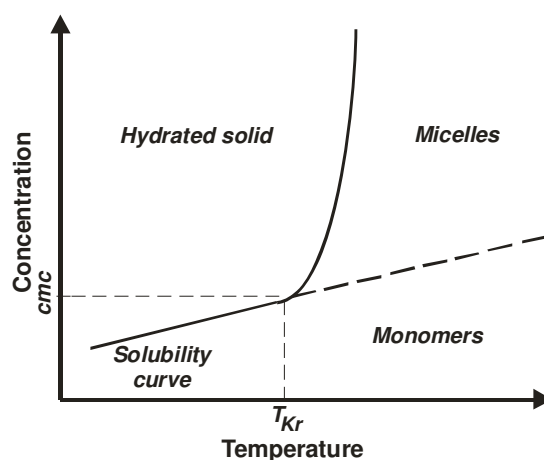


Figure 2.13: Binary phase diagram of a surfactant solution in water in the region of the Krafft temperature.

A decrease of the Krafft temperature can be achieved by hindering the crystal packing of the monomers, for example by using highly hydrated polar head groups or counterions [56, 92, 93, 115]. Recently, Collins concept of matching water affinities was applied to regulate the Krafft temperature [116-118]. It was shown that the combination of large polarisable head groups with a counterion with the same water affinity results in an increase of the Krafft temperature. In contrast, the combination of the head group with a small less polarisable counterion delivers an amphiphile with a higher solubility and a decreased Krafft temperature [119].

The temperature dependent behaviour of a nonionic surfactant is different. The characteristic feature of nonionic surfactants is the phase separation with increasing temperature. The characteristic point is called the cloud point and depends strongly on the chain length and the number of polar groups like ethoxy groups in the hydrocarbon chain [92, 120, 121]. The driving forces for the

2. Fundamentals

solubilisation of a nonionic surfactant like an alkyletherglycol are the hydration of the hydrophilic head group and the formation of hydrogen bonds between the ether units and the water. The strength of the H-bonds is strongly temperature dependent and decreases with increasing temperature, resulting in phase separation above the cloud temperature [56]. However, this behaviour can be influenced strongly by the addition of cosolutes [122, 123].

2.4 Cosolutes

2.4.1 Hydrotropes

The term hydrotrope was introduced for the first time by Neuberg to describe organic molecules with a hydrophilic as well as hydrophobic part which increase the solubility of organic compounds like alcohols, hydrocarbons, oils, etc (Fig. 2.14) [124]. They are surface active like surfactants but in contrast to surfactants the hydrophobic part is too small to cause defined self assembling in well-determined structures, therefore these compounds show no cmc [125, 126]. Hydrotropes are used to increase the solubility of e.g. surfactants. Investigations have shown that the dilution with water induces the precipitation of the solute because a high amount of hydrotrope is required to exhibit hydrotropic activity [127]. The concentration which needs to be exceeded is known as the “minimal hydrotropic concentration” (MHC) [125]. Above the MHC the hydrotropes change the solubility properties, the micellar characteristics like cmc and aggregation number and the adsorption of the surfactant at the interface [92, 128, 129]. One apposite approach to describe hydrotropes is the comparison with salting-in additives [125, 130]. Hydrotropes are used in industrial applications to avoid the formation of liquid crystals, by decreasing surfactant-surfactant interaction, to increase the cloud point and in separation processes [92, 128, 131].

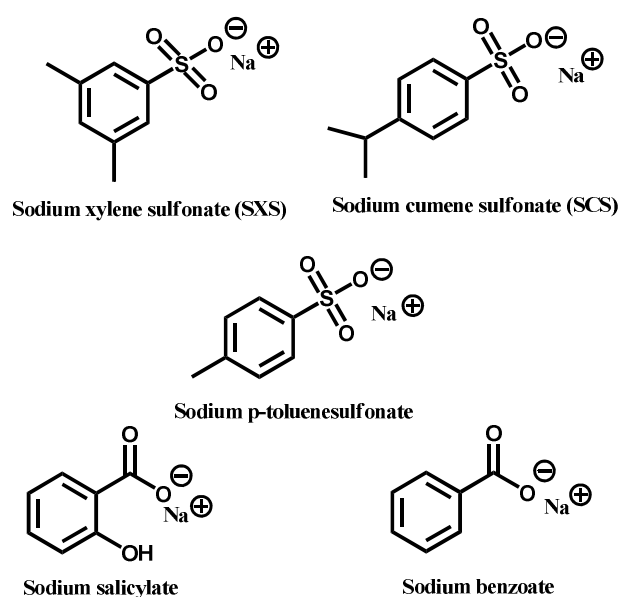


Figure 2.14: Structures of different common hydrotropes

2.4.2 Cosurfactants

Cosurfactants are molecules which have nearly the same properties as surfactants, but they are insufficiently hydrophilic to form micelles or other mesophases with water alone. However, they have a strong impact on surfactant mesophases. Depending on the strength of the polar head group they can act more like an oil, enriching in the interior of the micelles and adsorbing to the micelle surface or like a surfactant participating in the mesophase. Hence, they affect the curvature of the micelles and therefore, the structure of formed liquid crystalline phases. Typically used cosurfactants are alcohols, fatty acids and long chain aldehydes. In industrial applications they are used to reduce the amount of required surfactant to form microemulsion [56, 92-94, 98].

2.5 Microemulsion

One main aim in the washing process is the dissolution of oil in water. However, oil and water are not miscible spontaneously, anyhow under significant mechanical agitation emulsions can be formed but these are, in contrast to microemulsions, not thermodynamically stable. Emulsions consist of a dispersed and a continuous phase. Typical droplet diameters range from 0.1 to 1 micrometer, therefore emulsions appear turbid [92]. The addition of emulsifiers like surfactants can extend the stability, even so the emulsion is still a dispersion which will separate into the two phases water and oil, by either breaking, coalescence, creaming, Ostwald ripening or flocculation after a certain time [92, 93, 132-135]. Nevertheless, emulsions are important for many applications of daily life, like washing, cosmetic formulations or food products [93, 136].

Composed of the same components, but thermodynamically stable and clear, which finds wide application in a variety of products and processes is microemulsion. It was investigated the first time by Hoar and Schulman [137]. Finally, the latter one of the both introduced the term microemulsion [138]. A multitude of succeeding investigations have shown that these “dispersions” of water, oil and amphiphile are actually solutions [139]. So the great advantage of this species is the thermodynamical stability [139]. Further benefits of microemulsions for applications are the spontaneous formation, solubilisation of a high amount of oil and water, the low interfacial tension, the fine microstructure and the transparent appearance, due to the small droplet diameter of typically 2-20 nm [99, 140]. However, the small droplet size complicates the structural investigation of microemulsions. Commonly used techniques are amongst others NMR self diffusion, freeze fracturing transmission electron microscopy (cryo-TEM) and small angle neutron and X-ray scattering (SANS, SAXS) [141-144]. Adversely is also that the formation of microemulsions requires a big amount of surfactant and they do not solubilise triglycerides in high amounts without the addition of cosolutes, due to their high molecular weight [81, 145-155]. However, triglycerides are one of the main components of typical household laundry [8].

Structure of microemulsion

Three different structures are known for microemulsions (Fig. 2.15) [95]. They vary in the curvature of the oil/water interface. The curvature depends beside temperature, salinity, oil properties and surfactant concentration on the packing parameter of the surfactant [156]. This parameter results from the geometry and the chemical structure of the surfactant as well as from the intermolecular forces between the surfactant molecules [95, 157]. The repulsive, hydrophilic forces between the surfactant head groups determine the effective area per head group a of the surfactants, whereas the repulsive sterical interactions between the surfactant tails and the attractive oil penetration determine the volume V and the extended chain length l of the hydrocarbon tail. For a packing parameter less than one a positive curvature occurs and an oil-in-water (o/w) structure is formed and for a parameter greater than one the curvature of the interface becomes negative and a water-in-oil structure (w/o) occurs [137, 158-160]. These two structures are separated by a bicontinuous sponge-like phase with a packing parameter of about one and saddle shaped surfaces with positive and negative curvature resulting in a mean curvature of zero [92, 142, 157, 159, 160].

As already mentioned above, the curvature also depends on the concentrations of surfactant, oil and water. The three structures are continuously progressed by varying the oil to water ratio. For low oil concentrations oil in water droplets are formed. With increasing amount of oil the micelles expand to swollen micelles and after a certain oil concentration the micelles become cylindrical and sponge like and at least for a very high fraction of oil water in oil droplets are formed. Alternative abbreviations for the different structures are L1-phase for an o/w, L2 phase for a w/o and L3-phase for a bicontinuous systems.

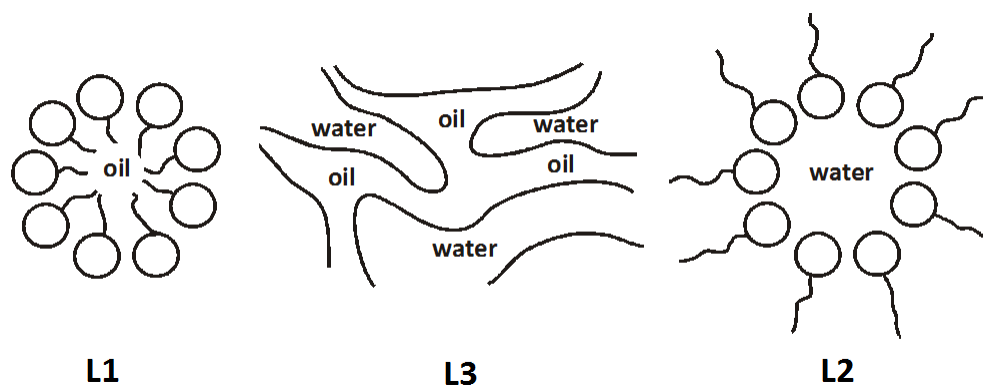


Figure 2.15: Structure of microemulsions as a function of water to oil ratio with the highest fraction of water in L1 and the lowest one in L2.

Conductivity of microemulsions

Conductivity is linked to the diffusion coefficient, hence the conductivity of a microemulsion depends on the structures in the system. Precondition for conductivity is the presence of ions in the microemulsion. These might originate from ionic surfactants or, in the case of microemulsions formed with nonionic surfactants, from added salt. However, the amount of added salt has to be small to avoid an influence on the phase behaviour of the system.

For a w/o system the ions are dissolved in the inner sphere of the reversed micelles. Due to the low mobility of the micelles, the conductivity is low. With an increasing fraction of water the micelles grow and begin to percolate, hence the ion transport becomes more efficient and the conductivity increases. For a bicontinuous system all isolated micelles accumulated to a system of fluctuating channels, yielding a maximum in the mobility of the ions and consequently in a maximal conductivity of the system. With increasing fraction of water the channels cross-link which hardly enhances the mobility of the ions. Additionally, the dilution of the ion concentration compensates this effect, therefore the conductivity decreases after the bicontinuous region.

Due to this change in conductivity, the measurement of conductivity κ as a function of water fraction, ϕ_w is an appropriate, easy method to determine the structure of microemulsions (Fig. 2.16).

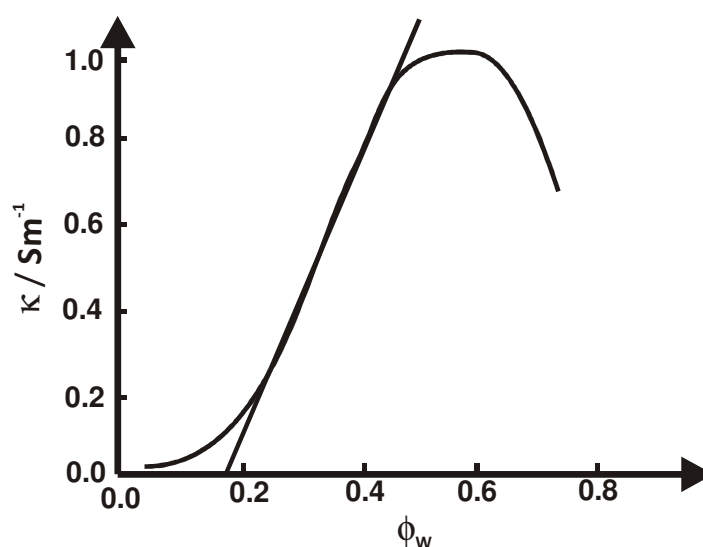


Figure 2.16: Specific conductivity κ of microemulsion as a function of water fraction ϕ_w .

2.6 Hansen Solubility Parameters

The importance to predict solubility is ubiquitous. The basic principle is “like dissolves like” or more generalized “like seeks like” [161]. Hildebrand did the first attempt to quantify this general concept. He related the cohesive energy E on the one hand and the enthalpy of evaporation and the molar volume on the other hand (equation 2.8).

$$\frac{E}{V_m} = \frac{\Delta H_v - RT}{V_m} \quad (2.8)$$

E is the energy of vaporization, V_m the molar volume of the pure solvent, ΔH_v the free enthalpy of vaporization, R the gas constant and T the temperature. Together with Scott he introduced in 1950 the term of the solubility parameter δ (equation 2.9) [162, 163].

$$\delta = \left(\frac{E}{V_m} \right)^{\frac{1}{2}} \quad (2.9)$$

The thermodynamic criterion for the miscibility of two solvents is that the free energy of mixing ΔG^{mix} is zero or negative (equations 2.10 and 2.11) [162, 164, 165].

$$\Delta G^{mix} = \varphi_1 \varphi_2 V_M (\delta_1 - \delta_2)^2 - T \Delta S_{comb}^{mix} \quad (2.10)$$

$$\Delta G^{mix} = \Delta G_{noncomb}^{mix} - T \Delta S_{comb}^{mix} \quad (2.11)$$

The φ_1 and φ_2 are the volume fractions of the solvent and the solute, V_m is the volume of the mixture, δ_1 and δ_2 are the solubility parameters of compound 1 and compound 2, ΔS_{comb}^{mix} is the combinatorial entropy change and $\Delta G_{noncomb}^{mix}$ is the noncombinatorial free energy of solution which includes all enthalpic effects due to simply mixing. The equations 2.3 and 2.4 visualize the importance of the similarity of solvent and solute. The more similar the solubility parameters the smaller is the contribution of the noncombinatorial free energy. Additionally, they also illustrate the importance of the entropy change for the solubilisation. However, the validity of this concept is restricted to regular mixtures and to small molar volumes. Many

scientist like Barton, Burrell, Blanks and Prausnitz and further, tried to improve this concept [162, 166, 167]. One of the most widely used developments of the concept is the one of Charles M. Hansen. It is a three dimensional solubility parameter model [95]. He considers that there are several contributions to the cohesive energy of evaporation. The energy of evaporation is the sum of dispersion cohesive energy E_D , polar cohesive energy E_P and the hydrogen cohesive energy E_H (equation 2.12) [162, 168-170].

$$E = E_D + E_P + E_H \quad (2.12)$$

The division by the molar volume V_m gives square of the total Hildebrand solubility parameter δ as a sum of the single contributions (equations 2.13 and 2.14) [95].

$$\frac{E}{V_m} = \frac{E_D}{V_m} + \frac{E_P}{V_m} + \frac{E_H}{V_m} \quad (2.13)$$

$$\delta^2 = \delta_D^2 + \delta_P^2 + \delta_H^2 \quad (2.14)$$

All these three parameters can be determined experimentally or calculated by increments (equations 2.15 – 2.17) [95]. This calculation is based on attractive constants F_{Di} and F_{Pi} for the dispersion and the polar part and the cohesive energy constant E_{Hi} [95].

$$\delta_D = \frac{\sum_i F_{Di}}{\sum_i V_i} \quad \delta_P = \frac{\sqrt{\sum_i F_{Pi}^2}}{\sum_i V_i} \quad \delta_H = \sqrt{\frac{\sum_i E_{Hi}}{\sum_i V_i}} \quad (2.15-2.16)$$

For the visualization of good solvents the Hansen parameters are plotted in the three dimensional Hansen space [95].

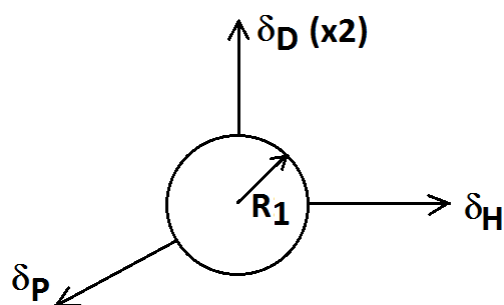


Figure 2.17: Illustration of the Hansen solubility parameters in the three dimensional solubility parameter space giving a spherical solubility space [95].

Solutes with Hansen solubility parameters within this spherical space are dissolved. Skarup developed an equation for the distance R_a between miscible compounds (equation 2.18) [162]. This is a good description, however, the geometrical averaging of the polar part is only approximative and the fact that hydrogen bonds are just formed in the presence of donor- and acceptor groups is unconsidered in this equation [95].

$$(R_a)^2 = 4(\delta_{D2} - \delta_{D1})^2 + (\delta_{P2} - \delta_{P1})^2 + (\delta_{H2} - \delta_{H1})^2 \quad (2.18)$$

The relative energy difference RED can be calculated when the interaction radius R_0 is considered (equation 2.19). Two solvents are alike and should mix completely for RED smaller than 1 and they will partially get mixed for RED about 1. When the molecules are very different, they will not dissolve and the RED is greater than 1. The RED allows a fast prediction of good solvents for a given substance. But unfortunately the R_0 value is not known for all combinations of solvent and solute which can be imagined and it can not be calculated.

$$RED = \frac{R_a}{R_0} \quad (2.19)$$

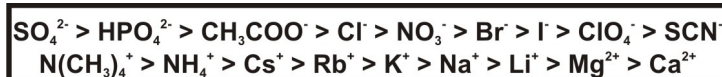
So the Hansen Solubility Parameters (HSP) permit a very fast qualitative comparison of a list of solvents for a special solute. It enables a more reliable prediction of good solvents than the Hildebrandt solubility parameter does. But it reaches its limitations for the quantitative solubility prediction. Therefore, as shown

in the subsequent study, the solvent screening for solid tripalmitin is unsatisfactory.

2.7 Hofmeister Series and Collins Concept

Specific ion effects are known for a very long time and still studied today by many scientists for various applications. For example for the design of new ionic liquids and for the aligned change of the solubility of surfactants [171]. For monoatomic ions the main features determining short-range specific ion interactions are their charge, their size, their polarizability and the availability of electrons and/or orbitals for covalent contributions. For polyatomic ions, additionally the charge density distribution and in some cases the presence of hydrophobic groups are essential [172, 173].

One of the first, investigating the specific ion effects systematically, was Franz Hofmeister and still today he is the reference for any investigations done within this field [174, 175]. He and his co-workers reported the effect of various salts on the solubility of proteins in water in a series of papers [174, 176-178]. They found that some salts precipitate proteins (salting out) while others improve the solubility of the proteins (salting in). There is a relation between the charge density of the salts and their effect on the protein solubility. Small, hard anions with high charge density are strongly hydrated and tend to cause salting out, whereas large, soft anions with low charge density are weakly hydrated and tend to cause salting in [172]. Also very common for the description of the ion behaviour are the terms cosmotropic and chaotropic. These terms take the ability to influence the structure of the water in account. However, the series is reversed for anions and cations. In the Hofmeister series the ions are ordered as a function of their charge density. Usually, anions and cations are listed in separated series (Fig. 2.18).



***cosmotropic
salting out***

***chaotropic
salting in***

Figure 2.18: A typical Hofmeister series.

Hofmeister series in which some ion have another position within the series are also known. This is due to the fact that in the series only the ions are considered

but whether they are salting in or salting out depends strongly on the counter ion [174].

A further approach to the explanation of specific ion effects was done by Collins with his concept of matching water affinities [118, 174, 179, 180]. Whenever salts are dissolved in water the structure of the solvent is changed [181]. The solvent surrounds the ion, which is described as a point charge and the region of modified solvent is denoted as the cosphere of the ion [172, 182]. According to Collins the water structuring of ions can be explained as a competition between the ion-water interaction, dominated by the charge density effects and the water-water interaction, dominated by the hydrogen bonding [116]. Small ions with a high charge density interact strongly with the water in the first water shell, structuring the water (cosmotropic) whereas larger ones have a lower tendency to structure the surrounding water [172]. Collins also postulated that the influence of cations on water structure is less pronounced than the influence of anions due to the fact that the negative partial charge of the water is nearer to the centre than the positive one [172].

Referred to Collins concept of matching water affinities contact ion pairs are only formed spontaneously for oppositely charged ions with an equal water affinity (Fig. 2.19) [116, 171, 174, 179]. The electrostatic interaction between two small hard ions is stronger than the ion-water interaction. Therefore, the ions come very close, forming a contact ion pair. For big oppositely charged ions the water-water interaction is stronger than the ion-water interaction and thus the centre of the two big ions can come close enough to form a contact ion pair too. Collins concept is an advancement of the general rule “like seeks like” [183, 184].

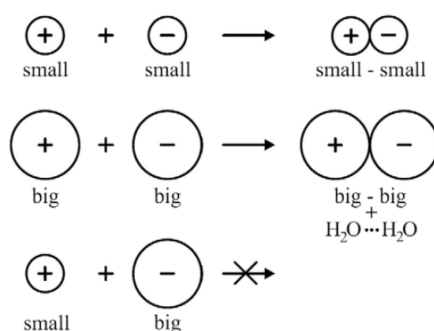


Figure 2.19: Collins concept of matching water affinities.

2.8 Characterization Methods

2.8.1 Ternary Phase Diagram

Searching for the best surfactant or combination of surfactant/surface active additive (which can be either a cosurfactant or a cosolute) to dissolve triglycerides, mixtures of oil, surfactant or rather surfactant/additive and water are investigated in order to find the combination with the most extended microemulsion or emulsion area. For a mixture of three components the state is determined by three variables, the temperature and the content of two of the components. The phase diagram of such a mixture is represented in a three dimensional diagram, the so called Gibbs triangle (Fig. 2.20) [185]. The mass, volume or mole fraction of the components are plotted along the axis of the equilateral triangle and the corner corresponds to the pure components. Hence, on the axis between the corner B and C the binary mixtures of oil and surfactant/cosurfactant are plotted [56]. In such a triangle the arising phases like microemulsions, emulsions, liquid crystalline phases and areas of precipitating surfactant can be illustrated easily. The comparison of different phase diagrams provided at the same temperature enables a fast estimation which surfactant/cosurfactant combination is most suitable to dissolve triglycerides and therefore probably the most promising for further washing applications.

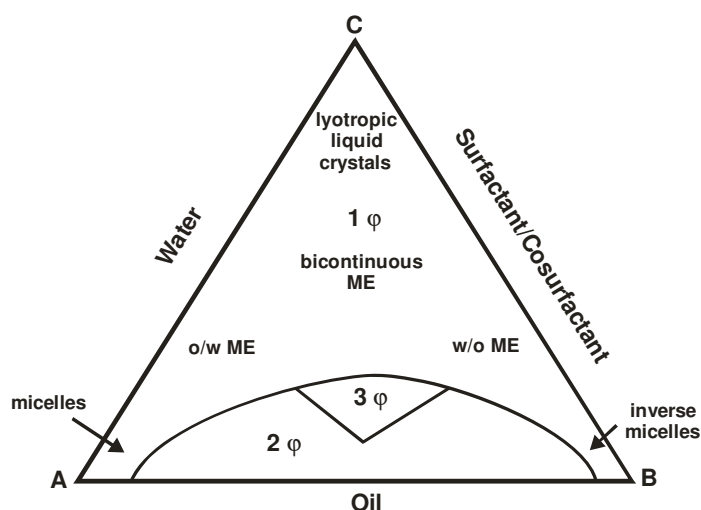


Figure 2.20: Schematic phase diagram of a ternary system of oil, surfactant/cosurfactant and water at given temperature. The symbols 1ϕ , 2ϕ and 3ϕ indicate regions of one, two and three phases. In the region of one phase typically regions of micelles, various microemulsions and liquid crystals are distinguished.

2.8.2 Differential Scanning Calorimetry

The Differential Scanning Calorimetry (DSC) is a thermal analysis technique to determine thermodynamic processes initiated by heating or cooling the sample [186]. The advantages of DSC are the high degree of certainty and reproducibility as well as the small amount of sample required for the determination of the melting point and melting enthalpy [187]. Typically it finds application in the determination of phase transitions and the determination of heat capacity [188]. For the purpose within this thesis we contemplate the fusion. For the determination of the melting point and the accompanied enthalpy the DSC has to be calibrated with calibrating substances like indium. For a calibrated DSC the transition enthalpy $\Delta H_{\text{fus}}(p,T)$ of fusion is proportional to the peak area $A(p,T)$ and can be calculated by equation 2.20 [189]. M is the molar mass of sample substance, m is the mass of sample and $k(p,T)$ is the calibration constant of the DSC.

$$\Delta H_{\text{fus}}(p,T) = \frac{A(p,T) * M}{m} * k(p,T) \quad (2.20)$$

It was shown that for measurements at normal pressure the calibration factor k is independent of the phase transition temperature [189]. Therefore, the equation is valid for the complete temperature range.

In the DSC device the sample and a reference are placed in a thermal isolated measuring cell. Both are heated by two independent ovens. Pt sensors determine the temperature difference between sample and reference during the measurement and the ovens try to compensate the difference. The melting of a substance is corresponding to the classification by Ehrenfest a phase transition of first order [96, 188]. Thus, the temperature of the sample does not change during the melting and the enthalpy increases abrupt at the melting point [187]. To gain the same temperature in sample and reference the heat flow in the reference has to be adapted. Accordingly, this setting enables the direct determination of formed or consumed quantity of heat (Fig. 2.21) [188].

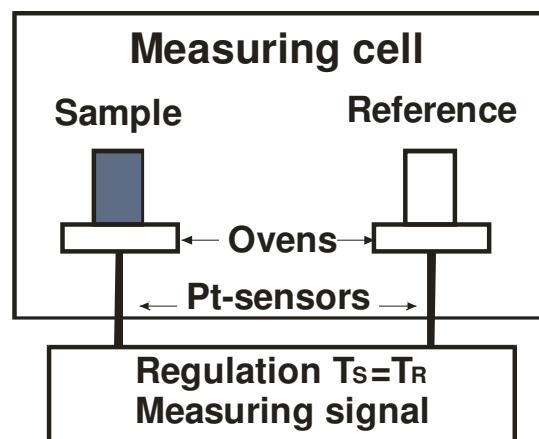


Figure 2.21: Schematic illustration of a DSC device.

The change of the heat flow is plotted as a function of the temperature (Fig. 2.22). The drift of the base line is due to the changed heat capacity during the melting process [188, 190]. For the peak integration a linear interpolation is done [188].

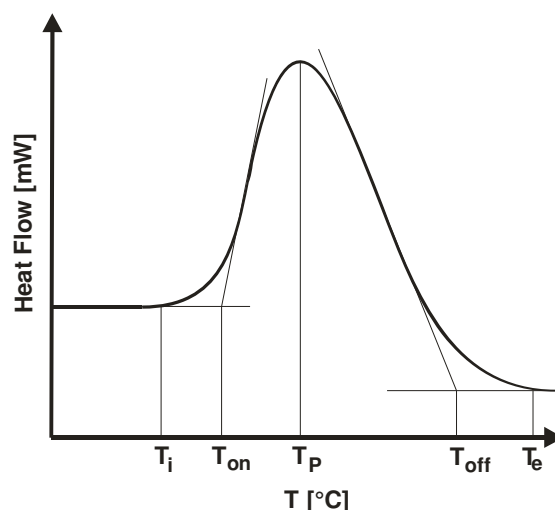


Figure 2.22: Schematic illustration of a typical endothermic melting peak yielding by DSC measurement.

The temperatures which can be gained from the peak are the temperature of the beginning of the peak T_i , of the onset of the peak T_{on} , of the peak maximum T_p , of the peak offset T_{off} and of the peak end T_e . If the heating rate is increased the melting peak becomes sharper. Hence, it is advised to use the peak onset for the characterisation of the phase transition, because this temperature is less dependent on the heating rate [188, 191].

2.8.3 NMR

General Aspects

The requirement for the beginning of NMR (nuclear magnetic resonance) spectroscopy was the discovery of the nuclear magnetic resonance in 1945 [192-195]. During the last decades it became one of the most important analytical techniques in chemistry to control the purity and to determine the molecular structure of products, to persecute dynamics in samples, to examine liquid crystals formed by amphiphiles and much more. Due to its versatile applicability it also became very important in biochemistry, medical science, pharmacy, materials science, physics and more. This widespread scope results from the application of superconductive magnets, the use of Fourier transform and multidimensional techniques [196-200].

Most important structural parameters gained from NMR measurements are the chemical shift, the scalar coupling constant, the multiplet structure and the integral intensity of the resonance signal. Further parameters for structure determination are the Kern-Overhauser effect, the temperature coefficient of the chemical shift, the diffusion coefficient, the coalescence temperature and the dipolar residual coupling. The information gained from all this parameters enable the determination of the constitution, the conformation, the dynamics and the detection of intermolecular interactions [201, 202]. In the following section a short overview of the fundamentals is given [203, 204].

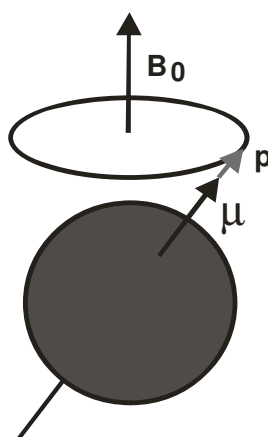


Figure 2.23: Representation of a spinning proton in a magnetic field of magnitude B_0 .

2. Fundamentals

Every nuclei carries charge and in some nuclei the charge “spins” on the nuclear axis, inducing a magnetic dipole along the axis (Fig. 2.23) [205].

The angular momentum of the nuclei is described by the quantum spin number I , which is odd ($1/2$, $3/2$ and so on) for an odd nucleon number and even (0 , 1 , 2 and so on) for an even nucleon number. The spin I for some nuclei is given in table 2.6 [206].

Table 2.6: Nuclear spin quantum number of some nuclei.

<i>Nuclei</i>	<i>Nucleon number</i>	<i>Atomic number</i>	<i>Spin I</i>
^1H	Odd	Odd	$1/2$
^2H	Even	Odd	1
^{31}P	Odd	Odd	$1/2$
^{23}Na	Odd	Odd	$3/2$
^{14}N	Even	Odd	1
^{13}C	Odd	Even	$1/2$
^{19}F	Odd	Odd	$1/2$
^7Li	Odd	Odd	$3/2$
^{87}Rb	Odd	Odd	$3/2$
^{137}Cs	Odd	Odd	$7/2$

The magnitude of the resulting magnetic dipole is expressed by the nuclear magnetic moment μ_0 . Nuclei with a spin $I > 1$ have a non spherical charge distribution inducing an electrical quadrupole moment (eQ) [201, 203, 204].

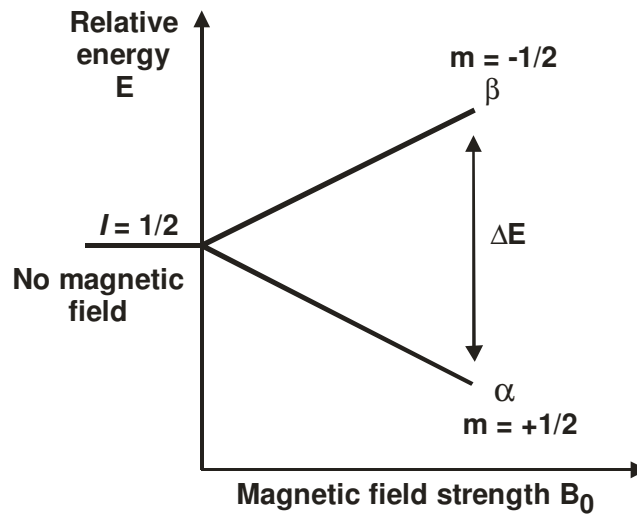


Figure 2.24: Energy profile of a nuclei with spin $I = \frac{1}{2}$ applied in a magnetic field of magnitude B_0 .

If the nucleus is brought into an external magnetic field it has $2I + 1$ possibilities to orientate. This orientations are characterised by m_I and the magnetic quantum number takes values from $-I$ to $+I$. Accordingly, a nucleus with spin $I = \frac{1}{2}$ has two orientations of different energy, labelled as α ($m = +1/2$) and β ($m = -1/2$) (Fig. 2.24). Spins parallel orientated to the applied magnetic field have a lower energy than the antiparallel orientated ones [201].

The energy difference between the two states is given by the larmor frequency ω_0 (equation 2.21 and 2.22) [201]. The larmor movement is a precession of the spins around the static magnetic field B_0 (figure 2.23).

$$\omega_0 = \gamma B_0 \quad (2.21)$$

$$\Delta E = \hbar \omega_0 = \left(\frac{h\gamma}{2\pi} \right) B_0 \quad (2.22)$$

$$\gamma = \frac{2\pi\mu}{hI} \quad (2.23)$$

Planck's constant h , π and the gyromagnetic ratio γ are constants, however γ is a fundamental nuclear constant, the proportionality factor between the magnetic moment μ and the spin number I (equation 2.23) [201]. Therefore, the energy difference is dependent on the nucleus and directly proportional to the magnetic field B_0 [205].

2. Fundamentals

Modern NMR devices are FT-(Fourier Transformation)-spectrometer (figure 2.25) [203, 204]. The sample is placed in a constant magnetic field of the magnitude B_0 and irradiated with a pulse of high power radiofrequency energy with a frequency range sufficiently large to cover the entire range [201]. If the frequency is equal to the Larmor frequency the nuclei are transferred from the α state to the β state. Immediately following the pulse, the excited nuclei begin to return to the ground level releasing energy, which is detected and transformed to a free induction decay (FID). The FID is the sum of all the nuclei emitting over time, therefore a function of time and is converted via Fourier transform (FT) to a spectrum, a function of frequency.

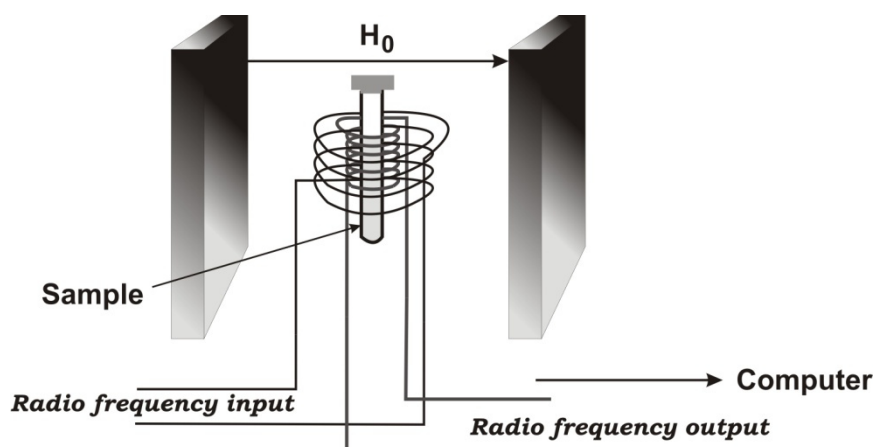


Figure 2.25: Schematic representation of a nuclear magnetic resonance spectrometer.

The magnitude of energy a nucleus can absorb depends on the population difference Δn between the two states α and β , which can be calculated from the Boltzmann distribution [201, 205] (equation 2.24).

$$\frac{n_{\alpha}}{n_{\beta}} = e^{\frac{\Delta E}{kT}} = e^{\frac{\gamma \hbar B_0}{2\pi kT}} \quad (2.24)$$

Quadrupole Splittings

As already mentioned above, nuclei with a spin $I > 1$ have a non spherical charge distribution inducing an electrical quadrupole moment (eQ) [201, 203, 204]. Examples for such nuclei are, ^2H ($I = 1$), ^7Li ($I = 3/2$), ^{23}Na ($I = 3/2$), ^{37}Cs ($I = 7/2$) and ^{87}Rb ($I = 3/2$). In an anisotropic environment, for example a liquid

crystalline phase, the electric field gradient at the nucleus is inhomogeneous and some orientations are favoured over others [207]. The interaction of the electrical quadrupole moment with the electric field gradient results in quadrupole splitting. The resonance signal splits into $2I$ equidistant signals, in the simplest case of $I = 1$ into two peaks [208-212]. The frequency difference between the two peaks is given by equation 2.25, where eQ is the electric quadrupole moment of the nucleus, eq is the electric field gradient, h is Planck's constant and Θ is the angle between the electric field gradient and the magnetic field director [207, 213].

$$v_Q = \frac{3}{4} \frac{e^2 q Q}{h} (3 \cos^2 \Theta - 1) \quad (2.25)$$

The resulting quadrupole splitting Δ is a weighted average of the values at the i different sites, due to the rapid exchange (equation 2.26) [213], where p_i is the fraction of the ions at the site i , v_{Qi} is the effective quadrupole coupling constant and S_i (equation 2.27) [214].

$$\Delta = \left| \sum_i p_i v_i S_i \right| \quad (2.26)$$

$$S_i = \frac{1}{2} (3 \cos^2 \Theta_{DMi} - 1) \quad (2.27)$$

S_i describes the orientation of the fraction of molecules at the site i , with Θ_{DMi} the angle between the electric field gradient and the director of the liquid crystal axis. Relaxation studies have shown that the quadrupole coupling constant $E_Q = \frac{e^2 q Q}{h}$ is approximately constant [215]. Therefore, changes in quadrupole splitting results primarily from different S_i . This enables the determination of the fraction of bound water p_b^w in liquid crystals (equation 2.28 and 2.29). The quadrupole splitting of free water Δ_f^w is zero [65, 215].

$$\Delta = \Delta_f^w + \Delta_b^w = p_b^w \delta_b^w = p_b^w \frac{3}{4} E_{Q,b}^w S_b^w \quad (2.28)$$

$$p_b^w = n_b \left(\frac{x_s}{x_w} \right) \quad (2.29)$$

The fraction of bound water is given by the molar amount of bound water per surfactant head group n_b and the mole fractions of surfactant x_s and water x_w . In

analogy the fraction of bound counterions can be calculated. This enables for example the study of the ion specificity of surfactants with different head groups in lamellar phases, as has been done recently [208].

Study of ion specificity

The requirements for the determination of ion specificities of surfactants by NMR is the assembling in liquid crystals and the existence of a quadrupole moment for the investigated counterions. Only for an anisotropic environment the determination of quadrupole splitting is possible and the fraction of bound ions can be determined. To simplify the following description only the lamellar phase is considered.

A lamellar phase has a regular structure of surfactant bilayers separated from water layers. The surfactant layer consists of surfactant and hydrotrope. The lamellar surface and the counter-ion binding is shown in figure 2.26 [208, 216]. There are three possible binding sites. The ion can be moving freely in the water layers between the surfactant bilayers. This location is characterized by $S = 0$ and the ions do not contribute to the quadrupole splitting. Alternatively, the ions can be bound, either next to the polar head group of the surfactant, resulting in an average angle between the director (D) and the electric field gradient (M) of 0° or between the polar head groups [216]. The existence of three binding sites became obvious by measuring the quadrupole splitting of sodium in the sodium octanoate/decanol system. From previous studies it was known that the octyl sulphate/decanol lamellar phase gives Δ values in the range 9–16 kHz, while the octyl sulphonate/decanol system gives 10–14 kHz. In contrast to the roughly constant Δ values for the sulphate and sulphonate systems, previous data for sodium Δ values in the sodium octanoate/decanol system demonstrated that the simple bound/free model did not fit the data, particularly at higher concentrations. Some compositions gave ^{23}Na Δ values that were much smaller, even approaching zero. These were highly temperature dependent, both increasing and decreasing with temperature (although not at the same time). Changes in the fraction of “bound” ions could not account for the behaviour. It was necessary to invoke a second binding site with a very different value of Δ_b , one that was of opposite sign to that of the

first binding site. The data were fitted with Δ_b values of +12 kHz for the normal ion binding site and -7 kHz for the second, which was thought to be from Na ions located between the head groups. Low temperatures and higher surfactant concentrations favoured the second site. The data indicated that as the water layer thickness became smaller, the location of the bound ions altered, with the more ions moving into positions between the head groups.

Previous studies of ionic surfactants have shown that the Δ values are broadly consistent with the “ion condensation” model, where ion binding (and Δ) is invariant over a fairly large water concentration. Therefore, fraction of the ions in the second and third binding site can be calculated from the quadrupole splitting as mentioned above.

Because of the difficulties in obtaining the absolute values of the quadrupole coupling constant the method has fallen into disuse. But it should be ideal for monitoring competitive ion binding. In a mixture of two ions, A & B , if B displaces A then the Δ values of A will decrease on addition of B . Those of B will also decrease because the highest fraction of bound B ions occurs with small additions of B . Fortunately, there are several cations that possess nuclear quadrupole moments [208].

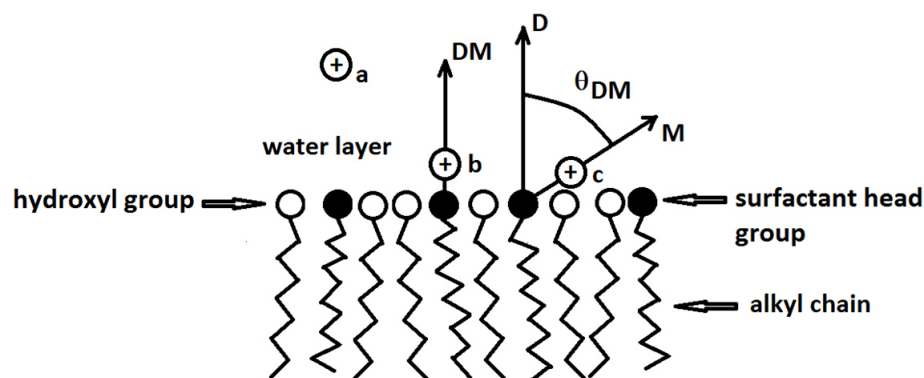


Figure 2.26: Schematic representation of the counter-ion binding at the lamellar surface. Three possible binding-sites are shown: (a) The counter-ion is moving freely in the water layers. (b) The counter-ion is located symmetrically with respect to the amphiphile polar end-group. (c) The counter-ion is located between amphiphile polar head groups.

2.8.4 Colorimetry

A more and more important quality criterion in industry is the colour of products [217]. The human eye can distinguish ten million colours and the colour perception depends basically on three elements which are the light source, the object and the observer. Hence, the description of the colour in precise mathematical terms is necessary [217, 218]. A great contribution to standardize the colour control was done by the CIE (Comission Internationale de l'Eclairage). They defined the light source as the amount of emitted energy at each wavelength (=relative spectral power distribution) [218]. The light interacts with the object and is transmitted, absorbed and reflected. But for the colour perception only the reflected light, which reaches the observer is relevant. The human eye possess three different types of cone shaped receptors which are sensitive to red, green and blue light [219]. Due to that the XYZ colour space was introduced. Each colour can be described by the three non-negative tristimulus coordinates X, Y and Z representing the answers of the three receptors [219, 220]. Colorimeters working on this principle are called tristimulus colorimeter (Fig. 2.27). The reflected light passes a red, green and blue filter and the amount of passing light is detected by photodetectors beyond each filter giving the X, Y and Z values [219].

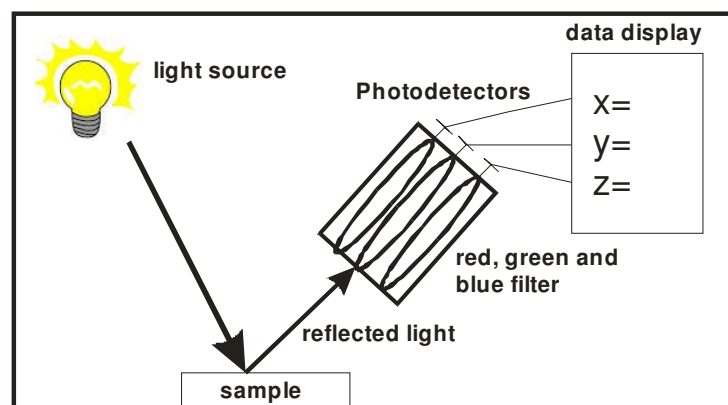


Figure 2.27: Schematic illustration of a tristimulus colorimeter.

However, these three values give not a uniform colour space and therefore these values are not capable to determine colour differences. Hence, a further colour scale was introduced. A theory says that the responses of the three different cones are mixed to an opponent response on its way to the brain [219, 221]. Thus, Hunter introduced the three dimensional $L^*a^*b^*$ colour space (Fig. 2.28) [218]. The L-axis

represents the lightness and scales from 0 (black) to 100 (white). The a-axis, also known as the red-green axis represents red for positive values and green for negative ones. The b-axis, also called blue-yellow axis illustrates yellow for positive values and blue for negative ones [171, 218].

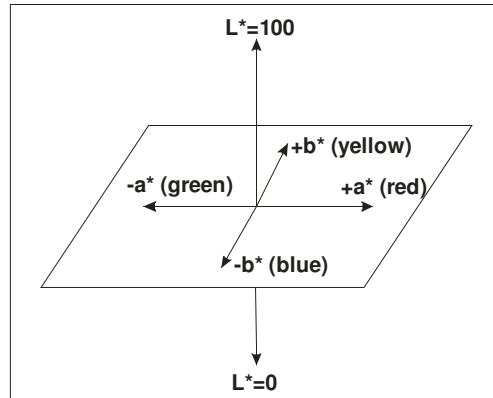


Figure 2.28: Schematic illustration of the $L^*a^*b^*$ space.

Within this system all colours can be plotted. However, the CIE refined the initial Hunter Lab space to the $L^*a^*b^*$ space [219]. The $L^*a^*b^*$ values are calculated from the measured X , Y , and Z values (equation 2.30-2.35) [220]. However, for the transformation a reference white point (n) with the values X_n , Y_n and Z_n is required.

$$X_1 = \frac{X}{X_n} \quad (2.30)$$

$$Y_1 = \frac{Y}{Y_n} \quad (2.31)$$

$$Z_1 = \frac{Z}{Z_n} \quad (2.32)$$

$$L^* = 116Y_1 - 16 \quad (2.33)$$

$$a^* = 500(X_1 - Y_1) \quad (2.34)$$

$$b^* = 200(Y_1 - Z_1) \quad (2.35)$$

In the daily praxis the colour difference between two samples is more interesting than the absolute $L^*a^*b^*$ values [218, 219]. The commonly used value is the total change of colour ΔE^* (equation 2.36) [171, 218, 219].

2. Fundamentals

$$\Delta E^* = \sqrt{(\Delta L^*)^2 + (\Delta a^*)^2 + (\Delta b^*)^2} \quad (2.36)$$

However, the use of ΔE^* is restricted because the same ΔE^* value can be obtained for completely different looking samples. But it is very well suitable for a fast pass/fall decision in industry. For the exact determination of colour differences the individual colorimetric components ΔL^* , Δa^* and Δb^* have to be used.

Chapter 3

Experimentals

3.1 Materials

DSC, microscopy and XRD samples

Triolein (TO, technical grade 60 %), tripalmitin (TP, technical grade 85 %), highly pure TO (≥ 99 %), highly pure TP (≥ 99 %), Lutensit ALB-N (linear Alkyl-Benzene-Sulfonate, technical grade), Lutensol GD70 (non-ionic alkyl polyglucoside, ~ 70 %), Lutensol AO0 (ROH; R = C13H15 oxo alcohol, ≥ 99 %), Lutensol AO3 (RO(CH₂CH₂O)₃H; R = C13C15 oxo alcohol, ≥ 99 %), Lutensol AO7 (RO(CH₂CH₂O)₇H; R = C13C15 oxo alcohol, ≥ 99 %), and Lutensol AO20 (RO(CH₂CH₂O)₂₀H; R = C13C15 oxo alcohol, ≥ 99 %) were received from BASF. Choline hexadecyl sulphate was synthesized by ion exchange of sodium hexadecyl sulphate, choline chloride and choline hydroxide. Sodium hexadecyl sulphate (99 %) was purchased from ALFA AESAR, choline chloride (≥ 98 %) was received from Sigma Aldrich, and choline hydroxide (45 %) was provided from Taminco. Lauryl alcohol (C12-OH, 98+ %) and myristyl alcohol (C14-OH, 97 %) were received from Sigma Aldrich. Chloroform (CHCl₃, 99.0 – 99.4 %) was purchased from Merck and diethylether (100 %) was obtained from VWR.

Solvent Screening and Karl Fischer

Anethole (99 %), α -terpinene (85 %), benzene (≥ 99.7 %), dihydrocarvenone (98 %), γ -valerolactone (99 %), mesitylene (98 %), p-cymene (99 %), tetrahydrothiophene (99 %) and tripalmitin (TP, 85 %) were received from Sigma Aldrich. α -Pinene (≥ 95 %), chloroform (CHCl₃, 99 – 99.4 %), limonene (≥ 94 %), o-xylol (≥ 98 %), pyridine (≥ 99.5), thiophene (≥ 99 %) and triolein (TO, 60 %) were purchased from Merck. 1-Ethyl-2-pyrrolidinone (98 %), menthone (98 %) and 2-penten (98 %) were obtained from Alfa AESAR. Cyclohexane (99.99 %), hexane (99.02 %) and tetrahydrofuran (99.99 %) were purchased from Acros Organics. Vertocitral was received from Symrise GmbH. 2-Methyltetrahydrofuran (2-MTHF, 99 %) and tetrahydrofurfurylalcohol (THFA, 98-100 %) were purchased from PENNAKEM.

Washing tests

The hydrophilic cotton fibres named Wool Galoon Fabric (style: N-500) were purchased from testex. Sudan black B, triolein (TO, 65 %), tripalmitin (TP, 85 %)

oleic acid (94.5 %), ethyl oleate (contains 74.5 % oleic acid), cholesterol (95 %) and cholesteryl palmitate (97 %) were received from Sigma Aldrich. Squalene (99 %) was obtained from Fluka. Culminal MHPC 500PF was gained from Hercules.

Samples for the determination of the Krafft temperature

Betaine (≥ 99 %) were received from Sigma Aldrich (Germany), sodium dodecyl sulphate (SDS, ≥ 99 %), L-lysine monohydrate (≥ 99 %) and trehalose (≥ 99 %) were obtained from Merck (Germany), carnitine (≥ 99 %) was purchased from Alfa Aesar, trimethylamine N-oxide (TMAO, ≥ 99 %) and sodium dodecanoic acid (SDC, ca. 99 %) were received from Fluka (Germany) and L-proline (99.8 %) was obtained from Clabiochem. Ectoine (98.3 %) was received from AppliChem (Germany).

NMR samples

Dodecanoic acid (COOH, 99.6 %) was received from Alfa AESAR, lithium dodecyl sulphate (LiDS, ≥ 99 %) was obtained from AppliChem (Germany), sodium dodecyl sulphate (SDS, ≥ 99 %) and lithium hydroxide (LiOH, 98 %) were purchased from Merck (Germany) and SDC sodium dodecanoic acid (SDC, ≥ 99 %), Caesium hydroxide (CsOH, 50 wt% in H₂O, 99.9%), rubidium hydroxide (RbOH, 50 wt% in H₂O, 99.9%) and octanol were obtained from Sigma Aldrich (Germany). Deuterated water was purchased from Deutero (Kastellaun, Germany) with a purity of 99.95 %.

All chemicals were used as received.

3.2 Methods

3.2.1 Differential Scanning Calorimetry

Differential scanning calorimetry of triolein was performed with a DSC 30 from Mettler Toledo (DSC-1). The tripalmitin samples were measured with a second calorimeter, a Perkin & Elmer DSC 7 (DSC-2). To check the comparability of the results measured on different instruments some of the tripalmitin samples were also measured with DSC-1. For the mixed samples triglyceride/surfactant the technical grade triglycerides were used. About 200 mg samples were weighed in 5 ml tubes and dissolved in about 0.5 ml chloroform. In the case of Lutensit ALB-N, diethylether was chosen as solvent. 2 to 3 drops of solution were transferred to aluminium sample pans and warmed up to 60 °C for at least 1 h in a heating chamber to evaporate the solvent. Afterwards the pans were sealed.

The triolein samples were cooled to -80 °C or -120 °C, depending on the surfactant. The triolein samples were equilibrated for 10 min at the minimum temperature before a scan was initiated. The heating/cooling rate was 5 °C/min or 10 °C/min and the sample was held for 5 min at 120 °C, the maximum temperature. In the case of pure TO, the maximum temperature was 50 °C. Two cycles were recorded for all TO samples.

The tripalmitin samples were cooled to -50 °C and held for 30 min at this temperature. The samples were then heated with a rate of 5 °C/min to 120 °C and equilibrated for further 30 min. Afterwards, the samples were cooled down again to -50 °C with a rate of 5 °C/min. This scanning cycle was performed 3 times.

In each case the reported values of melting enthalpy and melting temperature were determined from the second cycle to ensure that the thermal history was identical for all samples. The transition temperature was evaluated as the peak position of the transition and the corresponding enthalpy was determined by integrating the area under the peak. Both calorimeters were calibrated with indium. The standard deviation of the devices was determined from the results of pure triglyceride measured for at least three times.

3.2.2 Microscopy

For optical investigations of pure TP, a Leitz LINKAM LTS 350 light microscope with crossed polar filters and a temperature-controlled sample stage was used. Due to the very low melting point of TO, only TP was explored optically. Two drops of the samples dissolved in chloroform were placed on a microscope slide. The slide was then heated to 80 °C and held for 30 min at this temperature to evaporate the solvent. Afterwards, the cover slide was placed on the sample which was then cooled down to room temperature. The samples were heated again to 80 °C with 20 °C/min and cooled to 10 °C with 5 °C/min. During the temperature scans pictures were taken with a JVC TK-C1380 COLOR VIDEO Camera.

3.2.3 X-Ray powder diffraction

For XRPD (X-ray powder diffraction) measurements, pure TP and mixtures of 60 wt% TP with 40 wt% Lutensol AO3 and accordingly Lutensol AO7 were weighed into glass vials, melted and stirred. After cooling down to room temperature they were measured with a STOE STADI P powder X-ray diffractometer.

3.2.4 COSMOtherm

Theoretical melting points of TP in binary mixtures with surfactants were calculated by COSMO-RS (Conductor-like Screening Model for realistic solvation) [222]. This approach enables the prediction of the behavior of molecules in a liquid phase by calculating the solid-liquid equilibrium (SLE) (equation 3.1), with the enthalpy of fusion ΔH_{fus} , the activity coefficient of solute in liquid phase $\gamma_{\text{solute}}^{\text{L}}$, the mole fraction of the solute in liquid phase $\chi_{\text{solute}}^{\text{L}}$, the universal gas constant R , the melting temperature T_{m} and the temperature T [223, 224]. The calculations are based on screening charge density, called σ -profiles. These describe the surface charge of the molecule [222]. The considered interactions are the hydrogen bond interaction, the Van der Waals interaction, and a combinatorial term.

3. Experimentals

$$\ln(\gamma_{\text{solute}}^L \chi_{\text{solute}}^L) = \frac{-\Delta H_{\text{fus}}^x}{RT_m} \left(\frac{1}{T} - \frac{1}{T_m} \right) \quad (3.1)$$

With the help of COSMOtherm, COSMO-RS results are translated to thermodynamic values such as the maximum fusion free energy ΔG_{fus}^x for a range of mixtures at different temperatures and ideal conditions (equation 3.2) [225]. Therefore, the melting point and ΔH_{fus}^x of the pure molecule has to be known.

$$\Delta G_{\text{fus}}^x(T) = \Delta H_{\text{fus}}^x \left(\frac{T}{T_m^x} - 1 \right) \quad (3.2)$$

3.2.5 Determination of triglyceride solubility

The solubility of triglyceride was determined visually during the stepwise addition of an increasing amount of triglyceride. After each addition the sample was stirred and checked whether it was still clear. In the case of the tests of molten tripalmitin the samples were heated after each addition of tripalmitin.

3.2.6 Washing test

3.2.6.1 Sample Preparation

For the washing test stripes of standardized hydrophilic cotton fibres with a dimension of 2 cm length and 5 cm width were used. The soil was dyed with 0.5 wt% sudan black B, a lysochromic, fat soluble azo dye with a adsorption maximum at 598 nm (Fig. 3.1.)

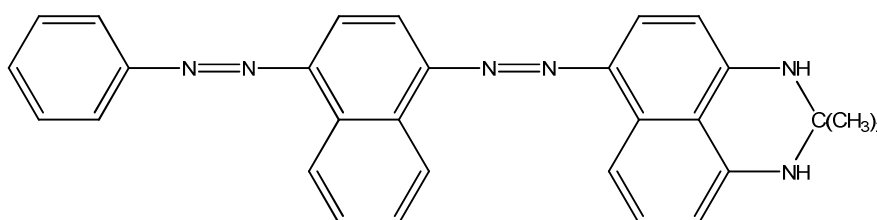


Figure 3.1: Molecular structure of sudan black B.

The stripes were soiled with either standardized soil, a mixture of several fats and oils, triolein, tripalmitin or mixtures of triolein and tripalmitin. The standardized soil has a similar composition like soil secreted from the human body [8]. It contains:

29 wt% triolein (purity = 65 %, Sigma Aldrich), 28.5 wt% oleic acid (purity 94.5 %, Sigma Aldrich), 18.5 wt% ethyl oleate (contains 74.5 % oleic acid, Sigma Aldrich), 14 wt% squalene (purity = 99 %, Fluka), 7 wt% cholesterol (purity = 95 %, Sigma Aldrich), 3 wt% cholesteryl palmitate (purity = 97 %, Sigma Aldrich) [171].

The mixtures of triolein and tripalmitin had a ratio of 3:1, 2:1, 1:1 and 1:3.

The fatty, stained soil was dissolved in chloroform and the stripes were dipped into the solution to gain a homogenous distribution of the soil on the cotton. After drying an uniform soiled cotton stripe with a contamination of about 0.2 g soil per g cotton was obtained. For each combination of soil and washing solution three stripes were prepared.

3.2.6.2 Washing Process

The soiled cotton was placed in a 100 ml beaker filled with 20 ml washing solution and stirred for 10 min. Afterwards, the step was repeated in 20 ml fresh washing solution. The stripe was then placed in a 250 ml beaker with 50 ml distilled water and stirred for further 10 min. This step was repeated for two further times. Subsequent the stripe was hang up to dry.

3.2.6.3 Colorimetric determination

The washing efficiency was controlled by measuring the cotton stripes on the spectrophotometer Elrepho SE 071 from Lorentzen & Wettre in the soiled condition and after washing and drying. The resulting L*(lightness), a*(red/green content), b* (blue/yellow content) values enable the calculation of the total colour change ΔE^* (equation 3.3).

$$\Delta E^* = \sqrt{(\Delta L^*)^2 + (\Delta a^*)^2 + (\Delta b^*)^2} \quad (3.3)$$

3.2.6.4 Conductivity measurements

To distinguish the region of continuous ME from the region of bicontinuous ME the conductivity was measured at 25°C, using pHenomenal PC 5000L of VWR. Depending on the used electrode, this device enables the simultaneous measurement of temperature and either pH or conductivity. The sample was placed in a glass envelope and 0.01 wt% sodium chloride was added. The fluid was stirred during measurement. The sample was diluted progressively with millipore water, using an Eppendorf pipette and the corresponding conductivity κ was recorded. The measurement was finished when the conductivity decreased with the addition of water (Fig. 2.16).

3.2.6.5 Determination of density

In order to determine the viscosity of the washing solutions, initially the density has to be known. Therefore, the density was measured with a vibrating tube densimeter (DMA5000M, Anton Paar, Asutria) according to the method of Kratky et al. [226]. The liquid is filled in U-shaped borosilicate glass and the eigenfrequency τ , which depends on the density of the liquid, is measured. The density is calculated by equation 3.4.

$$\rho = A \times \frac{\tau}{\tau_0} \times f_1 - B \times f_2 \quad (3.4)$$

A and B are calibration constants, τ_0 is the period of a reference oscillator and f_1 and f_2 are correction terms.

3.2.6.6 Determination of viscosity and rheological behaviour

The viscosity of some solutions was determined using a rolling-ball viscometer (AMVn, Anton Paar). The solution was filled in a glass capillary, containing a steel ball of known density ρ_{sb} . The capillary was fixed in a defined angle and the rolling time t of the steel ball was measured. The viscosity of the sample was calculated according to equation 3.5 with K as a temperature and angle dependent calibration constant and ρ_{sample} the density of the fluid.

$$\eta = K \times (\rho_{sb} - \rho_{sample}) \times t \quad (3.5)$$

The viscosity and rheological behaviour of the thickened solutions was determined on CVO 120 high resolution rheometer of Bohlin Instruments, a cone-plate rheometer. The space between cone and plate is filled with 5 ml fluid, which gets sheared with constant shear velocity by the rotation of the cone, yielding a constant shear stress τ in the sample. It can be calculated from the measured angular velocity ω , the torsional moment M of the tongue and the radius r_0 of the cone (equation 3.6). For a known shear stress the viscosity η can be calculated by equation 3.7, with the gradient angle α of the cone [227, 228].

$$\tau = \frac{3M}{2\pi r_0^3} \quad (3.6)$$

$$\tau = \eta \frac{\omega}{\alpha} \quad (3.7)$$

However, to classify the fluid, the viscosity was determined for varying shear velocity (5 rps to 500 rps). For a Newtonian Fluid the shear stress increases linear with increasing shear velocity, resulting in a constant viscosity with increasing shear stress [227, 229].

3.2.7 Krafft temperature determination

3.2.7.1 Sample Preparation

Each sample contains an additive and a surfactant. The surfactant is either sodium dodecyl carboxylate (SDC) or sodium dodecylsulphate (SDS). The used additives are carnitine, betaine, lysine, proline, trimethylamine oxide (TMAO) and trehalose. Stock solutions of 1 wt% surfactant in ultra pure water were prepared. That is consistent with 0.045 mol/L SDC, 0.035 mol/L SDS, respectively. The pH of the solutions was determined as pH = 9 for SDC and pH = 8 for SDS. The stock solution was placed in a tube and the required amount of osmolyte was added. The concentration of osmolyte in the surfactant solution reaches from 0 mol/L to 1.5 mol/L. 16 mixtures of osmolyte/surfactant were prepared for each osmolyte. The samples were stirred and heated up to 60 °C for at least 30 min.

3. Experimentals

3.2.7.2 Determination of the solubility temperature

The measurements of the solubility temperature, the temperature at which the solutions become absolutely clear and isotropic, of the samples with SDC were performed using a home-made device [230]. The detected data is the amount of transmitted laser light. When the solution becomes clear the transmission increases. The solubility temperature, of the samples with SDS was determined by direct visual observation. For both methods the mixtures were cooled to about -5 to -15 °C. All samples were turbid after cooling. Afterwards, they were reheated with a rate of 5 °C per h.

3.2.8 Nuclear Molecular Resonance

^{23}Na -, ^7Li -, ^{87}Rb - and ^{137}Cs -NMR measurements were performed using a Bruker Avance 400 spectrometer working with a 30 ° pulse. The operating parameters are summarized in table 3.1.

Table 3.1: Operating parameter for measuring the quadrupole nuclei.

<i>Nucleus</i>	<i>Frequency</i>	<i>Pulse length</i>
^{23}Na	105.84 MHz	8.70 μs
^7Li	155.51 MHz	7.10 μs
^{87}Rb	130.39 MHz	7.00 μs
^{137}Cs	52.48 MHz	10.90 μs

The number of scans varied for ^{23}Na and ^7Li spectra from 128 to 1024, but most of the spectra were collected with 512 scans. The ^{87}Rb and ^{137}Cs spectra were all collected with 1024 scans.

^{23}Na and ^7Li were measured in samples of liquid crystals formed by dodecyl sulphate or rather dodecyl carboxylate surfactants, whereas ^{87}Rb and ^{137}Cs were only measured in samples of liquid crystals formed by dodecyl carboxylate surfactants.

The measurements with the sulphate SDS, LiDS as well as the measurements of RbDC and CsDC were performed at 300 K. However, the measurements of the carboxylate SDC and LiDC were performed at 300 K and at 310 K. The temperature

range for the measurements of SDC and LiDC was selected so small in order to ensure liquid crystals are present.

Each sample (3g) was prepared in a tube, heated to 60 °C and mixed with a magnetic stirrer for at least one week. Afterwards, about 700 - 800 mg are transferred in a NMR tube (5 mm o.d.).

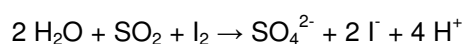
Each sample contains D₂O, octanol and surfactant. The surfactants are either carboxylate surfactants (SDC, LiDC, RbDC and CsDC) or sulphate surfactants (SDS and LiDS). LiDC, RbDC and CsDC were prepared in situ by mixing dodecanoic acid and the corresponding alkali metal hydroxide.

The molar ratio of the sodium surfactant to lithium surfactant varies from 0 to 100 % sodium surfactant in 20 % steps. In each sample the molar ratio of SDS + LiDS to octanol was 1:1, and due to the lower solubility of carboxylates in water, the molar ratio of SDC+LiDC to octanol was reduced to 1:3. The concentrations of SDS+LiDS+octanol and SDC+LiDC+octanol in D₂O were 35 wt% to 75 wt% in 10 wt% steps.

The molar ratio of CsDC and RbDC varies from 0 to 100 % caesium surfactant in 20 % steps. In each sample the molar ratio of surfactant/octanol was 1:3. The concentrations of surfactant+octanol in D₂O are 45 wt% to 85 wt% in 10 wt% steps. In order to identify the lamellar phase, the samples were observed visually via crossed polar filters. All the samples appeared as single phases with typical lamellar textures [107].

3.2.9 Karl Fischer titration

The Karl Fischer titration is a method to determine the water content. The technique is based on the reaction of sulphur dioxide with iodine which works only in the presence of water.



In principle, there are two methods which are based on the Karl Fischer titration. These two methods are the volumetric titration and the coulometric titration. The required iodine is generated by electrolytic oxidation on the anode from iodide in

3. Experimentals

the Karl Fischer reagent. The formed iodine reacts with the water and sulphur dioxide. At the end of the process excess iodine can be detected electrically. The amount of generated iodine is in proportion to the quantity of electricity. The water content is determined by the amount of the required electricity to the point where excess iodine is produced [231].

The determinations performed within this work were done by coulometric titration at a CA-02 from Mitsubishi Chemical ind Ltd. The water content of fresh 2-MTHF, o-Xylol and CHCl_3 and after storage over water under stirring for 16 h was determined.

Chapter 4

Results and Discussion

4.1 Investigation of triglycerides and binary mixtures with surfactants

4.1.1 Introduction

The washing active agents in detergents are the surfactants. They interact with the soil and the fiber surface, changing the interfacial tensions and resulting in soil release. And as mentioned above the soil release mechanism depends on the state of soil matter [11]. Typically the liquid soil release by the roll-up mechanism is faster and more efficient than solid soil removal. Consequently, the liquefaction of the soil increases the efficiency [232]. Investigations by Venkatesh et al. have shown that the main components of usual household laundry soil are fatty substances [8]. Therefore, the particulate soils are mainly solid triglycerides. An obvious way to liquefy the triglycerides is the increase of the temperature above the melting point. However, to save energy and to wash cloth with care, low washing temperatures are desired. And daily practice shows that it is possible to wash successfully triglycerides at temperatures below the melting point. Accordingly, the solid triglyceride might be liquefied by the interaction with surfactant. To proof the assumption, binary mixtures of triglycerides and surfactants were investigated without the addition of water, even though the concentration of the surfactants in the washing liquor is only about 0.1 wt%. But, locally the concentration of the surfactant is supposed to be far higher. It may accumulate at the soil surface.

The investigated triglycerides were triolein and tripalmitin. Both triglycerides are main components of household laundry soil and representative for the two states of soil matter [233]. The fatty acids of the liquid triolein are unsaturated (oleic acid) and the fatty acids of solid tripalmitin are saturated (palmitic acid). The explored surfactants were either ionic or non-ionic. For the nonionic alcohol surfactants, Lutensol AOx, the influence of the degree of ethoxylation was investigated. The used techniques were microscopy, DSC, XRD and COSMO-RS calculations.

4.1.2 Results

4.1.2.1 Microscopy

As mentioned above and known from literature triglycerides are polymorphic [84]. The three main polymorphs of triglycerides with three identical fatty acids are α , β' and β [66]. They are characterized by the subcell and chain length structure and were named by Larsson [234]. The α and β polymorphs show textures under polarizing optical microscope. During the crystallization usually the three polymorphs occur in the sequential stability of α , β' to β [66]. During heating the α to β transformation takes place. Depending on the chain length of the fatty acids the α structure transforms to the β polymorph with or without melting and recrystallization. For long fatty acids (C18) the stability of the α -form is higher than for shorter ones and the transition will occur via melting [235].

TP samples were investigated under a light microscope with crossed polarisation filters (Fig. 4.1). The sample was heated and cooled with 5 °C/min from 10 °C to 120 °C. At 10 °C the sample was anisotropic. At a temperature of 40 °C the sample became isotropic, due to the melting of the α -form. The triglyceride remained isotropic up to 50 °C. At this temperature the triglyceride started to recrystallize and was anisotropic until 60 °C. At temperatures above 60 °C TP was completely molten and isotropic.

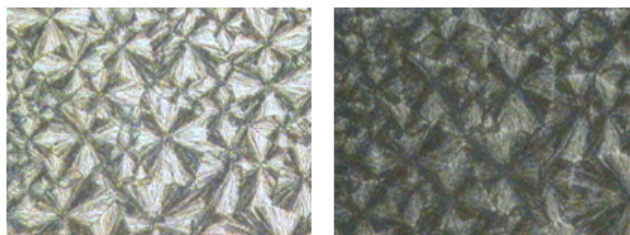


Figure 4.1: Microscopy picture of 100 wt% technical grade TP at 25 °C (left) and 52 °C (right) under polarizing optical microscope.

4.1.2.2 DSC

Investigation of pure triglyceride

Several groups investigated the polymorphism of triglycerides by DSC before [90, 236]. They found multiple transitions upon first heating [90]. The number of transitions and the reproducibility in further cycles depends strongly on the

4. Results and Discussion

heating rate (in addition to the thermal sample history). The samples investigated within this thesis were heated and cooled for three times. For highly pure TP, technical grade TP and 1:1 mixture of both an exothermic transition between two endothermic ones was observed (Fig. 4.2). These observations are in good accordance to the observation at the polarizing optical microscope. The exothermic transition results from the recrystallization after the melting of the α -form. The melting of α - and β -polymorph is endothermic. In the cooling period of the tripalmitin samples only the crystallization of the triglyceride into the kinetically preferred α polymorph occurred.

For highly pure and technical grade triolein similar polymorph transitions were observed (Fig. 4.2). However, for technical grade TO only upon the first heating the multiple transitions were observed. This difference might result from the lower starting temperature for highly pure TO. In the cooling curves, either one or two crystallizations peaks occur depending on the purity of the triglyceride. For the highly pure triolein only one crystallization peak is observed whereas the technical grade one shows two exothermic peaks upon cooling.

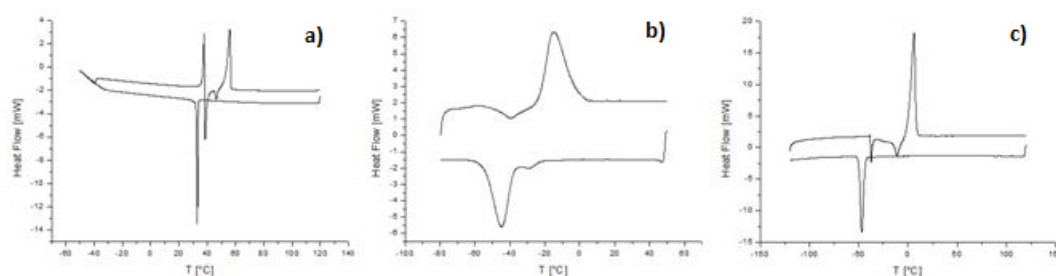


Figure 4.2: (a) Second cycle of DSC measurement of 100 wt% technical grade TP. (b) First cycle of DSC measurement of 100 wt% technical grade TO. (c) Second cycle of DSC measurement of 100 wt% highly pure TO.

Beside the qualitative analysis of polymorphism by microscopy and DSC the melting and crystallization were also evaluated quantitatively by DSC. The melting temperature of pure TP samples was determined to be 58.1 °C, which is comparable to the value found in the literature [237]. The melting enthalpy values found in literature reach from 158.7 J/g to 222.0 J/g [90, 237]. The measured melting enthalpy of pure technical grade TP was 158.8 J/g. The determined standard deviations of melting and crystallization temperature and of corresponding enthalpies are given in table 4.1. The transition temperatures and enthalpies of highly pure TP and 1:1 mixture of technical grade and highly pure TP are within the standard deviation (Tab. 4.1). Accordingly, the impurities in the technical grade TP

have only a slight influence on the melting temperature and the transition enthalpies of tripalmitin.

Table 4.1: Influence of impurities in technical grade TP on the melting/crystallization points and on the melting and crystallization enthalpies.

	Highly pure TP		1:1		Technical grade TP	
Melting	<i>Onset [°C]</i>	56.5	<i>Onset [°C]</i>	54.9	<i>Onset [°C]</i>	53.1 ± 0.6
	<i>Peak [°C]</i>	58.1	<i>Peak [°C]</i>	57.1	<i>Peak [°C]</i>	56.0
	<i>Enthalpy [J/g]</i>	174.0	<i>Enthalpy [J/g]</i>	170.7	<i>Enthalpy [J/g]</i>	158.8 ± 14.2
Crystallization	<i>Onset [°C]</i>	34.4	<i>Onset [°C]</i>	34.2	<i>Onset [°C]</i>	33.9 ± 0.1
	<i>Peak [°C]</i>	33.3	<i>Peak [°C]</i>	33.3	<i>Peak [°C]</i>	33.0
	<i>Enthalpy [J/g]</i>	-108.5	<i>Enthalpy [J/g]</i>	-117.5	<i>Enthalpy [J/g]</i>	-115.3 ± 13.7

The determined melting temperature of highly pure TO was 7.08 °C and the corresponding enthalpy was 109.47 J/g. The evaluated standard deviations are given in table 4.2. The melting temperature and enthalpy measured for technical grade TO are not within the standard deviation. The impurities in technical grade TO have an great influence on the melting/crystallization behaviour of the triglyceride.

Table 4.2: Influence of the impurities in technical grade TO on the melting/crystallization points and on the melting and crystallization enthalpies.

	Highly pure TO		Technical grade TO	
Melting	<i>Onset [°C]</i>	1.8 ± 1.5	<i>Onset [°C]</i>	-23.8
	<i>Peak [°C]</i>	7.1	<i>Peak [°C]</i>	-12.1
	<i>Enthalpy [J/g]</i>	109.5 ± 3.6	<i>Enthalpy [J/g]</i>	69.7
Crystallization	<i>Onset [°C]</i>	-43.7	<i>Onset [°C]</i>	-38.0
	<i>Peak [°C]</i>	-46.9	<i>Peak [°C]</i>	-60.7
	<i>Enthalpy [J/g]</i>	-58.6	<i>Enthalpy [J/g]</i>	-46.0

Investigation of mixtures triglyceride/Lutensit ALB-N

Lutensit ALB-N is a linear alkyl benzyl sulfonate and a commercially widely used anionic surfactant (Fig. 4.3). At room temperature the surfactant is a slight

4. Results and Discussion

yellowish, granular powder. DSC measurements of pure Lutensit ALB-N have shown no phase transition in the temperature range from -150 °C to 120 °C.

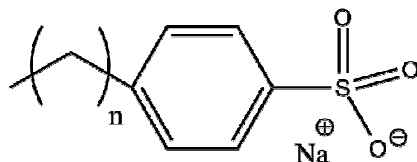


Figure 4.3: Structure of Lutensit ALB-N. n varies from 9-11.

The addition of varying amounts Lutensit ALB-N to technical grade TO seemed to retard the crystallization but had no influence on the polymorphism of the triglyceride. Also the melting point of TO was not influenced. The heating curves for the mixtures were the same like for pure TO. Hence, the surfactant does not interact with triolein and no mixed crystals are formed. Due to the low melting and crystallization points a quantitative analysis of the DSC curves was not possible.

Similar conclusions can be drawn from the DSC results gained for the mixtures Lutensit ALB-N with technical grade TP. Independently on the surfactant content in the mixture, the melting temperature and enthalpy of tripalmitin stayed constant. Also the polymorphism of tripalmitin was not influenced by the added surfactant. Lutensit has no impact on the melting behaviour of either triolein or tripalmitin.

Investigation of mixtures triglyceride/choline hexadecyl sulphate

Choline hexadecyl sulphate is an ionic surfactant (Fig. 4.4). At room temperature it appears as a white powder with a high affinity to water. The melting point is at temperatures above 120 °C. In the temperature range from -50 °C to 120 °C a solid to solid, a solid to semi crystalline and a semi-crystalline to lamellar transition is observed [238].

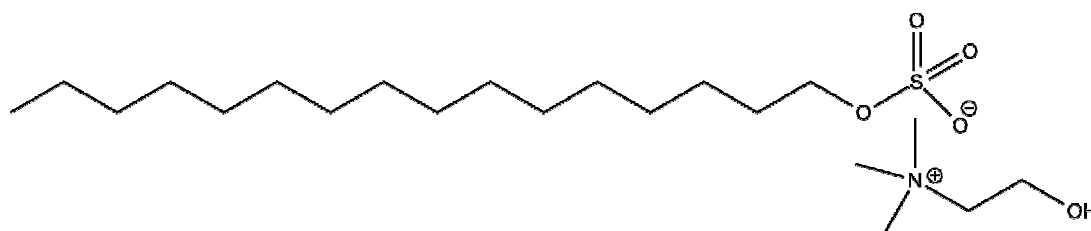


Figure 4.4: Structure of choline hexadecyl sulphate.

The addition of this surfactant to TP, similar as Lutensit ALB-N, also has no influence, neither on the melting point nor on the melting enthalpy of TP. Potentially, it has an impact on the polymorphism of TP. However, this cannot be stated with certainty, because the transition temperatures of surfactant and TP are

very similar. If any, interactions between choline hexadecyl sulphate and TP are very small in the binary mixtures. Similarly, we did not observe any influence of this surfactant on TO.

Investigation of mixtures triglycerides/Lutensol GD70

Lutensol GD70 is a commercial nonionic polyglycoside surfactant (Fig. 4.5). At room temperature it appears as a yellow honey-like liquid. The melting point is $-42\text{ }^{\circ}\text{C}$, but the onset of the transition is already at $-68.73\text{ }^{\circ}\text{C}$. The transition points of TO are in a similar temperature range. Hence, it is not possible to differentiate between TO and the Lutensol GD70 signals in DSC.

The investigation of mixtures Lutensol GD70 with TP showed that the presence of TP hindered the crystallisation of Lutensol GD70. Therefore, no signals of GD70 appear in the curves. The heating scans of the mixtures are very similar to the DSC curves of pure TP. The melting temperature of TP did not change either. We conclude that there is no significant interaction between TP and the surfactant in their binary mixtures.

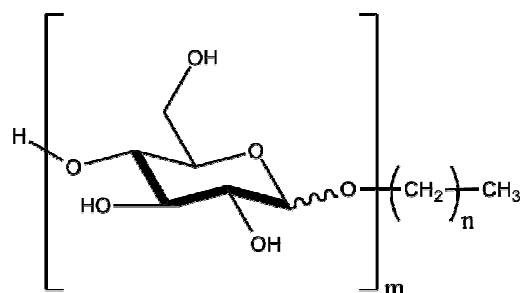


Figure 4.5: Structure of Lutensol GD70. n varies from 11-15 and m varies from 1-5.

Investigation mixtures triglyceride/Lutensol AOx

Lutensol AOx are nonionic ethoxylated C13/C15 alcohols with the structural formula $\text{RO}(\text{CH}_2\text{CH}_2\text{O})_x\text{H}$. The average degree of ethoxylation is given by x . In the present study, the investigated surfactants were Lutensol AO0, Lutensol AO3, Lutensol AO7 and Lutensol AO20. Except of Lutensol AO20, a yellowish solid, all surfactants appear liquid at room temperature. Lutensol AO3 and Lutensol AO7 are turbid liquids at room temperature and become clear upon heating. Lutensol AO0 is already clear at room temperature.

The determined melting point of pure Lutensol AO0 is $9.00\text{ }^{\circ}\text{C}$, of pure Lutensol AO3 is $-4.43\text{ }^{\circ}\text{C}$, that of pure Lutensol AO7 is $14.77\text{ }^{\circ}\text{C}$ and that of pure Lutensol AO20 is $29.77\text{ }^{\circ}\text{C}$. The impact of Lutensol AO0, AO3 and AO7 on the melting point of TP is comparable. In contrast, Lutensol AO20 sticks out. It has nearly no influence on the melting temperature of triglyceride. This might be due to the

4. Results and Discussion

insolubility of TP in AO20 also at temperatures above the melting point of TP, whereas AO0, AO3 and AO7 give a homogeneous solution with molten TP. Up to a Lutensol AOx:TP molar ratio of ~ 0.5 , all studied AOx species with less than 20 EO groups yield similar melting point reductions of TP, as would be expected for purely colligative behaviour (Fig. 4.6). For molar ratios above 0.5, it seems that the lower the degree of ethoxylation, the higher is the influence of the surfactant on the melting temperature at comparable molar ratios. Hence, in molar excess, Lutensol AO0 induces the strongest and Lutensol AO7 the lowest reduction of the melting temperature of TP. But the absolute influence of the degree of ethoxylation on the melting point is small, given that the surfactant and TP are miscible in the liquid state. For all surfactants Lutensol AOx, a very high amount of surfactant is required to reduce the melting point markedly. For the washing process this effect can be expected to be negligible, even assuming a potential enrichment in the soil from a diluted washing liquor. A reduction below room temperature seems to be illusive.

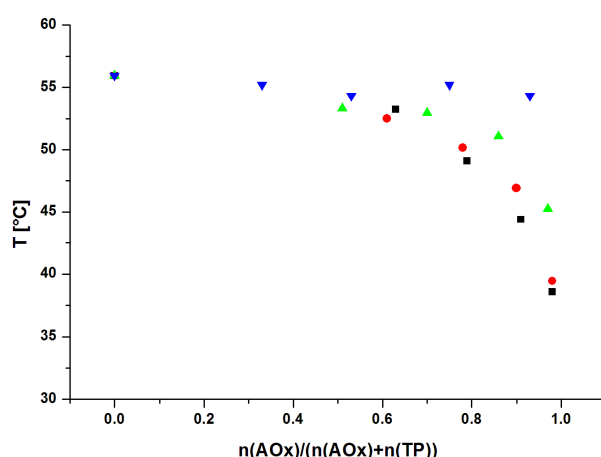


Figure 4.6: The influence of the degree of ethoxylation of Lutensol AOx on the melting point of TP. ■: AO0; ●: AO3; ▲: AO7; ▼: AO20. The x-axis shows an increasing surfactant molar fraction.

The interaction of surfactant with TP could potentially also result in the generation of mixed crystals, which would be detectable in the DSC curves. The cooling DSC curves of mixtures of TP with Lutensol AOx show two crystallization peaks for TP (Fig. 4.7). The second detected peak might result from a mixed crystal, built up from TP and AO3. The samples show no polymorphism of TP upon heating (Fig. 4.7).

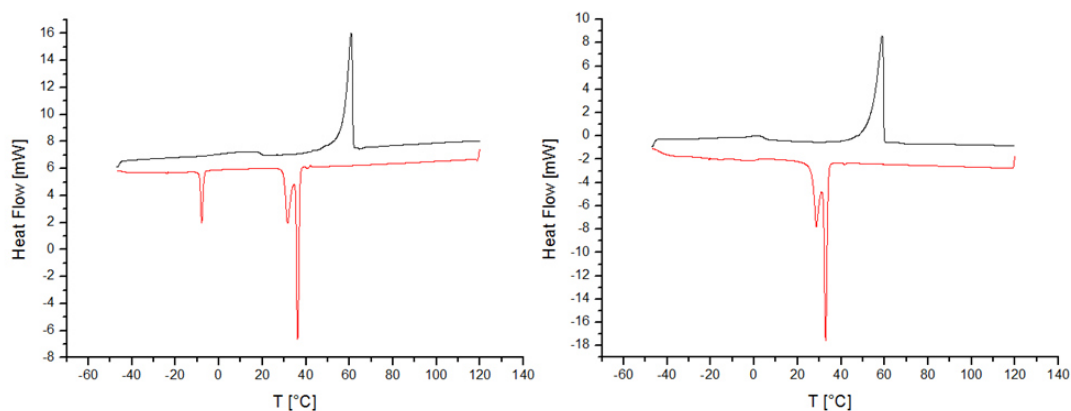


Figure 4.7: DSC curves of 60 wt% TP/40 wt% AO7 (left) and 60 wt% TP/40 wt% AO3 (right).

4.1.2.3 COSMO-RS

COSMO-RS enables the calculation of the theoretical melting point for binary mixtures (Fig. 4.8). The results of the COSMO $therm$ calculations are in good accordance to the experimental results. Also the distinct behaviour of Lutensol AO20 is predicted by COSMO-RS. The calculated data confirm the lower influence of the degree of ethoxylation of Lutensol AO x and the lower melting point reduction also for very high surfactant concentrations.

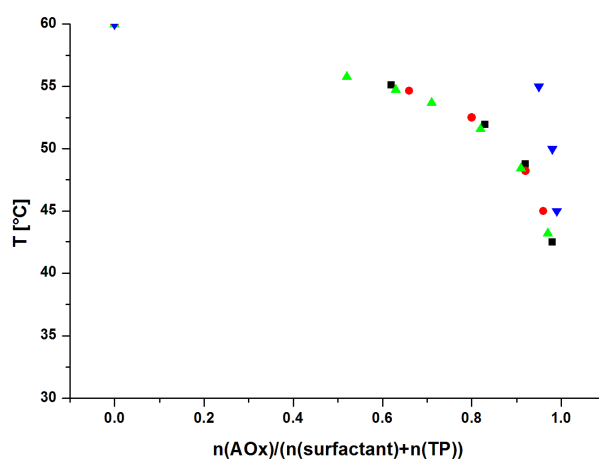


Figure 4.8: COSMO $therm$ calculation of the theoretical melting point of TP after the addition of different surfactants. ■: C13-OH; ●: C15-OH; ▲: AO7; ▼: AO20. The x-axis shows an increasing molar fraction of surfactant.

4.1.2.4 X-Ray powder diffraction

To analyse the possible existence of mixed crystals of TP/AO3 and TP/AO7 respectively, powder diffractograms of the mixtures and the pure TP were measured. The results at 298.15 K are shown in figure 4.9 and figure 4.10.

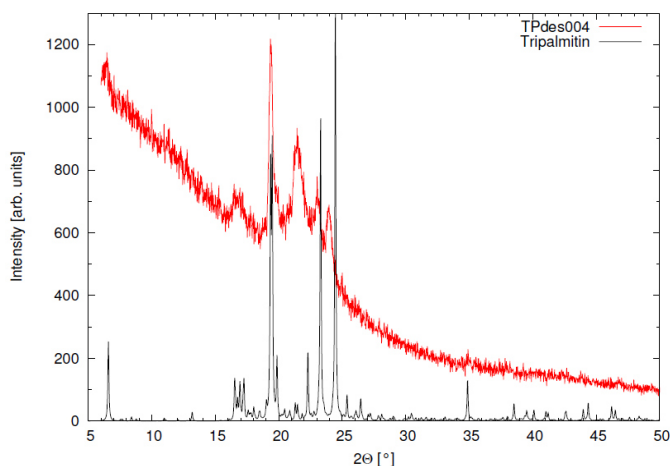


Figure 4.9: Experimental powder diffractogram of pure TP at 298.15 K (red) and from single crystal data calculated diffractogram (black).

The experimental powder diffractograms of the mixtures look very similar to the calculated diffraction pattern based on single crystal data of β -TP. In contrast, the diffractogram of pure TP differs from the calculated one. Probably, in the pure TP in native state a mixture of β' -TP and β -TP coexists.

In contrast, powder diffractograms of the mixtures of TP with Lutensol AO3 and AO7 show that the addition of surfactant promotes complete crystallization of TP in the β -morphology, but no hint at mixed crystals between surfactants and fat can be found.

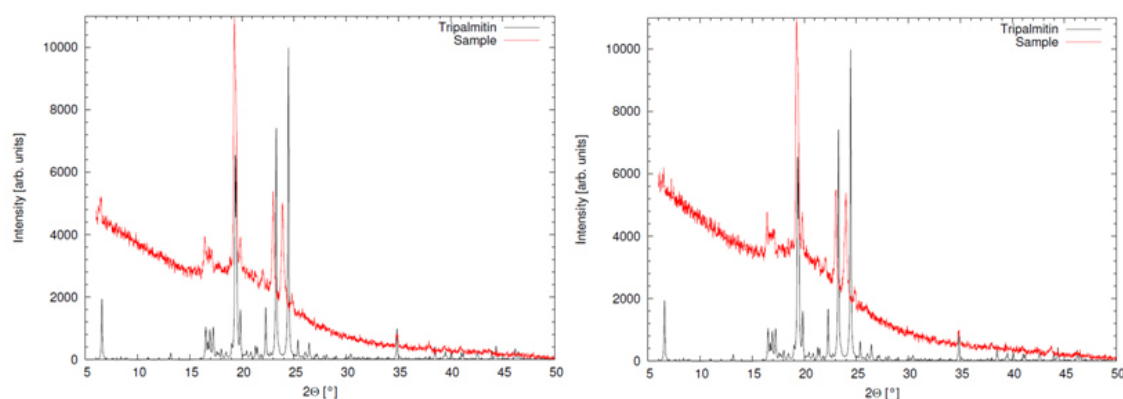


Figure 4.10: Experimental powder diffractogram of 40 wt% TP/60 wt%AO7 (left) and 40 wt% TP/60wt% AO3 (right) at 298.15 K (red) and from single crystal data calculated diffractogram of pure TP (black).

4.1.3 Conclusion

The investigation of the interaction between the triglycerides with ionic surfactants shows that these surfactants neither have a significant influence on the melting point nor on the melting enthalpy of the triglyceride. All detergency found for such surfactants for greasy soils in a washing liquor obviously is only based on their classical surfactant action, i.e. their amphiphilicity and the interactions at the water/grease interface.

The investigation of nonionic surfactants, represented by different Lutensols AOx, shows a noticeable but limited reduction of the melting point of TP in some cases. It turns out that the miscibility in the liquid state is a prerequisite for any melting point depression. Miscibility is given for AOx as long as the ethoxylation degree is low enough. In summary, the influence of the surfactants on the melting point of TP is marginal and requires very high amounts of surfactants. Again, any detergency of nonionic surfactants seems to be exclusively related to their interfacial activity in the presence of water and does not involve liquefaction of crystalline domains.

From the investigation of the binary mixtures of surfactants and triglycerides, the liquefaction of triglycerides with surfactants at room temperature seems utopian today. A further promising approach might be the investigation of solubilisation of triglycerides by solvents.

4.2 Solubilisation of triglycerides in organic solvents

4.2.1 Introduction

The removal of solid soil at low temperatures is a challenge. As mentioned above, solid triglycerides are not liquefied during the washing process by surfactants. Therefore, the success of soil release might result from the solubilisation of the triglycerides. The investigation of the binary mixtures of surfactant and triglyceride showed that the selected surfactants do not solubilise tripalmitin. Hence, solubilisation might result from surfactants with another chemical structure or from further ingredients in detergents. To determine the impact of triglyceride solubilisation on soil release several organic solvents were investigated regarding their tripalmitin solubilisation power. In addition, different models to predict the solubility were used. Experimental and theoretical results were compared and to affirm the results and conclusions the solubility of the liquid triolein was investigated in these too. The used theoretical methods are Hansen solubility parameters and COSMO-RS calculations.

However, these examinations do not consider the presence of water. The so far investigated systems were binary mixtures of triglyceride and solvent. But in the washing process a quite high amount of water is present. Therefore, the influence of water on the solubilisation properties of the solvents with the highest TP solvation power was determined.

4.2.2 Results

4.2.2.1 Hansen Solubility Parameters

For the description of the interaction between solutes and solvents Hildebrandt introduced the solubility parameter δ [95, 163]. This concept was extended by Hansen to the three dimensional solubility parameter model [162, 168-170]. Hansen considers that there are several contributions to the energy of evaporation. The solubility parameter is divided into the energy densities of the dispersion part, δ_D , the polar part, δ_P , and the hydrogen bond part, δ_H . Simplified, neglecting the interaction radius, R_0 , the more alike the parameters of solvent and solute the higher the solubility. This model is very suitable for the qualitative comparison of

different solvents in a special application and is commonly used in the polymer research.

The DSC samples were prepared using chloroform as solvent. The solubility limit of tripalmitin in CHCl_3 is about 22 wt%. The Hansen parameters of tripalmitin and chloroform, calculated by increments are given in table 4.3. The R_a value of a mixture of TP with chloroform is $3.15 \text{ (J/cm}^3\text{)}^{1/2}$. Solvents which give a similar R_a -value are supposed to solubilise TP in a comparable magnitude. Hence, potentially appropriate solvents of different solvent classes were tested to check the validity of Hansen concept experimentally (Tab. A1 and Tab. A2).

Table 4.3: Hansen solubility parameters and R_a value for tripalmitin and chloroform calculated from increments.

	TP	CHCl₃
$\delta_D \text{ [MPa}^{1/2}\text{]}$	16.70	17.8
$\delta_P \text{ [MPa}^{1/2}\text{]}$	0.98	3.1
$\delta_H \text{ [MPa}^{1/2}\text{]}$	4.94	5.7
$R_a \text{ [(J/cm}^3\text{)}^{1/2}\text{]}$	3.15	

Classical Alcohols

All investigated alcohols have one hydroxyl group and are aliphatic (Tab. 4.4). They differ in the alkyl chain length. With the exception of dodecanol and tetradecanol, which have melting points at 24 °C and 38 °C, respectively, the melting point of the solvents is distinctively below room temperature.

Table 4.4: Calculated R_a values for mixtures of tripalmitin and classical alcohols and examined solubility limits at room temperature.

Solvent	R_a value [(J/cm³)^{1/2}]	Molecular weight [g/mol]	wt% TP
Methanol	20.22	32.04	<1
Ethanol	15.76	46.07	<1
2-Propanol	12.94	60.10	<1
Butanol	11.09	74.12	<1
Hexanol	8.57	102.18	<1
Octanol	6.94	130.23	<1
Nonanol	6.31	144.26	<1

4. Results and Discussion

Decanol	5.78	158.28	<1
Dodecanol	4.71	186.34	<1
Tetradecanol	4.02	214.39	<1

With increasing chain length the δ_D value increases slightly (14.48 MPa^{1/2} for methanol, 16.38 MPa^{1/2} for tetradecanol) and the δ_P and δ_H values decrease considerably (δ_P : 11.49 MPa^{1/2} for methanol, 1.98 MPa^{1/2} for tetradecanol; δ_H : 21.63 MPa^{1/2} for methanol, 8.78 MPa^{1/2} for tetradecanol). By elongating the alkyl chain of the alcohol the δ values approximate to the Hansen parameter of tripalmitin, resulting in a decreasing R_a value. Based on the R_a values, an increasing solubilisation power with increasing alkyl chain length is supposed. However, none of the alcohols dissolves at least 1 wt% tripalmitin at room temperature or at 30 °C. They are unsuitable solvents for solid triglycerides. The fact that dodecanol and tetradecanol, the only solvents with a comparable R_a value to chloroform, are also poor solvents gives a hint on the importance of low solvent melting temperature.

Linear and branched alkanes

The chosen alkanes are liquid at room temperature and linear except of isooctane (Tab. 4.5). Independently of chain length and branching, the δ_P and δ_H values are zero for all alkanes. With increasing chain length the δ_D value increases (14.31 MPa^{1/2} for pentane, 15.32 MPa^{1/2} for dodecane), approaching the value of tripalmitin and resulting in a decreased R_a value. Comparing the R_a values of octane and isooctane gives, that branching reduces the tripalmitin solubilisation power of solvents.

Except of dodecane the R_a values for the alkanes are smaller than for the comparable alcohols. Hence, they are supposed to dissolve more TP than alcohols. While also none of the alkanes dissolve at least 1 wt% TP at room temperature, pentane, hexane and octane do dissolve at least 1 wt% TP at 30 °C. So far, the trend of experimental results and R_a values are in good agreement.

Table 4.5: Calculated R_a values for mixtures of tripalmitin and alkanes and examined solubility limits at room temperature.

Solvent	R_a value [[J/cm³]^{1/2}]	Molecular weight [g/mol]	wt% TP
Pentane	6.94	72.5	<1
Hexane	6.54	86.18	<1

Isooctane	6.59	114.23	<1
Octane	6.04	114.23	<1
Dodecane	5.74	170.34	<1

Dowanols

Dowanols are glycol ether, gained from Dow Chemicals. The chemical structures are given in the supplementary. Except of PMA (Propyleneglykolmethylether acetate), the dowanols are alcohols. All dowanols are liquid at room temperature. PM (Monopropylenglykolmonomethylether), DPM (Dipropylenglykolmonomethylether) and TPM (Tripropylenglykolmonomethylether) vary in the number of propylene groups. These three solvents contain an ethyl ether. This ether is replaced by a propyl ether in DPnP (Dipropylene Glycol n-Propyl Ether). Apart from that, DPnP has the same structure like DPM. PMA is comparable to PM, only the alcohol group in PM is replaced by an acetate. The chemical structure is given in supplementary.

With increasing number of propylene groups the δ values decrease whereat δ_D departs from TP value and δ_P and δ_H approach. For DPM the δ values are most alike to the tripalmitin ones. The elongation of ethyl ether to propyl ether reduces all δ values, but affects mainly the δ_H value and results in a decreased R_a value. The replacement of the alcohol group by an acetate results in an increased δ_D value and reduced δ_P and δ_H values and the lowest R_a value for this series of Dowanols. Hence, PMA might be the Dowanol with the highest tripalmitin solubilisation power. However, based on the previous results, none of the investigated Dowanols are supposed to and do dissolve at least 1 wt% TP at 30 °C (Tab. 4.6).

Table 4.6: Calculated R_a values for mixtures of tripalmitin and dowanols and examined solubility limits at room temperature. The Hansen solubility parameters of the dowanols are taken from the technical data sheet of Dow Chemicals [239].

<i>Solvent</i>	δ_D [MPa ^{1/2}]	δ_H [MPa ^{1/2}]	δ_P [MPa ^{1/2}]	R_a value [(J/cm ³) ^{1/2}]	<i>Molecular weight</i> [g/mol]	<i>wt% TP</i>
PM	15.60	7.20	13.60	10.89	90.1	<1
TPM	15.10	3.50	11.50	7.72	206.3	<1
DPM	15.50	4.00	11.50	7.61	148.2	<1
DPnP	15.00	3.00	9.60	6.11	176.2	<1
PMA	16.10	6.10	6.60	5.51	132.2	<1

4. Results and Discussion

Terpene and natural oils

In order to find natural and cheap solvents we calculated the R_a value for various terpenes and natural oils (Tab. 4.7). The solubility of tripalmitin was tested in 14 of these solvents. The investigated solvents were chosen due to their different R_a values and their comparable chemical structure. All solvents are cyclic, some are aromatic and have functional groups. They differ in the number of side chains and in the steric configuration. The chemical structures of the solvents are given in the supplementary. This assortment of solvents improves the understanding of the relationship between solvent structure and tripalmitin solubilisation power.

Table 4.7: Calculated R_a value and molecular weight of various terpene and natural oils and experimentally determined solubility of tripalmitin, sorted for decreasing R_a value.

Solvent	R_a value [[J/cm³]^{1/2}]	Molecular weight [g/mol]	wt% TP
Ethyllaurate	1.69	228.37	/
Ethyldecanoate	1.95	200.32	/
Anethole	2.17	148.20	2±0.5
Ethyl octanoate	2.38	172.26	/
1,8-Cineol	2.77	154.25	/
Ethylpentanoate	3.51	130.19	/
Citral	3.60	152.23	/
D-Dihydrocarvone	3.79	152.23	<1
Carvone	4.08	150.22	/
Menthone	4.11	154.25	1.5±0.5
2-Methyl THF	4.69	86.13	9±0.5
o-Xylol	4.98	106.17	8.2±0.5
Limonene	5.05	136.24	2.2±0.5
p-Cymene	5.05	134.21	3.5±0.5
Vertocitral	5.14	138.21	1.5±0.5
a-Terpinene	5.26	136.24	2.5±0.5
Mesitylene	5.38	120.19	7.5±0.5
α-Pinene	5.74	136.24	1.5±0.5
γ-Decanolactone	5.98	170.25	/
Geraniol	6.04	154.25	/

Citronellol	6.22	156.27	/
Citronellal	6.38	154.25	/
Menthol	6.42	156.27	/
3,7-Dimethyl-6-oxoctanal	7.78	170.25	/
Pivaldehyd	9.07	86.13	/
Tetrahydrofurfuryl alcohol	10.93	102.13	<1
γ -Valerolactone	12.03	100.12	<1
1-Ethyl-2-pyrrolidinone	12.65	113.16	<1

Except of 1-ethyl-2-pyrrolidinone, γ -valerolactone, tetrahydrofurfuryl alcohol and dihydrocarvone all tested solvents dissolved at least 1 wt% tripalmitin at room temperature. The low TP solubilisation power of the first three solvents was expected, due to the high R_a values. However, the slight solubility in Dihydrocarvone is surprising.

There is no consequent trend between R_a value and tripalmitin solubilisation power. But, first relations between solvent structure and tripalmitin solubilisation power are in evidence. Aromatic solvents dissolve more TP than comparable non aromatic ones and the smaller and less polar the side chains, the higher the solubility of triglyceride. Additionally, classical solvents were tested to affirm the assumptions and to get a clearer idea of the relations.

Classical solvents

Table 4.8: Experimentally determined solubility of tripalmitin in various classical solvents at room temperature, sorted by decreasing R_a value.

Solvent	R_a value [(J/cm³)^{1/2}]	Molecular weight [g/mol]	wt% TP
Pyridine	15.33	79.10	<3
Benzylic alcohol	12.08	108.14	<1
Thiophene	11.15	84.14	10.3±0.5
Benzene	8.31	78.11	14.3±0.5
Tetrahydrothiophene	7.91	88.17	5.8±0.4
2-Penten	7.81	70.13	2±0.5
Cyclohexane	6.84	84.16	4.2±.4
Diethylether	5.95	74.12	2.5±0.5
Tetrahydrofuran	4.67	72.11	14.7±0.3

4. Results and Discussion

There is no obvious trend between R_a value and amount of dissolved tripalmitin (Tab. 4.8). However, the comparison of all these solvents allows one to propose following guidelines for the choice of potentially applicable solvents:

- Cyclic molecules are better than non cyclic ones.
- Aromatic solvents are better than non aromatic ones.
- Less substituents are better than more.
- The smaller the substituent the better the solvent.
- The smaller the solvent the better.

The R_a value on its own does not enable a classification in good and unapt solvents. There are much more parameters which have to be considered for the choice of a capable solvent for tripalmitin solubilisation. One probably important, yet unconsidered, parameter is the crystallinity of tripalmitin. To confirm this assumption, the solubility of triolein and molten tripalmitin in the same solvents as tested for solid tripalmitin, was investigated. And indeed, all these solvents dissolve at least 50 wt% of liquid triglyceride.

Solubility limit of triolein

The Hansen solubility parameter is an appropriate method for solvent screening as long as the solute is liquid at investigated conditions. Therefore, the limit R_a value for triolein solubility was determined in order to predict suitable solvents. A small selection of tested solvents is shown in table 4.9.

Table 4.9: Experimentally determined solubility of triolein in various solvents at room temperature, sorted for decreasing R_a value.

Solvent	R_a value [[J/cm³]^{1/2}]	Molecular weight [g/mol]	wt% TP
1,2-Propandiol	23.62	76.09	<1
Methanol	20.29	32.04	<1
Propylencarbonat	19.92	102.09	<1
Ethanol	15.94	46.07	1-3
n-Propanol	13.55	60.10	>50
Benzylic alcohol	13.19	108.14	>50
Tetrahydrofurfurylalcohol	11.84	102.13	>50
Kresol	9.44	108.14	>50
Lutensol AO7	8.48	520	>50

Octanol	7.42	130.23	>50
Limonen	4.59	136.24	>50
Anethol	2.02	148.22	>50

Solvents giving a R_a value smaller than 14 for triolein dissolve more than 50 wt% of the liquid triglyceride. However, already for slightly increased R_a values the solubility decreases rapidly.

4.2.2.2 COSMOtherm calculations

COSMO-RS is a model, which enables the prediction of the behaviour of molecules in a liquid phase by calculating the solid-liquid equilibrium (SLE). In this model the crystallinity of solutes is considered and therefore, it is suitable for a tripalmitin solvent screening. COSMOtherm is an implementation of COSMO-RS, delivering thermodynamic values such as the maximum fusion free energy ΔG_{fus}^x for a range of mixtures at different temperatures.

We calculated the maximum fusion energy of various 1:1 mixtures of tripalmitin/solvent at 298.15 K (Tab. 4.10). For negative maximum fusion energy at least 1 wt% tripalmitin gets dissolved, except in octane, hexane and pentane. This aberration results from problems with the combinatorial term of the alkanes in the COSMO-RS software. Beyond that, the quantitative prediction of tripalmitin solubility, by COSMOtherm calculations is not possible.

Table 4.10: Results of COSMOtherm calculation and experimental determined solubility limit at 298.15 K with decreasing maximum fusion energy ΔG .

Solvent	ΔG [J/mol]	wt% TP
Methanol	0.467	<1
Ethanol	0.391	<1
Butanol	0.309	<1
Hexanol	0.257	<1
Octanol	0.219	<1
Decanol	0.193	<1
Anethole	-0.018	2±0.5
Octane	-0.070	<1
p-Cymene	-0.089	3.5±0.5

4. Results and Discussion

Tetrahydrothiophene	-0.091	5.8±0.4
Limonene	-0.094	2.2±0.5
Mesitylene	-0.096	7.5±0.5
Hexane	-0.096	<1
Thiophene	-0.098	10.3±0.5
o-Xylol	-0.099	8.2±0.5
Benzene	-0.108	14.3±0.3
Pentane	-0.113	<1
Cyclohexane	-0.115	4.2±0.4
Tetrahydrofuran	-0.134	14.7±0.3
Diethylether	-0.144	2.5±0.5
Chloroform	-0.229	22±0.3

4.2.2.3 System of three components

As known from the Indigo effect, the presence of water can change the solvent properties completely. Already dissolved solutes get displaced by water. And indeed, the same effect is observed for dissolved tripalmitin. Two of the best solvents were chosen for this experiment. The investigated solvents were chloroform and 2-methyl tetrahydrofuran. They were used, due to their good solubility properties and due to their comparable small toxicity. 5 wt% TP and an increasing amount of water were dissolved in these solvents. For 2-MTHF the addition of 2 wt% induces precipitation, whereas tripalmitin already precipitates from chloroform, with addition of less than 1 wt% water. The different amounts of water, required to induce the precipitation, are based on the differing solubility of water in the tested solvents. Karl Fischer measurements gave a water solubility limit of 0.08 wt% in chloroform and 6.5 wt% in 2-MTHF. The amount of precipitated tripalmitin from chloroform is very small, the samples become slightly turbid. However, a quantitative determination was not possible. The addition of various amounts of water (2-25 wt%) to a solution of 5 wt% tripalmitin in 2-MTHF induced the precipitation of 2.2±0.3 wt% tripalmitin.

4.2.3 Conclusion

The comparison of experimental solubility results with calculated R_a values shows that the model of Hansen solubility parameters is not suitable for the prediction of crystalline tripalmitin solubility.

However, for molten TP and triolein the results are in good accordance. Consequently, this model is suitable for the solvent screening for liquid solutes.

COSMOtherm calculations consider the melting enthalpy of the solute, giving results for tripalmitin solvent screening which agree with the experimental investigations. However, it is not possible to predict the solubility limit of tripalmitin. Only a ranking for a list of solvents can be gained from COSMOtherm calculations. Due to the restricted COSMO-RS database the solvents which can be calculated are limited.

The displacement of already dissolved tripalmitin by water and the generally low solubility makes the dissolution of tripalmitin from sourced cotton during the washing process illusive. However, practical experience shows that also solid triglycerides can be removed from cotton. Hence, the removal of solid triglycerides results from another mechanism. The investigations have shown that liquid triglycerides can be dissolved easily. Realistic fatty soils consist of a mixture of solid and liquid triglycerides. The liquid triglycerides act as a glue and we suppose that during the washing process the liquid triglycerides become dissolved and a very fragile frame of solid triglycerides remains. It breaks up mechanically during the washing process and gets suspended by the washing solution. This will be investigated in more detail in the further section.

4.3 Washing tests

4.3.1 Introduction

In various former studies the mechanism of soil release from cotton fibre was investigated. And as already mentioned, the soil release mechanism depends on the state of soil matter [11]. They found that liquid soil release by the roll-up mechanism is faster and more efficient than solid soil removal. Hence, an increased washing temperature improves the washing result [232]. However, the deepened environmental awareness of the population requires low washing temperatures to save energy, but without losing efficiency. Investigations by Venkatesh et al. have shown that the main components of usual household laundry soil are fatty substances [8]. Therefore, the particulate soils are mainly solid triglycerides. Accordingly, in the former sections the interactions with surfactants and solvents were investigated. Only a marginally influence of the surfactant on the melting point of the TP was found and the solubilisation of at least 50 wt% triglyceride worked only for liquid triglycerides. Further, it was shown that the addition of water to a binary systems of solvent and TP reduces the triglyceride solubilisation power dramatically. Therefore, to avoid the deposition of soil and surfactant on the laundry and in the washing machine the formation of microemulsions by soil and detergent is desired.

Therefore, various combinations of surfactants and cosurfactants with Lutensol AO7 were tested in combination with TO, in order to find systems forming microemulsions. Additionally, it was tested at which water content the solutions became turbid. The higher the amount of water the more extended is the region of microemulsion, approximately. For four very promising mixtures the ternary phase diagram was determined and the one with the most extended area of microemulsion was tested for washing cotton fibers soiled with triglyceride mixtures with varying content of TO/TP. Additionally, the ternary phase diagram of the mixture water/TO/AO7/citronellol was determined, due to the green character of the cosurfactant.

In the subsequent washing tests at room temperature, the following detergents were tested:

- Water
- Lutensol AO7 (varying concentration)
- AO7/AO3/benzyl alcohol (varying concentrations)

- AO7/AO3/benzyl alcohol/lecithin
- AO7/ChS
- AO7/2-MTHF (varying compositions)
- Spee (varying concentrations)

However, the viscosity of the washing liquors was very different. Hence, to determine the influence of the viscosity on washing efficiency, 1 wt% solutions of Lutensol AO7 were thickened by culminal MHPC 500PF and the washing results compared to the ones gained for non thickened solution.

A further factor, influencing the washing efficiency is the temperature. As already mentioned above, roll up mechanism is the more efficient mechanism. Therefore, washing at higher temperatures is supposed to give better washing results. Accordingly, washing tests with 1 wt% aqueous solution of AO7 as detergent at 10 °C and 40 °C were performed. Another relevant factor would be the water hardness. But all washing tests were performed using millipore water, without taking the water hardness into account.

The washing efficiency was determined by measuring the ΔE_{ab} value before and after washing. Therefore, the $L^*a^*b^*$ values of untreated cotton and washed cotton without previous soiling for every washing agent were measured at the colorimeter. The higher the resulting $\Delta\Delta E_{ab}$ value, the better is the washing result.

4.3.2 Results

4.3.2.1 Solvent mixtures forming microemulsion with TO

One challenge in detergency is to avoid the deposition of soil and surfactant in the washing machine. A promising approach is the formation of microemulsions during the washing process. Microemulsions are thermodynamically stable, hence the dissolved soil would remain in the washing liquor and could be removed easily without soiling the machine and hoses. Assuming that the liquid triglycerides acting as a glue retaining the crystalline triglycerides, a solvent for the oily soil has to be found which dissolves a preferably high amount and forms microemulsion by dissolution. Because Lutensol AO7 is a in detergency commonly used surfactant and triolein is one of the main liquid components of household laundry soil, mixtures of Lutensol AO7, various cosurfactants and triolein have been prepared and water was added stepwise, until the solutions became turbid. In all samples the ratio oil/surfactant was 1:1. Into some mixtures also ionic surfactants have

4. Results and Discussion

been added. Thereby it is easy to find out which cosurfactants are inept to dissolve triolein and the region of microemulsion is determined quickly. In table 4.11 the composition and the amount of water until the samples become turbid is given.

Table 4.11: Determination of the region of one phase for the addition of water to various mixtures TO/surfactant/cosurfactant at 298.15 K.

oil	surfactant	cosurfactant	oil/(surfactant+ cosurfactant)	surfactant/ cosurfactant	wt% (H ₂ O)
TO	AO7	butanol	1:1	1:1	5.6
TO	AO7	anethol	1:1	1:1	1.3
TO	AO7	octanol	1:1	1:1	3.3
TO	AO7	benzyl alcohol	1:1	1:1	3.9
TO	AO7	AO3	1:1	1:1	10.5
TO	AO7:X-AES = 1:1		1:1		0
TO	AO7	TPM	1:1	1:1	3.9
TO	AO7	DPM	1:1	1:1	1.1
TO	AO7	PM	1:1	1:1	2.8
TO	AO7	SXS	1:1	1:1	0
TO	AO7	SXS:EtOH = 1:1	1:1	1:1	0
TO	AO7	AO3:benzyl alcohol = 1:1	1:1	1:1	11.5
TO	AO7	AO3:benzyl alcohol = 1:2	1:1	1:1	8.2
TO	AO7	AO3:benzyl alcohol = 1:2	1:1	1:2	8.5
TO	AO7:SLES = 1:1	AO3	1:1	1:1	0
TO	AO7:SLES = 1:1	AO3:benzyl alcohol = 1:1	1:1	1:1	0

Without the addition of water all samples are one phase, except the samples containing X-AES, SXS or SLES. These compounds are ionic, whereas the others are nonionic. The best tested cosurfactant was Lutensol AO3, remaining a microemulsion until the addition of 10.5 wt% water. However, the region of one phase was extended by the addition of the second cosurfactant benzyl alcohol. But only for the ratio AO3/benzyl alcohol = 1:1 and AO7/cosurfactant = 1:1. For mixtures with a higher content of benzyl alcohol the one-phase region is decreased. However, these tests are only a first hint on promising washing liquors. They enable a fast screening of cosurfactants. To assure a mixture is promising for a high washing efficiency, the complete ternary phase diagram has to be determined. Therefore, the determined ternary phase diagram of various systems is given in the following section.

Water/TO/AO7

This mixture does not contain a cosurfactant (Fig. 4.11). All further phase diagrams are compared to this to see if the addition increases or decreases the region of microemulsion.

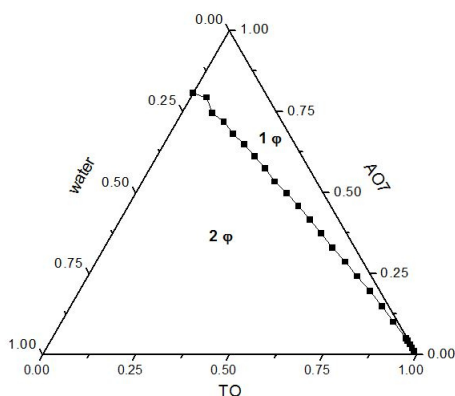


Figure 4.11: Ternary phase diagram with water/TO/AO7 at 298.15 K. The area of 1 ϕ gives the region of microemulsion and the area of 2 ϕ represents the region of emulsion.

Water/TO/AO7/AO3/Benzylic alcohol

All mixtures contain Lutenosl AO7 as surfactant and mixtures of AO3 and benzyl alcohol as cosurfactant. The ratio AO7/cosurfactant was either 1:1 or 1:2 and the composition of the cosurfactant AO3/benzyl alcohol was either 1:1 or 1:2 (Tab. 4.12). The resulting phase diagrams are given in figure 4.12.

Table 4.12: Composition of investigated samples containing AO7, AO3 and benzylic alcohol.

<i>mixture</i>	<i>AO7/cosurfactant</i>	<i>AO3/benzyl alcohol</i>
A	1:1	1:2
B	1:2	1:2
C	1:1	1:1

The addition of cosurfactant results in an expansion of the area of microemulsion for mixture A and C. For a higher content of cosurfactant, like in mixture B the one-phase region is nearly unchanged. For higher contents of AO3 in the cosurfactant mixture the microemulsion area is slightly extended. AO3 is more expansive than benzyl alcohol and is a surfactant on its own. Hence, for ecological and economical reason the mixture A containing less surfactant is the more favoured one for detergency. Nevertheless, the subsequent washing test was performed using mixture C.

4. Results and Discussion

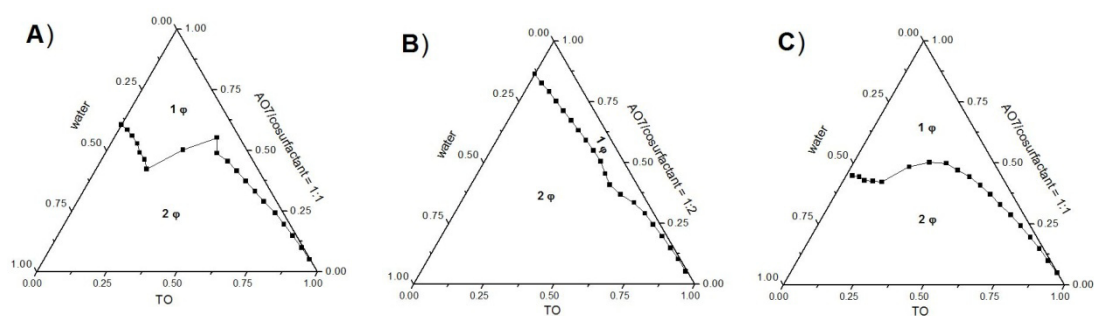


Figure 4.12: Ternary phase diagram with water/TO/AO7/AO3/benzyl alcohol at 298.15 K and varying ratio AO7/cosurfactant and AO3/benzyl alcohol. A) AO7/cosurfactant = 1:1 and AO3/benzyl alcohol = 1:2; B) AO7/cosurfactant = 1:2 and AO3/benzyl alcohol = 1:2; C) AO7/cosurfactant = 1:1 and AO3/benzyl alcohol = 1:1.

Water/TO/AO7/Citronellol

In comparison to AO3 and benzyl alcohol, citronellol is a cosurfactant derived from natural resources. It is found in the oil of roses and geraniums. With regard to our aim, making the washing process more environmentally friendly, the use of a natural cosurfactant instead of a synthesized one, is preferred. However, the determination of the ternary phase diagram using citronellol as cosurfactant gives only small area of microemulsion (Fig. 4.13). Therefore, this cosurfactant is not considered for the subsequent washing tests.

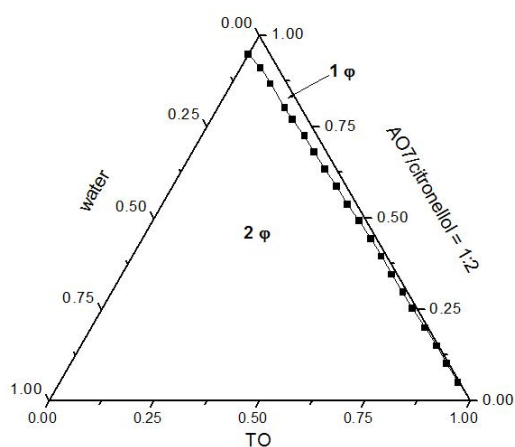


Figure 4.13: Ternary phase diagram with water/TO/AO7 at 298.15 K. Ratio AO7/citronellol = 1:2.

4.3.2.2 Washing of soiled cotton fibre

4.3.2.2.1 Washing at room temperature without thickeners

Detergent: Water

The most environmental friendly and cheapest washing liquor is pure water. However, triglycerides can not be dissolved in water at room temperature. Accordingly, soil release results from mechanical action during the washing process, exclusively. Except for cotton soiled with pure tripalmitin, no soil release is detected for water as detergent, resulting in $\Delta\Delta E_{ab}$ values about zero (Tab. 4.13). As soon as a small amount of liquid triglyceride is present in the soil, the crystalline triglyceride can not be broken up mechanically, any longer. These results affirm the assumption of triolein acting as a glue for tripalmitin, hindering the breaking up of crystalline particles.

Table 4.13: At the colorimeter determined $\Delta\Delta E_{ab}$ values for washing tests with washing liquor water with varying soil composition.

soil	$\Delta\Delta E_{ab}$
TO	-1.31
TO/TP = 3:1	0.52
TO/TP = 2:1	0.05
TO/TP = 3:2	0.16
TO/TP = 1:1	-2.74
TO/TP = 2:3	2.56
TO/TP = 1:2	0.48
TO/TP = 1:3	0.99
TP	13.51

Detergent: Lutensol AO7

The ternary phase diagram of water/TO/AO7 gives that AO7 and triolein are miscible in all ratios. Therefore, this surfactant is supposed to dissolve the liquid triglyceride from soiled cotton. Thus, the glue is removed leaving crystalline tripalmitin, which can be removed mechanically. Hence, the washing power of Lutensol AO7 detergent with varying concentration was investigated (Tab.4.15). The corresponding viscosity of the washing solutions is given in table 4.14.

4. Results and Discussion

Table 4.14: Concentration and corresponding viscosity of Lutensol AO7 detergents.

<i>wt% (AO7)</i>	<i>η [mPas]</i>
0.5	1.02
1	1.28
5	10.89
10	127.20

Table 4.15: At the colorimeter determined $\Delta\Delta E_{ab}$ values for washing tests with washing liquor Lutensol AO7 with varying surfactant concentration and soil composition.

<i>soil</i>	<i>0.5 wt%</i>	<i>1 wt%</i>	<i>5 wt%</i>	<i>10 wt%</i>
	$\Delta\Delta E_{ab}$	$\Delta\Delta E_{ab}$	$\Delta\Delta E_{ab}$	$\Delta\Delta E_{ab}$
TO	9.81	12.80	9.76	11.21
TO/TP = 3:1	10.21	14.97	15.34	20.01
TO/TP = 2:1	10.39	16.93	15.52	18.06
TO/TP = 3:2	15.20	23.47	20.93	22.92
TO/TP = 1:1	14.09	18.82	18.15	23.25
TO/TP = 2:3	15.41	20.24	24.46	26.56
TO/TP = 1:2	15.98	18.84	23.83	26.37
TO/TP = 1:3	24.33	28.43	24.94	26.69
TP	29.34	31.78	29.56	24.30

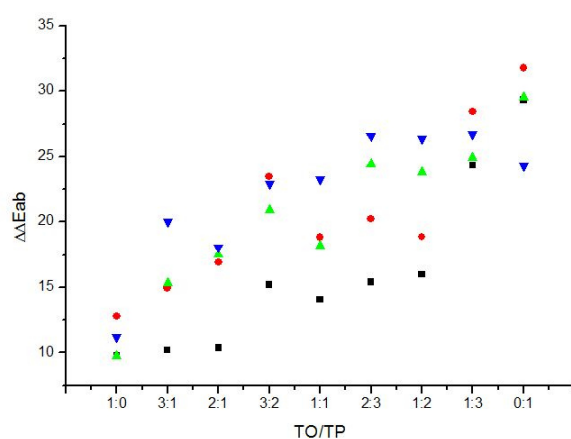


Figure 4.14: At the colorimeter determined $\Delta\Delta E_{ab}$ values for washing tests with washing liquor Lutensol AO7 with varying surfactant concentration and soil composition. ■: 0.5 wt% AO7; ●: 1 wt% AO7; ▲: 5 wt% AO7; ▼: 10 wt% AO7

The resulting $\Delta\Delta E_{ab}$ values, as a function of the surfactant concentration and the soil composition are given in table 4.15 and figure 4.14. In contrary to pure water, soil release is gained for all concentrations and soil compositions. Additionally, the washing result for pure tripalmitin was improved. And except of some outlier, the detergency power enhances with increasing tripalmitin content in soil. Comparison of the results gained for varying surfactant concentrations gives only for the increases from 0.5 wt% to 1 wt% a significantly increased $\Delta\Delta E_{ab}$ value and an improved washing result, consequently. Just for some soil compositions a higher detergent concentration results in a slightly improved result. Regarding to the environmentally friendly claim, the 1 wt% washing liquor is the favored one.

Detergent: Lutensol AO7/AO3/benzyl alcohol

Ternary phase diagrams of Lutensol AO7/AO3/benzyl alcohol were determined for varying ratios of surfactant/cosurfactant and AO3/benzyl alcohol. AO3 and benzyl alcohol act as cosurfactant. The composition with the most extended region of microemulsion was the mixture AO7/cosurfactant 1:1 and AO3/benzyl alcohol 1:1. Therefore, washing tests with varying concentrations of the mixture for varying soil compositions were performed. The tested concentrations with corresponding Lutensol AO7 concentration and viscosity are given in table 4.16.

Table 4.16: Concentration of AO7/AO3/benzyl alcohol mixture and corresponding Lutensol AO7 concentration and viscosity.

<i>wt% (mixtures)</i>	<i>wt% (AO7)</i>	<i>η [mPas]</i>
1	0.5	1.57
5	2.5	12.38
10	5	95.35
20	10	210.12

Table 4.17: At the colorimeter determined $\Delta\Delta E_{ab}$ values for washing tests with mixtures AO7/AO3/benzyl alcohol with varying surfactant concentration and soil composition. AO7/cosurfactant = 1:1, AO3/benzyl alcohol = 1:1

	<i>1 wt%</i>	<i>5 wt%</i>	<i>10 wt%</i>	<i>20 wt%</i>
<i>soil</i>	<i>$\Delta\Delta E_{ab}$</i>	<i>$\Delta\Delta E_{ab}$</i>	<i>$\Delta\Delta E_{ab}$</i>	<i>$\Delta\Delta E_{ab}$</i>
<i>TO</i>	5.70	5.44	5.90	2.02
<i>TO/TP = 3:1</i>	4.86	7.86	6.72	4.93
<i>TO/TP = 2:1</i>	7.84	8.37	11.29	5.30

4. Results and Discussion

TO/TP = 3:2	9.68	12.95	15.55	5.27
TO/TP = 1:1	13.83	15.06	12.83	5.59
TO/TP = 2:3	16.54	19.78	20.56	11.71
TO/TP = 1:2	14.04	18.36	17.16	10.83
TO/TP = 1:3	20.23	15.30	17.79	12.98
TP	23.52	25.38	29.12	19.32

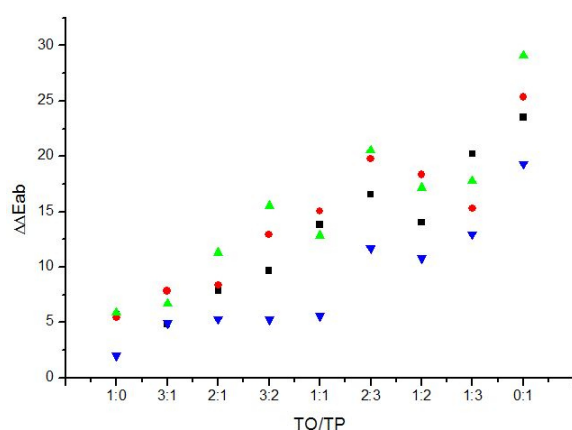


Figure 4.15: At the colorimeter determined $\Delta\Delta E_{ab}$ values for washing tests with mixtures AO7/AO3/benzyl alcohol with varying surfactant concentration and soil composition. AO7/cosurfactant = 1:1, AO3/benzyl alcohol = 1:1; ■: 0.5 wt% AO7; ●: 1 wt% AO7; ▲: 5 wt% AO7; ▼: 10 wt% AO7

The resulting $\Delta\Delta E_{ab}$ values, as a function of the surfactant concentration and soil composition, are given in table 4.17 and figure 4.15. The lowest washing efficiency is observed for the highest concentration of the mixture. However, this washing liquor has a distinctively higher viscosity than the other concentrations. Therefore, the diminished efficiency might result from longer diffusion times in the detergent. The soil release for the other washing liquors is nearly the same. Except of some outliers, the $\Delta\Delta E_{ab}$ value rises with increasing tripalmitin content in soil for all detergent concentrations. Comparing the results of 1 wt% mixture with the results of 0.5 wt% pure AO7, gives a lower efficiency of the mixture.

Detergent: Lutensol AO7/AO3/benzyl alcohol/lecithin

Lecithin is a green emulsifier of low toxicity and acceptable taste. Therefore, it is widely used in food, cosmetic and medical formulations [240]. Commercial lecithin derives from soybeans. But also other vegetable and animal sources, like corn oil, safflower and egg yolk are known. Depending on the source, the composition of lecithin differs. The three phospholipid types of lecithin derived from soybeans are phosphatidylcholine (main component), phosphatidylethanolamine and

phosphatidylinositol. Also the chain length and saturation of hydrocarbon chains may vary [241]. Emulsifier can decrease the interfacial tension between soil and water, yielding an increased detergency, supposedly. Therefore, a washing liquor, containing lecithin was tested for the soil release of varying ratios triolein/tripalmitin. The composition of the detergent was 0.45 wt% AO7, 0.225 wt% AO3, 0.225 wt% benzyl alcohol and 0.1 wt% lecithin. The viscosity was determined to be 1.18 mPas. The resulting $\Delta\Delta E_{ab}$ values as a function of soil composition is given in table 4.18 and figure 4.16. With increasing fraction of crystalline triaplmitn in contamination the soil release increases.

Table 4.18: At the colorimeter determined $\Delta\Delta E_{ab}$ values for washing tests with mixtures AO7/AO3/benzyl alcohol/lecithin with varying soil composition. AO7/cosurfactant = 1:1, AO3/benzyl alcohol = 1:1; 0.1 wt% lecithin

<i>soil</i>	$\Delta\Delta E_{ab}$
TO	3.99
TO/TP = 3:1	4.80
TO/TP = 2:1	3.28
TO/TP = 3:2	7.14
TO/TP = 1:1	9.62
TO/TP = 2:3	12.02
TO/TP = 1:2	12.52
TO/TP = 1:3	16.88
TP	23.53

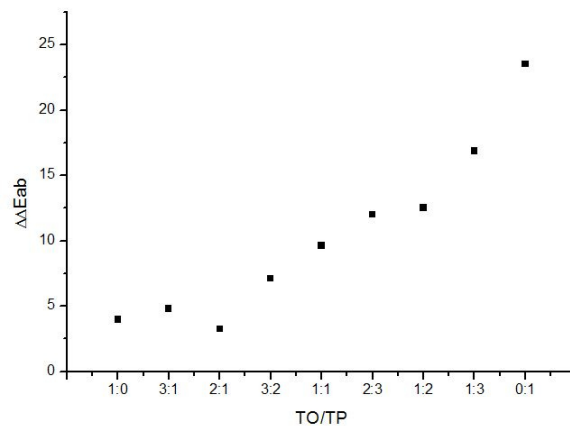


Figure 4.16: At the colorimeter determined $\Delta\Delta E_{ab}$ values for washing tests with mixture AO7/AO3/benzyl alcohol/lecithin with varying soil composition. AO7/cosurfactant = 1:1, AO3/benzyl alcohol = 1:1; 0.1 wt% lecithin.

4. Results and Discussion

Except the outlier at a soil composition TO/TP = 2:1, the soil release increases with increasing TP content in soil. However, the washing result is diminished compared to a washing liquor containing only 0.5 wt% AO7 or 1 wt% mixture of Lutensol AO7/AO3/benzyl alcohol as mentioned before. For this mixtures the addition of emulsifier did not improve the washing efficiency of the detergent.

Detergent: Lutensol AO7/ChS

A lot of studies about ionic and nonionic surfactants used in detergency, are published [242-244]. Mixtures of ionic and nonionic surfactants are supposed to have a higher washing ability than only one class of surfactant. Accordingly a 1/1 mixture Lutensol AO7/ChS as washing liquor for varying soil compositions was tested. Choline alkylsulphate has a varying C₁₆/C₁₈ alkyl chain length.

Table 4.19: At the colorimeter determined ΔE_{ab} values for washing tests with mixtures AO7/ChS with varying soil composition. 0.5 wt% AO7; 0.5 wt% ChS

<i>soil</i>	<i>ΔE_{ab}</i>
<i>TO</i>	3.50
<i>TO/TP = 3:1</i>	4.15
<i>TO/TP = 2:1</i>	6.20
<i>TO/TP = 3:2</i>	8.91
<i>TO/TP = 1:1</i>	10.91
<i>TO/TP = 2:3</i>	11.76
<i>TO/TP = 1:2</i>	15.99
<i>TO/TP = 1:3</i>	14.08
<i>TP</i>	20.13

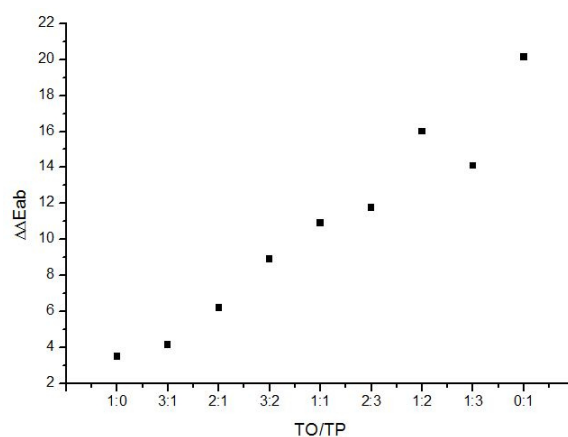


Figure 4.17: At the colorimeter determined $\Delta\Delta E_{ab}$ values for washing tests with the mixture AO7/ChS = 1/1 with varying soil composition. 0.5 wt% AO7; 0.5 wt% ChS.

The results of the washing tests with detergent containing 0.5 wt% AO7 and 0.5 wt% ChS are given in table 4.19 and figure 4.17. The viscosity of the washing liquor was determined to be 1.03 mPas. Except of one outlier at soil composition TO/TP = 1:3, the soil release increases with increasing content an crystalline triglyceride.

Detergent: Lutensol AO7/2-MTHF

2-MTHF is a side product of the industrial production of furfuryl alcohol and furfural [245]. Additionally, it is synthesized from renewable raw materials by hydrogenation of 2-Methylfuran or by cyclization and hydrogenation of levulinic acid [245, 246]. Accordingly, it is an environmentally acceptable organic solvent which dissolves about 9 wt% tripalmitin. In order to determine the influence of structuring in washing liquor, the ternary phase diagram of mixture 2-MTHF/Lutensol AO7/water was determined to find areas of microemulsion (Fig. 4.18). The regions of continuous and bicontinuous microemulsion were distinguished by conductivity measurements. Four different compositions of mixture Lutensol AO7/2-MTHF were investigated as detergents for washing tests (Tab. 4.20).

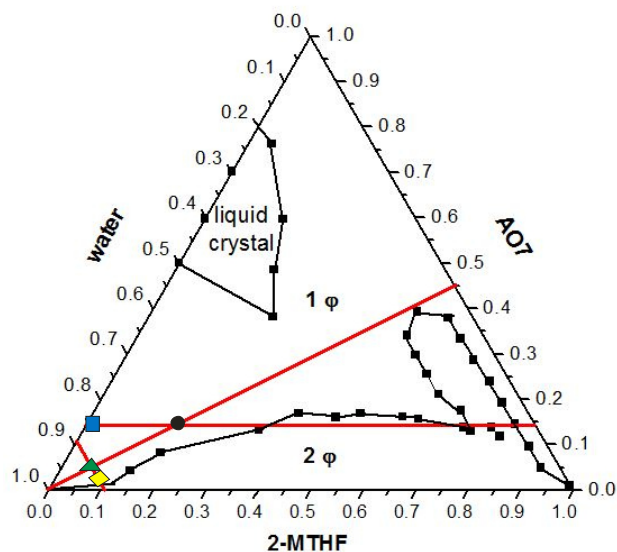


Figure 4.18: Ternary phase diagram of mixture 2-MTHF/Lutensol AO7/water at 298.15 K. ●: bicontinuous ME with 14.4wt% AO7 and 17.6 wt% 2-MTHF; ■: continuous ME with 14.4 wt% AO7 and 0.6 wt% 2-MTHF; ▲: continuous ME with 5 wt% AO7 and 6.11 wt% 2-MTHF; ◆: continuous ME with 1 wt% AO7 and 10.11 wt% 2-MTHF.

Table 4.20: Composition of mixtures Lutensol AO7/2-MTHF/water and corresponding viscosity.

<i>detergent</i>	<i>wt% AO7</i>	<i>wt% 2-MTHF</i>	<i>type of ME</i>	<i>η [mPas]</i>
1	1	10.11	continuous	1.39
2	5	6.11	continuous	2.31
3	14.4	17.6	bicontinuous	6.56
4	14.4	0.6	continuous	251.62

Detergent 1

This composition is plotted as ◆ in the ternary phase diagram of mixture Lutensol AO7/2-MTHF (Fig. 4.18). The solution is a continuous microemulsion, containing 1 wt% surfactant. The mass ratio Lutensol AO7/2-MTHF is 0.09. The results of washing test for cotton fibers soiled with triglycerides with varying ratio TO/TP are given in table 4.21 and figure 4.19.

Table 4.21: At the colorimeter determined $\Delta\Delta E_{ab}$ values for washing tests with mixtures AO7/2-MTHF with varying soil composition. 1 wt% AO7; 10.11 wt% 2-MTHF.

<i>soil</i>	$\Delta\Delta E_{ab}$
<i>TO</i>	4.97
<i>TO/TP = 3:1</i>	5.82
<i>TO/TP = 2:1</i>	8.56
<i>TO/TP = 3:2</i>	7.19
<i>TO/TP = 1:1</i>	10.14
<i>TO/TP = 2:3</i>	10.31
<i>TO/TP = 1:2</i>	10.35
<i>TO/TP = 1:3</i>	14.81
<i>TP</i>	29.54

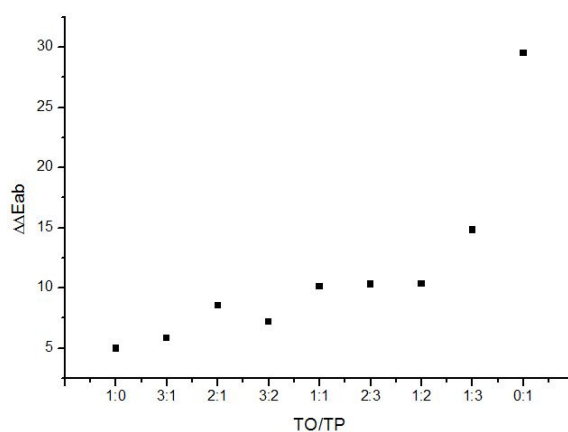


Figure 4.19: At the colorimeter determined $\Delta\Delta E_{ab}$ values for washing tests with mixture AO7/2-MTHF with varying soil composition. 1 wt% AO7; 10.11 wt% 2-MTHF.

Except the outlier at a soil composition $TO/TP = 3:2$, the soil release increases with increasing tripalmitin content in contamination. However, the $\Delta\Delta E_{ab}$ values are smaller than for washing with solution of 1 wt% Lutensol AO7. Structuring the surfactant in a microemulsion reduces the washing ability.

Detergent 2

This washing liquor contains the same amount of water like detergent 1 and is also a continuous microemulsion. But the surfactant content is increased to 5 wt%, resulting in a mass fraction Lutensol AO7/2-MTHF = 0.45. The composition is plotted as ▲ in the ternary phase diagram of mixture Lutensol AO7/2-MTHF/water

4. Results and Discussion

(Fig. 4.18). The $\Delta\Delta E_{ab}$ values determined for washing of cotton fibers soiled with triglycerides with varying TO/TP ratio are given in table 4.22 and figure 4.20.

Table 4.22: At the colorimeter determined $\Delta\Delta E_{ab}$ values for washing tests with mixtures AO7/2-MTHF with varying soil composition. 5 wt% AO7; 6.11 wt% 2-MTHF.

soil	$\Delta\Delta E_{ab}$
TO	8.62
TO/TP = 3:1	15.67
TO/TP = 2:1	19.36
TO/TP = 3:2	16.17
TO/TP = 1:1	20.90
TO/TP = 2:3	23.69
TO/TP = 1:2	26.47
TO/TP = 1:3	23.91
TP	30.58

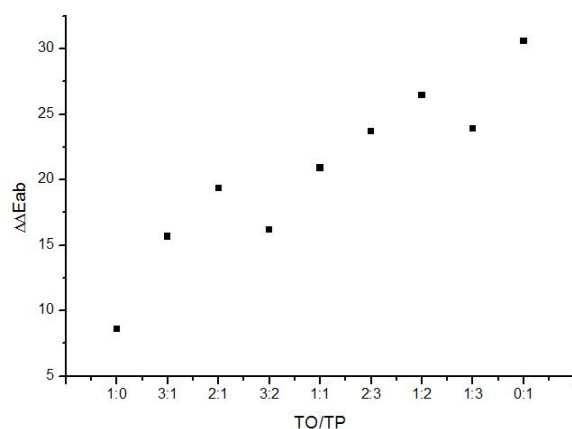


Figure 4.20: At the colorimeter determined $\Delta\Delta E_{ab}$ values for washing tests with mixture AO7/2-MTHF with varying soil composition. 5 wt% AO7; 6.11 wt% 2-MTHF.

With increasing TP content in the soil the $\Delta\Delta E_{ab}$ value increases, except for the outliers at soil compositions TO/TP = 3:2 and 1:3. Due to the higher surfactant concentration, the washing activity of the detergent 2 is higher than of detergent 1. However, the soil release is only comparable to washing with 5 wt% solution of Lutensol AO7. Hence, as already mentioned before, the washing activity of surfactant seems to be reduced by structuring in a microemulsion.

Detergent 3

This mixture is a bicontinuous microemulsion, containing 14.4 wt% Lutensol AO7. The composition is plotted as ● in the ternary phase diagram of mixture AO7/2-MTHF/water at 298.15 K (Fig. 4.18). The mass ratio AO7/2-MTHF is 0.45, the same as in detergent 2. The results of washing tests are given in table 4.23 and figure 4.21.

Table 4.23: At the colorimeter determined $\Delta\Delta E_{ab}$ values for washing tests with mixtures AO7/2-MTHF with varying soil composition. 14.40 wt% AO7; 17.6 wt% 2-MTHF.

<i>soil</i>	$\Delta\Delta E_{ab}$
TO	15.47
TO/TP = 3:1	18.46
TO/TP = 2:1	20.73
TO/TP = 3:2	25.63
TO/TP = 1:1	26.77
TO/TP = 2:3	26.09
TO/TP = 1:2	26.13
TO/TP = 1:3	24.81
TP	32.18

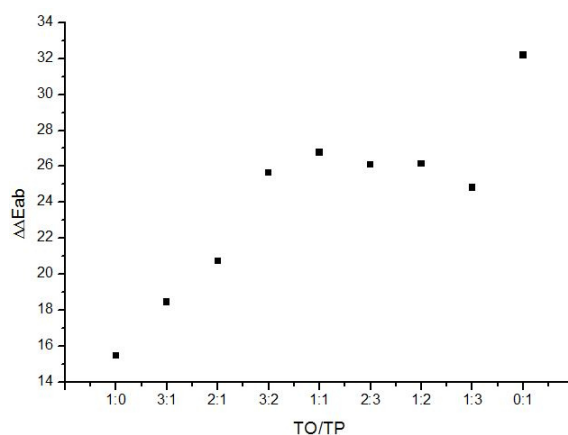


Figure 4.21: At the colorimeter determined $\Delta\Delta E_{ab}$ values for washing tests with mixture AO7/2-MTHF with varying soil composition. 14.40 wt% AO7; 17.6 wt% 2-MTHF.

With increasing TP content in soil the $\Delta\Delta E_{ab}$ values increases, except of the samples with soil composition TO/TP = 2:3, 1:2 and 1:3. The results are comparable to the results gained for washing with solution of 10 wt% Lutensol AO7.

4. Results and Discussion

Detergent 4

Detergent 4 is a continuous microemulsion, containing 14.4 wt% Lutensol AO7 and 0.6 wt% 2-MTHF. Accordingly, the ratio AO7/2-MTHF is 0.96. It is plotted as ■ in ternary phase diagram of mixture 2-MTHF/AO7/water at 298.15 K (Fig. 4.18). In contrast to the other tested detergents the viscosity is significantly higher. The results for washing tests with cotton fibres soiled with triglycerides with varying TO/TP content are given in table 4.24 and figure 4.22.

Table 4.24: At the colorimeter determined $\Delta\Delta E_{ab}$ values for washing tests with mixtures AO7/2-MTHF with varying soil composition. 14.40 wt% AO7; 0.06 wt% 2-MTHF.

soil	$\Delta\Delta E_{ab}$
TO	8.82
TO/TP = 3:1	12.05
TO/TP = 2:1	17.27
TO/TP = 3:2	24.04
TO/TP = 1:1	18.60
TO/TP = 2:3	26.93
TO/TP = 1:2	19.97
TO/TP = 1:3	27.13
TP	28.83

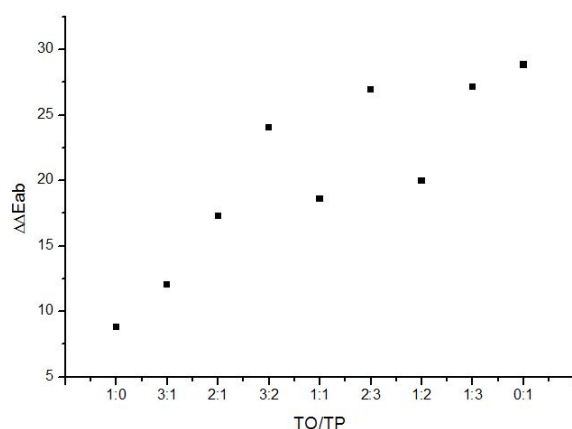


Figure 4.22: At the colorimeter determined $\Delta\Delta E_{ab}$ values for washing tests with mixture AO7/2-MTHF with varying soil composition. 14.40 wt% AO7; 0.06 wt% 2-MTHF.

With increasing TP content in triglyceride soil, the $\Delta\Delta E_{ab}$ values increase. Significantly higher values and, accordingly, better washing results are obtained for soil composition TO/TP = 2:3 and 3:2. Despite the same surfactant concentration

like in detergent 3 the washing results are slightly inferior. This might result from either the higher viscosity or the different structuring in microemulsion.

Detergent: Spee

Spee AktivGel is a commercial liquid detergent supplied by Henkel. It is developed for white and bright laundry and the use at 20 to 95°C. It is applicable in hand washing as well as in the washing machine. These washing tests were performed in order to get an idea of common $\Delta\Delta E_{ab}$ values in detergency. The tests were conducted with cotton fibres soiled with varying TO/TP mixtures and for varying washing agent concentrations. Spee was used undiluted, in a dilution with about 1-5 wt% overall surfactant content and in typically hand washing concentration. According to manufacturer's data the detergent contains <5 wt% nonionic surfactants and 5-15 wt% anionic surfactants. For hand washing, Henkel recommended a dilution of 40 ml Spee in 10 l water. That leads to an overall surfactant concentration of about 0.02-0.1 wt%. The viscosity of the solutions was determined as 142 mPas for undiluted Spee, 1.2 mPas for 1-5 wt% surfactant content and 1.5 mPas for hand washing dilution. The results are given in table 4.25 and figure 4.23.

Table 4.25: At the colorimeter determined $\Delta\Delta E_{ab}$ values for washing tests with varying dilutions of Spee with cotton fibers soiled with varying TO/TP compositions.

	<i>undiluted</i>	<i>1-5 wt% surfactant</i>	<i>hand washing dilution</i>
<i>soil</i>	<i>$\Delta\Delta E_{ab}$</i>	<i>$\Delta\Delta E_{ab}$</i>	<i>$\Delta\Delta E_{ab}$</i>
TO	3.52	5.29	2.96
TO/TP = 3:1	10.44	10.15	2.72
TO/TP = 2:1	14.41	13.42	5.13
TO/TP = 3:2	21.13	24.56	6.05
TO/TP = 1:1	17.48	7.93	2.79
TO/TP = 2:3	23.86	12.89	-0.19
TO/TP = 1:2	22.56	17.01	4.78
TO/TP = 1:3	23.81	15.26	5.05
TP	30.97	15.85	6.84

4. Results and Discussion

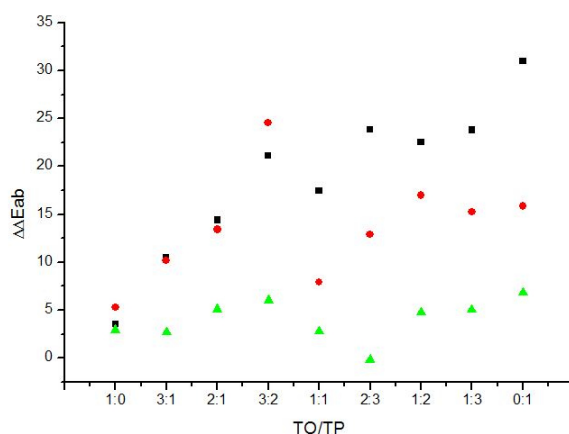


Figure 4.23: At the colorimeter determined $\Delta\Delta E_{ab}$ values for washing tests with varying dilutions of Spee and soil composition. ■: undiluted Spee; ●: dilution with 1-5 wt% overall surfactant concentration; ▲: hand washing dilution

The lowest washing efficiency is determined for hand washing dilution. Except of the kink at TO/TP = 1:1 and 2:3 the $\Delta\Delta E_{ab}$ values increase with increasing TP content in soil for this Spee dilution. However, the washing result for cotton fibres soiled with pure TP is lower than for washing with pure water.

The results for undiluted Spee and dilution with 1-5 wt% overall surfactant content are comparable for cotton fibres soiled with triglyceride mixtures with mainly TO. For contaminations with more TP than TO the undiluted Spee gives the best results. Following the trend the washing efficiency increases with increasing tripalmitin fraction in soil. For these detergents also a kink in $\Delta\Delta E_{ab}$ values at TO/TP = 1:1 was observed. But for washing cotton fibers, soiled with pure TP both give better results than for washing with pure water. Furthermore, the washing efficiency is comparable to a 1 wt% solution Lutensol AO7.

4.3.2.2.2 Washing at 40 °C without thickeners

Increasing the washing temperature results in an increased fraction of liquid soil and accelerates the dynamics in solution. The increase from 25 °C to 40 °C has a negligible influence on polarity and viscosity of washing liquor.

Detergent: Water

For washing with pure water at 40 °C the soil release is, like for washing at 25 °C, for mixtures TO/TP and pure TO insignificant (Tab. 4.26; Fig. 4.24). The result for pure TP contamination is decreased. The increased fraction of liquid triglyceride handicaps the mechanical release.

Table 4.26: At the colorimeter determined $\Delta\Delta E_{ab}$ values for washing tests with water at varying temperatures with cotton fibers soiled with varying TO/TP compositions.

<i>soil</i>	40 °C	25 °C
	$\Delta\Delta E_{ab}$	$\Delta\Delta E_{ab}$
TO	1.33	-1.31
TO/TP = 3:1	1.79	0.52
TO/TP = 2:1	-0.54	0.05
TO/TP = 3:2	-0.69	0.16
TO/TP = 1:1	-2.98	-2.74
TO/TP = 2:3	1.27	2.56
TO/TP = 1:2	2.79	0.48
TO/TP = 1:3	0.16	0.99
TP	7.10	13.51

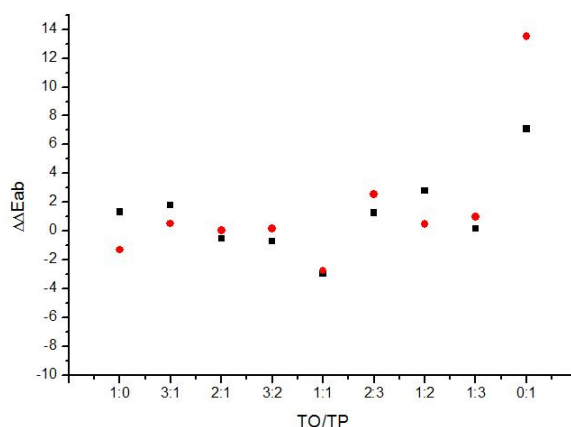


Figure 4.24: At the colorimeter determined $\Delta\Delta E_{ab}$ values for washing tests with water at varying temperatures and soil composition. ■: washing at 40 °C; ●: washing at 25 °C.

Detergent: Lutensol AO7

For washing with 1 wt% Lutensol AO7 at 40 °C instead of 25 °C the soil release is decreased, except of the soil composition TO/TP = 3:1 (Tab. 4.27 and Fig. 4.25). However, the impact is not the same pronounced for all compositions. These results are in agreement with the previous observation that with a decreased fraction of crystalline triglyceride the soil release decreases.

4. Results and Discussion

Table 4.27: At the colorimeter determined $\Delta\Delta E_{ab}$ values for washing tests with water at varying temperatures with cotton fibers soiled with varying TO/TP compositions.

soil	40 °C	25 °C
	$\Delta\Delta E_{ab}$	$\Delta\Delta E_{ab}$
TO	7.17	12.80
TO/TP = 3:1	17.67	14.97
TO/TP = 2:1	16.55	16.93
TO/TP = 3:2	9.22	23.47
TO/TP = 1:1	16.60	18.82
TO/TP = 2:3	19.50	20.24
TO/TP = 1:2	14.50	18.84
TO/TP = 1:3	16.20	28.43
TP	27.61	31.78

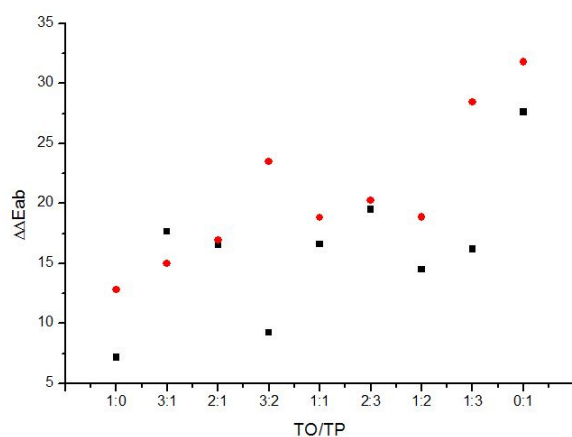


Figure 4.25: At the colorimeter determined $\Delta\Delta E_{ab}$ values for washing tests with water at varying temperatures and soil composition. ■: washing at 40 °C; ●: washing at 25 °C

4.3.2.2.3 Washing at 10 °C without thickeners

Decreasing the washing temperature might result in an increased fraction of solid soil and slow down the dynamics in solution. The decrease from 25 °C to 10 °C has a negligible influence on polarity and viscosity of the investigated washing liquors.

Detergent Water

For washing with pure water at 10 °C the soil release is, like for washing at 25 °C, for mixtures TO/TP and pure TO insignificant (Tab. 4.28; Fig. 4.26). The result for

pure TP contamination is considerably decreased. Reducing the washing temperature does not result in increased crystallinity of soil and enhanced mechanically soil release.

Table 4.28: At the colorimeter determined $\Delta\Delta E_{ab}$ values for washing tests with water at varying temperatures with cotton fibers soiled with varying TO/TP compositions.

<i>soil</i>	10 °C	25 °C
	$\Delta\Delta E_{ab}$	$\Delta\Delta E_{ab}$
TO	0.61	-1.31
TO/TP = 3:1	-1.19	0.52
TO/TP = 2:1	-0.02	0.05
TO/TP = 3:2	0.63	0.16
TO/TP = 1:1	-1.01	-2.74
TO/TP = 2:3	-0.66	2.56
TO/TP = 1:2	1.58	0.48
TO/TP = 1:3	1.55	0.99
TP	3.93	13.51

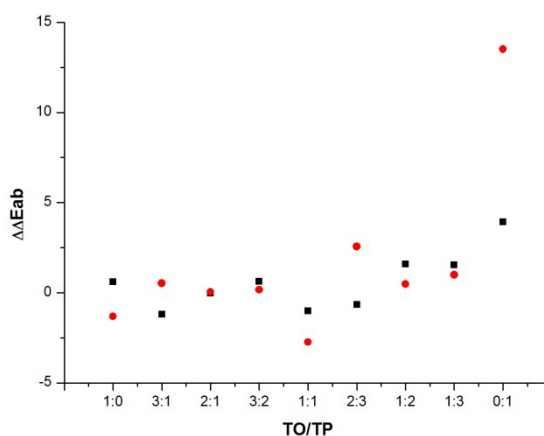


Figure 4.26: At the colorimeter determined $\Delta\Delta E_{ab}$ values for washing tests with water at varying temperatures and soil composition. ■: washing at 10 °C; ●: washing at 25 °C.

Detergent: Lutensol AO7

For washing with 1 wt% Lutensol AO7 at 10 °C instead of 25 °C the soil release is decreased, independently of soil compositions (Tab. 4.29 and Fig. 4.27). However, the impact is not the same pronounced for all compositions. These results are in

4. Results and Discussion

agreement with the previous observation that with decreased fraction of crystalline triglyceride the soil release decreases.

Table 4.29: At the colorimeter determined $\Delta\Delta E_{ab}$ values for washing tests with water at varying temperatures with cotton fibers soiled with varying TO/TP compositions.

<i>soil</i>	10 °C	25 °C
	$\Delta\Delta E_{ab}$	$\Delta\Delta E_{ab}$
<i>TO</i>	5.15	12.80
<i>TO/TP = 3:1</i>	9.43	14.97
<i>TO/TP = 2:1</i>	14.23	16.93
<i>TO/TP = 3:2</i>	12.55	23.47
<i>TO/TP = 1:1</i>	8.30	18.82
<i>TO/TP = 2:3</i>	14.39	20.24
<i>TO/TP = 1:2</i>	12.42	18.84
<i>TO/TP = 1:3</i>	12.33	28.43
<i>TP</i>	19.83	31.78

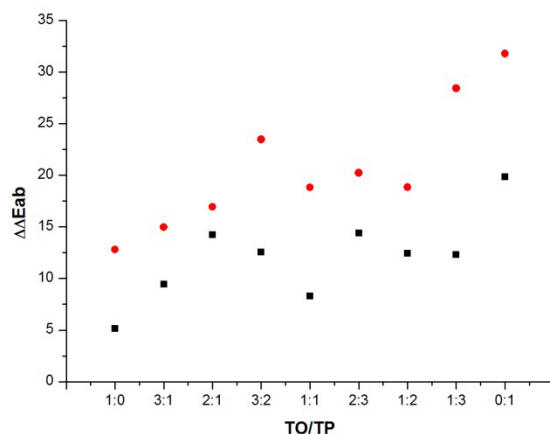


Figure 4.27: At the colorimeter determined $\Delta\Delta E_{ab}$ values for washing tests with water at varying temperatures and soil composition. ■: washing at 10 °C; ●: washing at 25 °C.

4.3.2.2.4 Washing at room temperature with thickeners

In order to determine the influence of viscosity on the washing efficiency of detergents, a 1 wt% solution of Lutensol AO7 was thickened and the washing results were compared with the results gained for not thickened solution.

Therefore, various thickeners were tested in order to find one which does not interact with the surfactant. Our criterion for a suitable thickener was the formation of a clear solution after the addition to a 1 wt% solution of Lutensol AO7. The thickener of choice was culminal MHPC 500PF, a nonionic cellulose ether. For the addition of 2.4 wt% thickener the viscosity of the washing liquor increased from 1.39 mPas to 170 mPas.

Table 4.30: At the colorimeter determined $\Delta\Delta E_{ab}$ values for washing tests with 1 wt% solution of Lutensol AO7 with and without thickener culminal and not at room temperature with cotton fibers soiled with varying TO/TP compositions.

	<i>with thickener</i>	<i>without thickener</i>
soil	$\Delta\Delta E_{ab}$	$\Delta\Delta E_{ab}$
TO	2.78	12.80
TO/TP = 3:1	2.80	14.97
TO/TP = 2:1	3.05	16.93
TO/TP = 3:2	4.08	23.47
TO/TP = 1:1	5.27	18.82
TO/TP = 2:3	5.10	20.24
TO/TP = 1:2	5.40	18.84
TO/TP = 1:3	12.97	28.43
TP	17.28	31.78

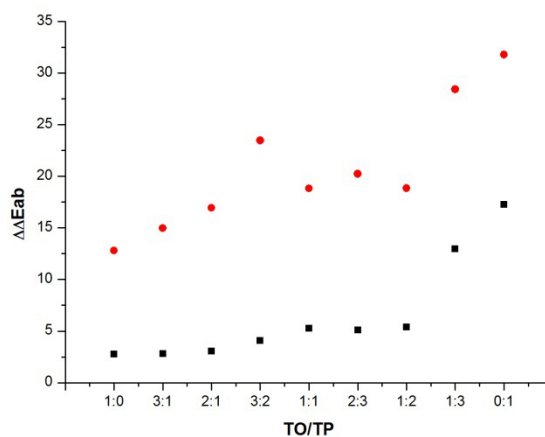


Figure 4.28: At the colorimeter determined $\Delta\Delta E_{ab}$ values for washing tests with water at varying temperatures and soil composition. ■: washing at 10 °C; ●: washing at 25 °C.

4. Results and Discussion

With an increased viscosity of the washing liquor, the soil release decreases (Tab. 4.30 and Fig. 4.28). The higher the fraction of oily soil in contamination the stronger is the reduction of washing efficiency. The higher viscosity decelerates the diffusion of solvent and the dissolution of liquid components, accordingly. Therefore, the magnitude of tripalmitin release is slightly better than for washing with pure water, a washing agent in which the diffusion of washing active agents also does not contribute to washing efficiency.

4.3.3 Conclusion

From the results of washing tests performed with cotton fibres soiled with mixtures of varying composition TO/TP it can be concluded that triglyceride solubilisation as well as mechanical impact are important for a good washing result.

Testing pure water at room temperature as well as at 40 °C and 10 °C has given that the lack of surfactant and, accordingly, of triglyceride solubilisation makes it impossible to release soil mixtures containing liquid components acting as a glue. However, pure TP can be released partially due to the mechanical impact during laundry but less than for washing with washing liquors containing a surfactant. Changing the temperature has an influence on the state of matter of TP, accordingly the soil release is decreased for higher washing temperatures and increased for decreased temperatures.

Washing with a solution of 1 wt% Lutensol AO7 at varying temperatures give the same observations. With increasing temperature the fraction of liquid triglyceride is increased and the soil release decreased. As can be seen for all further washing tests, the higher the fraction of crystalline triglyceride the higher the washing efficiency in washing test of cotton fibres.

Lutensol AO7 gives the best washing results. The addition of any additives like surfactant, cosurfactant, emulsifier and oil declines the results. They interact with Lutensol AO7, hindering the interaction between surfactant and soil. Therefore, less triolein is dissolved and less tripalmitin can get broken up mechanically.

The comparison of washing results of 1 wt% Lutensol AO7 solution with continuous and bicontinuous microemulsions gives higher washing efficiency for pure surfactant solution. Furthermore, it was found that bicontinuous microemulsion delivers better results than continuous one. However, the viscosity of continuous

microemulsion is distinctively higher than of bicontinuous one. Accordingly, the influence of viscosity on soil release was determined by thickening a 1 wt% solution of Lutensol AO7. It was found that with increasing viscosity the washing efficiency decreases. Therefore, the less soil release with continuous microemulsion might result from the higher viscosity and decelerated diffusion and dissolution of oily soil component.

From testing pure water we know for sure that surfactants are important for the washing process, therefore, the decrease of the solubility temperature is one potential contribution to decrease the washing temperature. A well known opportunity to reduce the solubility is the addition of additives like salts and osmolytes. Therefore, in the following section the influence of various osmolytes on the Krafft temperature of sodium dodecyl sulphate and sodium dodecyl carboxylate was investigated.

As already mentioned in the fundamentals, common laundry detergents consist of at least eight components. Accordingly, the investigated detergents within this work are far away from formulations which could be used in household laundry. But the limitation on only surfactant, cosurfactant and oil enables to determine the influence of structuring, temperature and viscosity.

4.4 The influence of osmolytes on the Krafft temperature

4.4.1 Introduction

Due to environmental and economical concerns reduced washing temperatures and biocompatible surfactants are desired. However, the washing result should be still the same or even better. A precondition for low washing temperatures is a sufficient solubility of the used surfactants. However, the oldest and most common surfactants, sodium and potassium carboxylates and alkyl sulphates, have Krafft temperatures (T_{Kr}) above room temperature; accordingly, they are not suitable for washing with cold water [92]. The Krafft temperature is the temperature at which the solubility of the surfactant is equal to the critical micellar concentration (cmc) and increases by orders of magnitude [247]. It is commonly defined as the clearing temperature of a 1 wt% ionic surfactant solution, since the cmc is generally far below 1 wt% [248]. Generally, the Krafft point is determined by two competitive thermodynamic forces. The competing energies are the free energy of the solid crystalline state and of the micellar solution. A good packing of surfactant head group and counterion increases the crystal stability and accordingly the solubility temperature. A low free energy of the micellar solution favours the dissolved state. The packing ability of the micelles and the head group/counterion interactions are relevant here [92]. With increasing alkyl chain length of alkylcarboxylates the surface activity, the washing ability and its solubilising power increases, but also the Krafft temperature increases [248-250]. However, it was found that the solubility temperature of ionic surfactants is strongly dependent on the head group and the counterion [251]. In several studies it was shown that the T_{Kr} can be reduced by replacing the alkali ion by quaternary ammonium ions [252, 253]. Admittedly, most of the quaternary ammonium ions are toxicologically critical due to acting as phase transfer catalysts and transporting ions across biological membranes [254, 255].

But also the addition of electrolytes to solutions of alkali surfactants influences the solubility and accordingly the Krafft temperature. Ions can be salting-in or salting-out. A systematic study was performed initially by Franz Hofmeister in 1888 [256]. Based on his work, ions are classified according to their charge density which influences their water affinity. Small anions with a high charge density have a high water affinity - they are called kosmotropic - and are salting-out [97]. Chaotropic

ions (low charge density) interact more strongly with chaotropic counterions than with kosmotropic ones, according to Collins' concept of matching water affinities, whereas kosmotropic ions interact more strongly with kosmotropic ones [117, 183]. This fact enables the use of classical laundry surfactants as washing active substance at low temperatures by adding additives decreasing the Krafft temperature.

In the context of our study it is important to note that alkylcarboxylates are known to be more kosmotropic than alkylsulphates [117]. Consequently more chaotropic cations should interact more strongly with alkylsulphates, resulting in an increased Krafft temperature. Probably, specific interactions of sodium alkylsulphates and alkylcarboxylates with common biological additives will also increase or reduce the solubility temperature of these surfactants. In particular, so-called osmolytes, which are known to act as protein-stabilizing salting-out agents but without direct interaction with proteins are considered [257-262]. A synonym for osmolyte is compatible solute. They are small organic molecules which are nonionic at physiological pH, but polar and bind a significant number of water molecules. If this binding is strong, they should be kosmotropic, otherwise they are chaotropic. Even for very high concentrations in cytoplasm they do not influence the cell metabolism [263-265]. Natural protein protecting osmolytes can be classified into three groups: polyols, amino acids (and derivatives thereof) and methylamines [258, 259]. L-proline is a common amino-acid. L-carnitine, betaine and ectoine can be chemically or biologically produced from common amino-acids and L-carnitine, betaine and Trimethylamine oxide are osmoprotectants of the methylamine class. L-Carnitine and betaine are a member of both groups, amino acids derivatives and methylamines. In the following, however, they will be discussed only within the methylamine group. Trehalose is a sugar and can be considered as a polyol. It is the only none zwitterionic additive for investigated conditions and is typical of non halophilic and halotolerant organisms like *E.coli*. It is synthesized and accumulated in the cytoplasm. The other investigated osmolytes are typical for enhanced salt tolerant organisms and are either accumulated by de-novo synthesis or by uptake from media. The latter one is the energetically preferred way [263-265].

It seemed logical to study the effects of common osmoprotectants like L-proline, L-carnitine, betaine, ectoine and the nonionic trehalose on the solubility temperature of micelles, as the later were often proposed as models for proteins in solutions (Tab. A3).

L-lysine was added to this study because this molecule was known to be implicated in the biological function of fatty acid transport and binding proteins (Tab. A3). This

4. Results and Discussion

function supposes then a contact of lysines with the fatty acids but drive also certainly to a reduction of the solubility temperature of the more hydrophobic fatty acid in the blood. This aspect seemed to be in an interesting opposition of action in contrast with the probable mode of action of osmoprotectant molecules, but can be also an interesting way to improve washing processes.

Biological relevance of investigated additives

a) Trehalose

Sugars are commonly used for food preservation [266]. Globular proteins are denatured in the presence of sugar, resulting in an increased melting point and for very high sugar concentrations the textural consistency prevents microbial attack in food [264]. These phenomena might result from water/sugar interaction. It was observed that the sugar concentration, mainly trehalose, increases during dehydration and the cells do not degrade and biomolecules maintain their native conformation by subsequent rehydration. Some organisms can survive water contents below 20 %. Accordingly, trehalose received great attention as potential natural preservative [267-269].

Within this study it is the only nonionic investigated osmoprotectant. It is a binary, non reducing sugar consisting of two α,α' -1,1 glycosidically linked glucose molecules [270, 271]. It is found in mushrooms, drought-adapted organisms, spores, yeasts and further more [272, 273]. All these organisms are able to produce trehalose under arid conditions.

b) L-Lysine

L-Lysine is an essential, basic proteinogenic amino acid. It influences the serotonin receptors. Hence it could be shown to be helpful for the therapy of anxiety state [274]. Further, it turned out to support cancer therapy [274]. It has a second amino group in ϵ position. The pK_a values are: $pK_{COOH} = 2.2$, $pK_{\alpha-NH_3^+} = 8.90$ and $pK_{\epsilon-NH_3^+} = 10.28$ [275].

c) L-Proline

Proline is a heterocyclic, zwitterionic not essential proteinogenic amino acid. Proline is necessary for the formation of collagen [276]. It serves as a precursor of hydroxyl proline which is a module of collagen [276]. The pK_a -values are: $pK_{COOH} = 1.99$ and $pK_{NH_3^+} = 10.60$ [277].

d) Ectoine

Ectoine is a cyclic imino acid. It is one of the most commonly found osmolytes in nature and was first discovered in *Ectothiorhodospira halochloris* [278-280]. It is strongly water binding and commercially used in skin care products and sunscreen. It stabilizes the structure of proteins, nucleic acids and biological membranes. Hence, it protects the skin from damages by stress factors like UV-radiation, dryness, heat or cold [281-284]. Accordingly, it is used to stabilize proteins and cells during freezing. It also induces a lasting increase of moisture and protects the immune system of skin [285-289]. Ectoine possesses the structural properties of betaines as well as of proline. It has the same charge and charge density as betaines and it has a ring structure of acetylated diamino acids similar to proline [290]. It is zwitterionic in aqueous solutions [283, 290, 291].

The biosynthetic pathway for ectoine biosynthesis is linked with the biosynthesis of L-threonine, L-methionine and L-lysine (Fig. 4.29) [292]. The main limiting factor for ectoine biosynthesis is aspartate kinase.

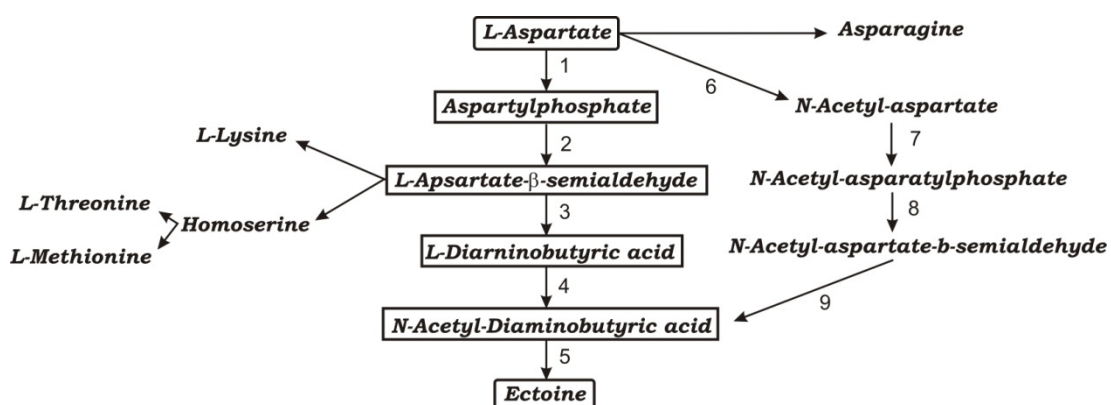


Figure 4.29: Biosynthetic pathway of the compatible solute ectoine (framed compounds). 1: L-Aspartate-kinase; 2: L-Aspartate- β -semialdehyde dehydrogenase; 3: L-2,4-diaminobutyric acid transaminase (*ectB*); 4: L-2,4-Diaminobutyric acid N- γ -acetyltransferase (*ectA*); 5: L-ectoine synthase (*ectC*); 6: L-Aspartate acetyl transferase; 7: N-Acetyl aspartokinase; 8: N-Acetyl-aspartate- β -semialdehyde dehydrogenase; 9: N-Acetyl-aspartate- β -semialdehyde transaminase.

e) Trimethylamine oxide

TMAO is a well known natural osmoprotectant, found in fish cells and helps preserving an isoosmotic situation within the micelles as compared to the outer salt water [293]. The protein stabilizing effect of TMAO was further shown by the fact that in presence of TMAO the required urea concentration for protein denaturation is increased [294].

f) Betaine

Betaine is a derivated glycine and an oxidation product of choline [295]. It is a quaternary ammonium compound carrying three methyl groups. It is an important donor of methyl groups for transmethylation in organisms for example for synthesis of creatine, methionine, lecithine and carnitine. Betaine is an amphoteric compound and in contrast to zwitterions like amino acids, the contrary charges can not be compensated by proton transfer. In combination with folic acid, vitamin B6 and B12 it is supposed to decrease increased homocysteine values in human blood. Accordingly, it is protective against arteriosclerosis [295].

g) L-Carnitine

L-Carnitine is one of the most discussed dietary supplements for athletes. It is present in every human cell, however the concentration depends, beside further factors, strongly on gender, age, dietary and physical stress. It is a kind of vitamin and plays an essential role for fat burning and energy production in the human body and for further biochemical processes. It was shown that the growth of rats with lack of carnitine was retarded. Various studies indicate, carnitine dietary supplements increase the activity and accelerate regeneration of athletes. Carnitine is also supposed to have a positive influence on the immune system [296].

L-Carnitine is known for its catalytic function as carrier of long chain fatty acids from the cytosol to the mitochondrial membrane where the β -oxidation takes place [297-299]. L-carnitine is a betaine, physiologically synthesized from the essential amino acids methionine and lysine (Fig. 4.30) [296, 300]. Precondition for the biosynthesis is a sufficient supply of vitamin C, B3, B6, B12, folic acid, iron and the essential amino acids. A lack of these reduces the rate of biosynthesis. Also a lack of riboflavin lowers the L-carnitine level because it is required for the protein turnover. The synthesis takes place in several human organs. The first four steps are executed in the skeletal muscles. The first step of the endogenous synthesis is the methylation of lysine by the methyl groups provided from methionine [301-305]. In the next step trimethyllysine is released which is oxidized in several steps to γ -butyrobetaine by trimethyllysine dioxygenase (TMLD), 3-hydroxy-N-trimethyllysine aldolase and butyrobetaine aldehyde-dehydrogenase [304]. Afterwards γ -butyrobetaine is hydrolyzed to carnitine by γ -butyrobetaine dioxygenase (γ -BBD) [302, 306].

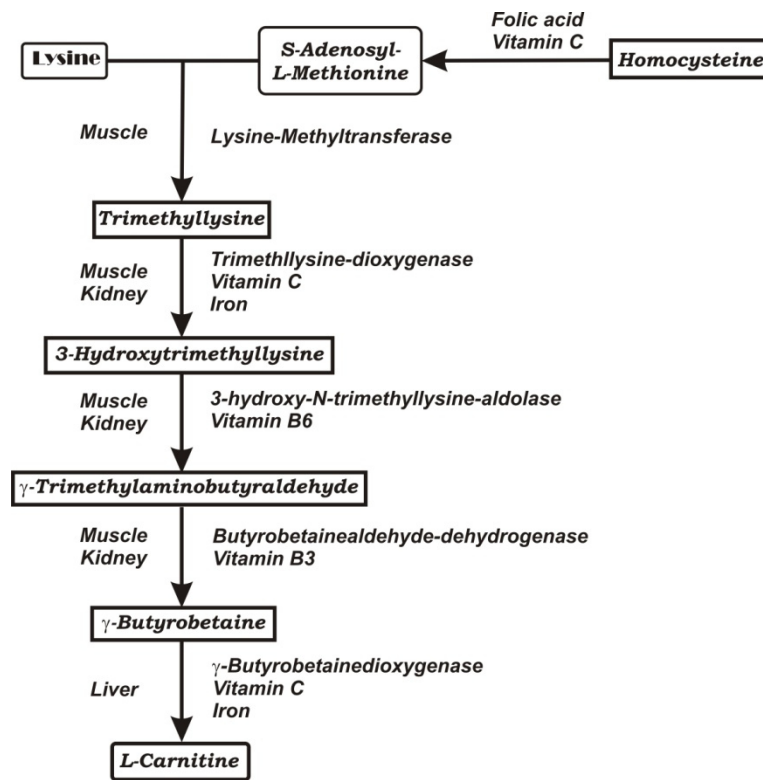


Figure 4.30: Schematic biosynthesis of L-carnitine.

4.4.2 Results

4.4.2.1 Small additive concentrations

Except of lysine, for all additives it is found that at very small additive concentrations (< 0.05 mol/L) the reduction of the Krafft temperature is very small (Fig. 4.31). The deviation of values for $c=0$ mol/L gives the error of the method. It is about 3 °C for SDC and about 1.5 °C for SDS.

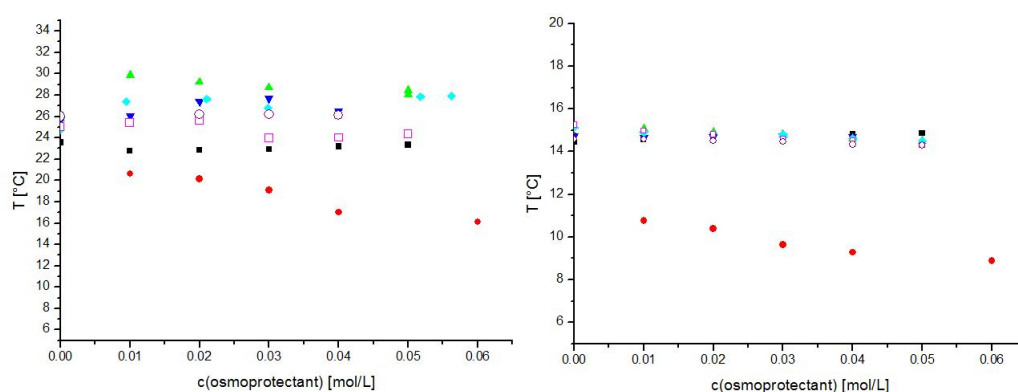


Figure 4.31: Influence of osmoprotectant concentration of trehalose (■), lysine (●), proline (▲), TMAO (▼), betaine (◆), carnitine (□) and ectoine (○) on the solubility temperature of a 1 wt% solution of SDC (left diagram) and of a 1 wt% solution of SDS (right diagram), respectively.

4.4.2.2 High additive concentrations

4.4.2.2.1 Trehalose

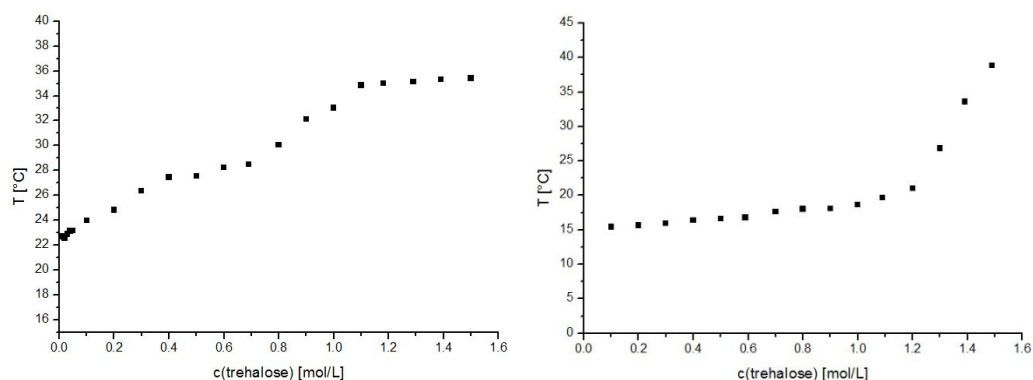


Figure 4.32: Influence of trehalose concentration on the solubility temperature of a 1 wt% solution of SDC (left diagram) and of a 1 wt% solution of SDS (right diagram), respectively.

The addition of trehalose significantly increases the Krafft temperature of both surfactants (figure 4.32). For SDC the increase is nearly linear with increasing trehalose concentration. For concentrations higher than 1.1 mol/L a plateau is reached. In the case of SDS the Krafft temperature is nearly constant for concentrations below 1.1 mol/L and increases at higher additive concentrations.

4.4.2.2.2 Amino acid and amino acid derivatives

a) Amino acids

The influence of L-lysine and L-proline on the Krafft temperature of SDS and SDC is depicted in figure 4.33. According to the pKa values of L-lysine ($pK_{\text{COOH}} = 2.2$, $pK_{\alpha\text{-NH}_3^+} = 8.90$ and $pK_{\epsilon\text{-NH}_3^+} = 10.28$) the carboxyl group is deprotonated and the $\epsilon\text{-NH}_3^+$ group is protonated for both the SDC and the SDS solution. The $\alpha\text{-NH}_3^+$ group is partially protonated in the SDC samples and completely deprotonated in the SDS samples.

According to the pKa values of L-proline ($pK_{\text{COOH}} = 1.99$ and $pK_{\text{NH}_3^+} = 10.60$) the carboxylic group is deprotonated and the amino group protonated for both surfactant systems at the investigated conditions.

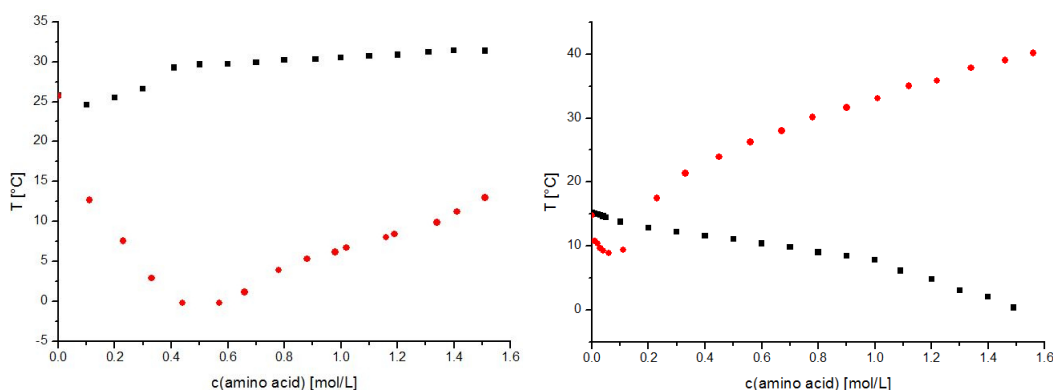


Figure 4.33: Influence of the amino acid concentration of lysine (●) and proline (■) on the solubility temperature of a 1 wt% solution of SDC (left diagram) and of a 1 wt% solution of SDS (right diagram), respectively.

For small L-lysine concentrations the Krafft temperature of both surfactants decreases (Fig. 4.33). The decrease is more pronounced for the SDC samples than for the SDS samples. For concentrations above 0.1 mol/L the solubility temperature of SDS increases sharply. The solubility temperature of SDC decreases until a salt addition of about 0.5 mol/L. At higher concentrations of additive the Krafft temperature also increases.

4. Results and Discussion

At low proline concentrations the solubility temperature of SDC decreases slightly and increases slightly for concentrations above 0.1 mol/L proline. Whereas the solubility temperature of SDS decreases continuously with increasing concentration of proline.

b) Cyclic, derivated amino acid

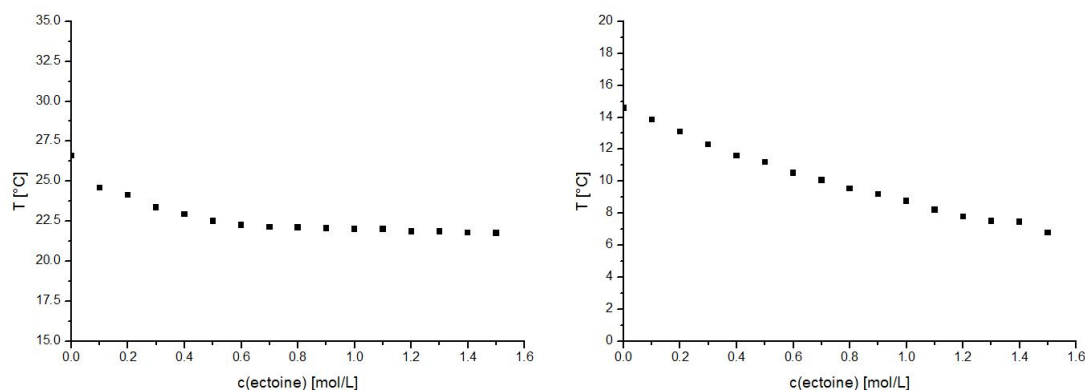


Figure 4.34: Influence of the ectoine concentration on the solubility temperature of a 1 wt% solution of SDC (left diagram) and of a 1 wt% solution of SDS (right diagram), respectively.

Upon the addition of ectoine the Krafft temperature of both surfactants decreases (Fig. 4.34). For SDS the decrease is more pronounced than in the case of SDC. And at concentrations higher than 0.6 mol/L the T_{Kr} of SDC remains nearly constant.

c) Methylamines

The influence of TMAO, L-carnitine and betaine (all of them are methylamines) on the Krafft temperature of SDC and SDS is shown in figure 4.35.

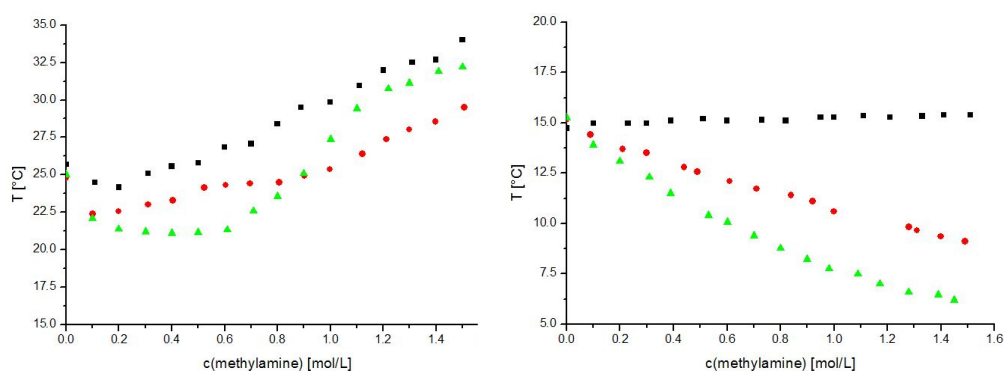


Figure 4.35: Influence of the methyl amine concentration of TMAO (■), betaine (●) and L-carnitine (▲) on the solubility temperature of a 1 wt% solution of SDC (left diagram) and of a 1 wt% solution of SDS (right diagram), respectively.

As can be seen from figure 4.35, TMAO only influences the T_{Kr} of SDC, whereas it does not change the solubility of SDS at all, even at high concentrations of osmolytes (Fig. 4.35). The Krafft temperature of SDC decreases at small TMAO

concentrations and increases then continuously with increasing osmolyte concentration above 0.3 mol/L.

For betaine at low concentrations the solubility temperature of both surfactants decreases (Fig. 4.31). At concentrations above 0.1 mol/L the Krafft temperature of SDC increases, whereas the solubility temperature of SDS still decreases (Fig 4.35). The decrease of the Krafft temperature of SDS is smaller for betaine than for carnitine (Fig. 4.35). For carnitine concentrations below 0.6 mol/L the Krafft temperature of SDC decreases, but for higher concentrations it increases (Fig. 4.35). The trend of SDC solubility is the same as for betaine but the kink is shifted towards higher osmolyte concentration. According to the pKa values of betaine (pKa = 1.83) and carnitine (pKa = 3.8) the carboxyl groups of both are completely deprotonated at the investigated condition in the SDC as well as in the SDS solution [307].

4.4.3 Conclusion

To describe the influence of osmolytes on the Krafft temperature of surfactants various effects have to be taken into account. According to Collins the sulphate head group interacts more strongly with chaotropic cations like trimethylamines than carboxylate does. Therefore, ionic interactions between surfactant and osmoprotectant are only observed for SDS. This ionic interaction results for non zwitterionic additives in an increased Krafft temperature of SDS, but for zwitterionic osmolytes the aggregate becomes more hydrophilic and the Krafft temperature decreases. A further effect is the water binding of osmoprotectants, resulting in dehydration of surfactant head group and thus a reduced solubility. Additionally, as shown by Marcus *et al.* osmolytes can have an effect on apparent pKa of SDC and therefore on its solubility [308].

The addition of osmolytes has an influence on either both, SDS and SDC, or at least one surfactant. For osmolyte concentrations lower than 0.05 mol/L the influence on the Krafft temperature of SDC and SDS is negligible, except for the addition of lysine. By trend, the Krafft temperature is reduced by the addition of osmolyte.

Trehalose is the only investigated additive which is not zwitterionic. Consequently, the increase of the Krafft temperatures of SDC and SDS with trehalose addition is not the result of ionic interactions. Former studies have shown that trehalose can also work as a protein denaturant [183]. The sugar is strongly water binding, thus effectively reducing the hydration of surfactant and the ionization of micelle. Due to the higher sensitivity of the apparent pKa of SDC towards additives and the lower SDC solubility, the increase of Krafft temperature of SDC is more pronounced than that of SDS.

For low lysine concentrations, a decrease of the Krafft temperature of both surfactants occurs. However, the Krafft temperature of SDS increases already at a lower additive fraction than the one of SDC does. This results from the different state of charge of lysine in the surfactant solutions. In the SDC solution the carboxyl group of lysine is completely deprotonated, the ϵ -amine group completely protonated and the α -amine group is partially protonated, accordingly it has a stronger influence towards the ionization of micelle and on apparent pKa of SDC. In the SDS solution the α -amine and the carboxyl group are completely deprotonated and the ϵ -amine group is protonated. The lysine appears less protonated in SDS

solutions than in SDC solution and it has nearly no influence on the apparent pKa of SDS. Therefore, the solubility in the SDS solution is lower than in the SDC solution. At low lysine concentrations the Krafft temperature of both surfactants decreases with increasing additive concentration. For SDC it is due to the change of apparent pKa, resulting in deprotonation of SDC. For SDS it results only from the increased hydrophilic character of formed SDS/lysine aggregate. It is less pronounced for SDS in function of concentration (Fig. 4.31). After exceeding a certain concentration the surfactants are completely deprotonated and the solubility can not be enhanced by the addition of lysine any longer. It can be speculated that lysine forms ion pairs with the surfactants resulting in a sort of highly water soluble double-dipole structure.

Proline has only a small influence on the Krafft temperature of SDC. The solubility temperature of the surfactant is slightly increased with increasing proline concentration. The decrease of soap solubility results from surfactant head group dehydration. But due to the weak hydration of proline the influence on the Krafft temperature is only small. However, the impact on SDS is more pronounced. According to Collins concept of matched water affinities a contact ion pair of sulphate head group and proline is formed, resulting in a more hydrophilic SDS/proline aggregate with increased solubility.

Except for pH 4, ectoine is zwitterionic in aqueous solutions [309]. The decrease of SDC Krafft temperature results from decreased apparent carboxylate pKa, leading to increasing micelle ionization. After exceeding 0.6 mol/L of additive, the Krafft temperature does not change, anyhow. There is currently no explanation for this behavior. By contrast, the increase of SDS solubility with the addition of ectoine might result from the ionic interaction of sulphate and amine groups of ectoine and the resulting increased hydrophilic character of the formed aggregate.

For low additive concentrations of the three methylamines the solubility temperature of SDC decreases. These results are in agreement with the observations of Klein *et al.*, who showed that ChCl and trimethylammonium chloride, also methylamines, are weakly associated to carboxylate compared as to sodium [247, 310]. For higher concentrations the osmolytes may act as co-surfactants and get incorporated in the interfacial film. Additionally, for high additive concentrations the strong ion-water interactions dominate, resulting in surfactant head group dehydration and Krafft temperature increase. After exceeding 1 mol/L of osmolyte concentration, the influence becomes non specific.

4. Results and Discussion

The Krafft temperature of SDS does not change for TMAO and decreases for the addition of betaine and carnitine. According to Collins, ionic interaction of trimethylamine group and sulphate head group occurs, resulting in a decreased solubility of surfactant. But due to the zwitterionic character of these three additives, the SDS/additive aggregate becomes more hydrophilic, resulting in a decreased Krafft temperature. For TMAO the negatively charged group is very close to the cationic group, resulting in only a weak dipole. As a result, its interaction with the head group is only weak and the solubility of SDS is not influenced by the addition of TMAO.

For L-carnitine the decrease of the Krafft temperature is more pronounced than for betaine. Due to that larger distance between cationic and anionic groups in L-carnitine, the intramolecular dipole moment of L-carnitine is stronger than that of betaine. Therefore, the aggregate appears more hydrophilic and the solubility increases more strongly. This new concept of salting in with zwitterionic compounds should be investigated in more details.

To sum up, the results show that the reduction of the Krafft temperatures of surfactants is linked to the nature of the additive and the surfactant. Zwitterionic additives such as lysine can significantly reduce the Krafft temperature of surfactants provided that:

- a) the positive and negative charges of the zwitterions are sufficiently separated and
- b) that there is a significant ion binding between one charge of the zwitterion and the opposite charge of the surfactant

The (although less pronounced) Krafft temperature lowering of SDS with L-carnitine further supports this hypothesis.

Obviously, the influence of the additives on the Krafft temperatures of the surfactants is the consequence of a subtle balance between various interactions. Among those are electrostatic and sterical interactions between head groups and ions, where ion and head group polarisabilities are important [311, 312]. Further, the change of head group hydration in the presence of additives plays also an important role, as well as pH. These results are a first and preliminary contribution to the study of surfactant-additive interactions beyond salts and co-surfactants. Despite of its preliminary character, they show that some natural additives, commonly used in formulation or other contexts, can indeed significantly lower the

Krafft points of important classes of surfactants. This finding is a first step towards washing with efficient longer-chain surfactants at low temperature.

4.5 NMR studies

4.5.1 Introduction

Still today many papers start with the statement that specific ion effects and especially the Hofmeister series are not yet understood. However, such a global conclusion is no longer valid. Significant progress has been made over the last twenty years. We quote only a few of the new insights:

- Collin`s concept of matching water affinities contributed much to a qualitative description of specific ion-ion and ion-head group interactions [119, 179]. Even rough predictions of ion behaviour in complex systems are possible.
- Since the landmark work by Jungwirth and Tobias it is clear that ions can adsorb into the first layer near the air-water interface, whereas the overall profile of the ion concentration shows depletion, in agreement with the Gibbs adsorption isotherm [311].
- In a recent work it was shown why different Hofmeister series may exist and why they can be partially or fully reversed, depending on the adjacent interface [313].

It seems to be clear now that the specific behaviour of an ion strongly depends on the ion`s environment and especially on the counterions. This is not a trivial statement, since it explains why engineers have difficulties to define single ion parameters.

Having now a basic understanding of specific ion effects and the related subtle balance between different interaction forces, it is tempting to go deeper and deeper into the details of such subtleties. But the danger is that we get lost in these details and that it is more and more difficult to infer generalisable trends. It is evident that spherical (e.g. chloride), linear (thiocyanate) and flat (nitrate) ions must behave differently at very short distances and that the structure of their hydration shells must be different, despite the same charge they bear. This is as true for ions as it is true for any other chemical species. Therefore, there is nothing to generalise when questions are asked that involve these details. As a consequence, related studies are only of limited value, because the results cannot be easily extended to other systems and situations.

Our conclusion is that it is important to answer the following two questions:

- (1) How specific are ion specificities? In which cases are predictions possible from general rules, in which cases does the ion behave so individually that

nothing can be predicted? Then only a particular experiment or simulation can help. We can formulate the problems in other terms: how close energetically are the states of different ions in similar systems? If they are very close, it is difficult or impossible to predict e.g. if there is a reversal of the ions in the Hofmeister series for that particular case or not.

- (2) When do specific ion effects appear? From numerous studies it is well-known that at very low concentrations ion interactions are dominated by electrostatic interactions and the Debye-Hückel theory is the appropriate description. No or minor specific ion effects are visible. At very high concentrations electrostatic interactions (now screened and therefore “only” short ranged) also dominate. For example even chaotropic ions begin salting out at sufficiently high concentrations. It is the intermediate concentration range, in which specific ion effects appear and this is also the concentration range of biological relevance.

Whereas this fact is well-known for the concentration range of the ions, it is much less investigated for the concentration range of the charged counterparts. For example, it would be interesting to study the relevance of specific ion effects close to charged membranes or layers as a function of their charge density-with possible impact on the understanding of biological systems.

In the following sections we tried to contribute to answer the first question. It is commonly accepted that according to Collins’ ideas more cosmotropic ions interact more strongly with more cosmotropic (oppositely charged) head groups and more chaotropic ions with more chaotropic head groups. For example lithium ions should have a stronger propensity to the head groups of alkylcarboxylate (cosmotropic) than sodium, and the contrary can be expected for alkylsulphate (a chaotropic head group) [179]. And rubidium ions should have a higher affinity to the head group of alkylcarboxylate than caesium ions [183]. The question is if the differences are comparably strong or if in one case the specificity is more pronounced than in the other case. A problem in the experimental determination of ion binding is to identify a well defined system where the measured parameters are directly related to ion binding, without other changes to the system.

To answer this question we performed NMR experiments in which we determined the quadrupole splitting of sodium (Δ_{Na}), lithium (Δ_{Li}), caesium (Δ_{Cs}) and rubidium (Δ_{Rb}) in lamellar liquid crystals. Amphiphile lamellar (L_α) phases consist of alternating surfactant and water layers (Fig 4.36).

4. Results and Discussion

The surfactant can be ionic, zwitterionic or nonionic, while the water layers can vary in thickness from ca. 1-2 nm up to >10 nm. Within the surfactant layers it is easy to mix different amphiphiles such as ionic surfactants and uncharged cosurfactants. Thus it is possible to vary both, the charge density of the amphiphile layers and the distance between opposing charged layers.

NMR spectroscopy is a possible method to monitor the behaviour of ions in liquid crystalline phases. In anisotropic media (such as a lamellar phase) the spectrum of ions like Na^+ , Li^+ , Cs^+ and Rb^+ (and many more) which possess a nuclear quadrupole moment is split into a number of peaks rather than the single peak observed in isotropic solutions. In the simplest case, for “well behaved” systems, the magnitude of the separation between the peaks (the quadrupole splitting, Δ) is proportional to the fraction of ions in contact with the head groups [209, 213]. Thus by measuring Δ it is possible to monitor how this fraction changes with composition, for example when competitive binding occurs (e.g. the displacement of sodium ions by lithium ions at an anionic surface). Both sodium and lithium ions possess a quadrupole moment, hence give multiple lines in the NMR spectra of anisotropic phases. Thus by selecting an appropriate lamellar phase system it should be possible to quantify the displacement of sodium ions by lithium ions from the changes in the Δ values of both. The objective of this initial study is to establish if a suitable system can be identified, where the changes in Δ reflect changes in ion-binding. If such a system can be found, then it should be possible to extend the studies to a very wide range of ions.

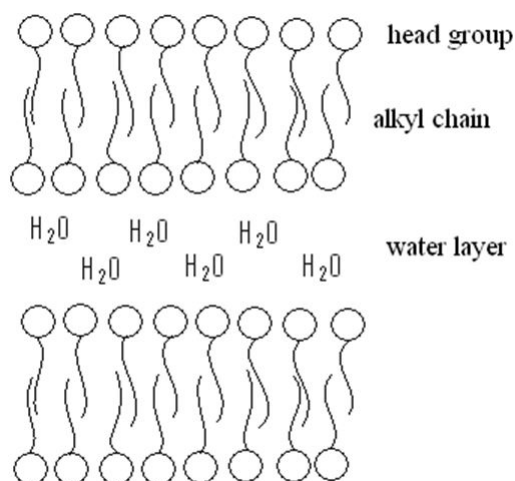


Figure 4.36: A schematic picture of a lamellar phase.

4.5.1.1 Lamellar phase-structure, charge density

The lamellar phase has a regular structure of repeating surfactant and aqueous layers, with the surfactant being organized in bilayers. Except for the restrictions on molecular configurations imposed by the layer structure, the system has liquid-like disorder. The repeat dimension of the structure can be measured by X-ray diffraction, hence the dimensions of the two layers can be calculated, provided that their densities are known [314]. In addition, the area per amphiphile can be calculated. Thus the charge density on the surface can be calculated precisely. Whilst we have not carried out X-ray measurements on the systems studied here, there is a substantial body of data available on similar systems [315-318]. These show that the area per amphiphile (a) for both sodium and potassium soaps in mixtures with decanol is of order 25–30 Å², and changes but little with water content. We were unable to find similar data for alkyl sulphates with octanol or decanol. The phase behaviours of alkylsulphates and carboxylates in water alone are known to be very similar as they are in the presence of cosurfactants [213, 315, 316]. Thus we take the area per amphiphile for the sulphate system to be similar to that of the carboxylate—probably slightly larger by 3–5 Å² [317]. We have studied two different ratios of surfactant/cosurfactant, these being 1:1 for the dodecyl sulphate/octanol system and 1:3 for the dodecyl carboxylate/octanol system. The lower charge density in the latter system was necessitated by the insolubility of the carboxylates. Taking the upper value of $a = 30$ Å² gives an area per charge of 60 Å² for the sulphate system, while for the carboxylate system we take the lower values of $a = 27$ Å² (area per charge = 108 Å²).

The ionic strength of the samples is very high and an estimate is given in table 4.31 and 4.32 for the carboxylate systems. Only the cations have been considered, whereas the carboxylate head group was ignored, hence the concentration of the ions in the water was halved. Since about 80% of the cations are bound to the head groups the effective ionic strength of the aqueous region is only about 20% of the calculated values. Similar, but somewhat higher values are estimated for the sulphate samples.

4. Results and Discussion

Table 4.31: Ionic strength of the sodium and lithium carboxylate samples for all compositions and all concentrations.

n(SDC):n(LiDC)	Ionic strength of Na (mol L ⁻¹)				Ionic strength of Li (mol L ⁻¹)				Total ionic strength (mol L ⁻¹)			
	25 wt%	35 wt%	45 wt%	55 wt%	25 wt%	35 wt%	45 wt%	55 wt%	25 wt%	35 wt%	45 wt%	55 wt%
0:1					0.23	0.33	0.22	0.55	0.23	0.33	0.43	0.54
1:4	0.05	0.05	0.09	0.11	0.19	0.27	0.35	0.42	0.24	0.33	0.43	0.52
2:3	0.09	0.13	0.17	0.22	0.14	0.19	0.26	0.34	0.23	0.33	0.44	0.55
1:1	0.12	0.17	0.22	0.27	0.11	0.17	0.22	0.27	0.23	0.33	0.44	0.54
3:2	0.14	0.20	0.26	0.32	0.09	0.13	0.18	0.21	0.24	0.33	0.44	0.54
4:1	0.19	0.27	0.35	0.43	0.05	0.07	0.09	0.11	0.24	0.33	0.43	0.54
1:0	0.23	0.33	0.43	0.54					0.23	0.33	0.43	0.55

Table 4.32: Ionic strength of the caesium and rubidium carboxylate samples for all compositions and all concentrations.

n(CsDC):n(RbDC)	Ionic strength of Cs (mol L ⁻¹)					Ionic strength of Rb (mol L ⁻¹)					Total ionic strength (mol L ⁻¹)				
	45 wt%	55 wt%	65 wt%	75 wt%	85 wt%	45 wt%	55 wt%	65 wt%	75 wt%	85 wt%	45 wt%	55 wt%	65 wt%	75 wt%	85 wt%
0:1						0.37	0.48	0.60	0.74	0.91	0.37	0.48	0.60	0.74	0.91
1:4	0.07	0.09	0.12	0.15	0.18	0.29	0.38	0.47	0.58	0.71	0.36	0.47	0.59	0.73	0.89
2:3	0.14	0.19	0.23	0.29	0.35	0.22	0.28	0.35	0.43	0.52	0.36	0.46	0.58	0.72	0.88
1:1	0.18	0.23	0.29	0.36	0.43	0.18	0.23	0.29	0.36	0.43	0.36	0.46	0.58	0.72	0.87
3:2	0.21	0.28	0.34	0.42	0.51	0.14	0.18	0.23	0.28	0.34	0.35	0.46	0.58	0.71	0.85
4:1	0.28	0.36	0.45	0.56	0.66	0.07	0.09	0.11	0.14	0.17	0.35	0.45	0.56	0.70	0.83
1:0	0.34	0.44	0.56	0.68	0.80						0.34	0.44	0.56	0.68	0.80

4.5.2 Results

4.5.2.1 Investigation of ^{23}Na and ^7Li nuclei

It is well known that lamellar phases are formed from mixtures of ionic surfactants with a long chain cosurfactant such as an alcohol [315, 316]. We have selected two ionic surfactants for study, dodecyl sulphate and dodecyl carboxylate, with sodium and lithium as counterions and octanol as the cosurfactant. These surfactants are thought to have very different specificities for Li or Na [179]. And lithium and sodium were selected due to their high sensitivity which makes them easy to measure with conventional multi-frequency high-resolution spectrometers. Additionally, they are reported to have different specific binding capabilities with different anions. Octanol is employed as a cosurfactant because it is necessary for the formation of lamellar phase. Our first step was to determine composition regions where a lamellar phases occur in dodecyl sulphate/octanol and dodecyl carboxylate/octanol mixtures for a reasonable range of water concentrations (45–75%). Then the ^{23}Na and ^7Li Δ values were measured as a function of water concentration at a fixed ratio of octanol/surfactant. Finally we selected several fixed values of the water concentration and measured the ^{23}Na and ^7Li Δ values as a function of the Na/Li ratio to investigate the binding competition.

Phase structure and NMR spectra

All of the samples examined appeared as single lamellar phases by polarising microscopy. However, there were problems with some compositions. Samples with 15% SDC/LiDC/octanol gave broad ^7Li NMR spectra without clear quadrupole splitting. This is discussed further below. For 65 and 75 wt% SDC/LiDC/octanol samples the spectra indicated that the samples were incompletely mixed. This is the composition region where solubility is most limited, and the samples were not examined further because of time constraints. In the ^{23}Na - and ^7Li -NMR spectra of the sulphate samples at 300 K and of the carboxylate samples at 300 K and 310 K a single quadrupole splitting was visible, except for the sample with 25 wt% with a composition of SDC : LiDC = 1 : 4, which shows no sodium splitting at 300 K.

In the figure. 4.37a and 4.37b typical ^{23}Na and ^7Li spectra of the carboxylate system can be seen. In the figure 4.38a and 4.38b typical ^{23}Na and ^7Li spectra

4. Results and Discussion

of the sulphate system are shown. (Note that the broad signal underlying the Na spectra arises from sodium in the glass NMR tubes.) All of these are typical powder patterns with a single quadrupole splitting.

The quadrupole splitting (Δ) is equal to one half the distance between the signals 1 and 1' and one quarter the distance between 2 and 2'. These distinct features can be seen for nearly all mixtures. In the sulphate as well as in the carboxylate systems the ^{23}Na splitting is much larger than the ^7Li splitting, the values of both being in good agreement with those in the literature [210, 319, 320]. In all of the spectra having well-defined powder patterns there is an asymmetry in their appearance (clearly visible in figure 4.38b). The outer features (2,2') are off-set compared to the inner peaks (1,1'). In addition, the central peak is asymmetric in shape. The cause is the well-known chemical shift anisotropy ($\Delta\sigma$) that occurs for liquid crystals [321]. This effect is very small, only ca. 100 Hz, but because the ^7Li splitting is small it is easily observed. We are currently examining the dependence of $\Delta\sigma$ for both the ^{23}Na and ^7Li spectra. It appears that $\Delta\sigma$ varies with the bulk compositions of the samples, rather than giving information on the molecular behaviour.

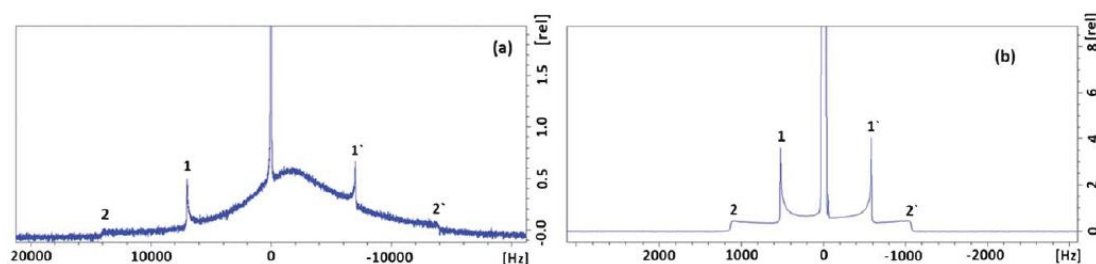


Figure 4.37: (a) ^{23}Na -NMR spectrum of a 35 wt% sample with a composition of SDC/LiDC = 2/3 at 300 K. The relative intensity of the signals is plotted against the frequency in [Hz]. (b) ^7Li -NMR spectrum of a 35 wt% sample with a composition of SDC/LiDC = 2/3 at 300 K. The relative intensity of the signals is plotted against the frequency [Hz].

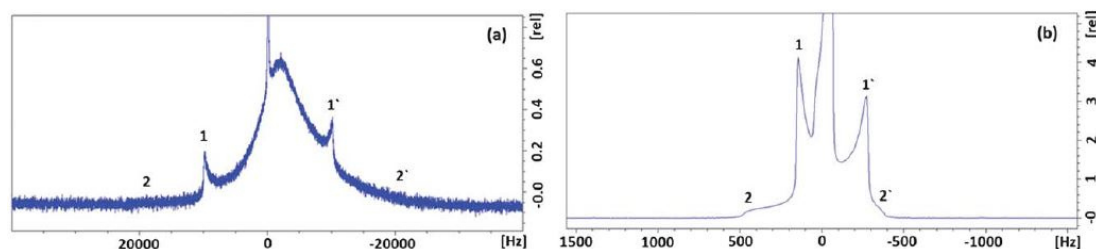


Figure 4.38: (a) ^{23}Na -NMR spectrum of a 65 wt% sample with a composition of SDS/LiDS = 2/3 at 300 K. The relative intensity of the signals is plotted against the frequency in [Hz]. (b) ^7Li -NMR spectrum of a 35 wt% sample with a composition of SDS/LiDS = 2/3 at 300 K. The relative intensity of the signals is plotted against the frequency [Hz].

Influence of surfactant concentration on the quadrupole splitting

In figure 4.39 the sodium and the lithium Δ values with increasing concentration are shown for the single ion systems. The lithium splittings are roughly constant for the carboxylate samples, as expected. However, the sodium splitting decreases with concentration in both the carboxylate and the sulphate samples, up to 65% after which it increases. Moreover, in the sulphate samples the lithium splitting also decreases with increasing concentration up to 65%. It seems highly unlikely that the ion binding would decrease with increasing surfactant concentration. Hence, as described above, we attribute this decrease to the existence of two distinct locations for the bound ions, one on the surface of the head groups (positive Δ values, Δ_{bs}) and the second, in between the head groups (negative Δ values, Δ_{bb}). Of course, these are average values since both sites will include ions having a distribution of positions. The increase in Δ values for the highest sulphate concentration simply represents the movement of ions from site bb to site bs because head groups move closer together.

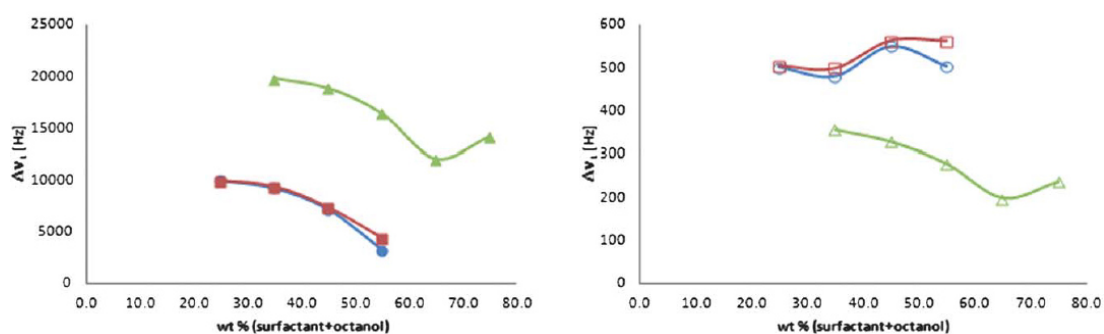


Figure 4.39: Sodium splitting with increasing concentration of surfactant and octanol (left) and lithium splitting with increasing concentration of surfactant and octanol (right). ● pure SDC at 300 K, ■ pure SDC at 310 K, ▲ pure SDS at 300 K, ○ pure LiDC at 300 K, □ pure LiDC at 310 K, △ pure LiDS at 300 K.

Ion specificity of carboxylate

The Δ values of ^{23}Na and ^7Li for a mixture of 25 wt% SDC/LiDC/octanol in D_2O in figure 4.40 show only a marginal increase at the higher temperature. Thus the fraction of ions in site bb is small. However, the sodium Δ values increase with increasing amount of sodium, while the lithium Δ values decrease with an increasing amount of lithium. Moreover, the relative magnitude of the changes is the same for both, but of opposite sign. That is strong evidence that the

4. Results and Discussion

changes in Δ values reflect changes in ion binding and that Li binding to carboxylate is stronger than Na. The addition of Li ions displaces Na ions from the surface, decreasing the Na Δ values. For the Li ions, the largest fraction of bound ions occurs at the lowest Li concentration, and this decreases with added Li ions because a larger fraction must replace the free Na ions. The data suggest that the fraction of bound Li ions is ca. 28% larger for the 0.2 fraction Li mixture than for the pure Li system.

Similarly to the 25 wt% sample, at 35 wt% the sodium splittings increase with increasing amount of sodium and the lithium splitting decreases with increasing fraction of lithium (Fig. 4.41). Hence, these results confirm the stronger binding of lithium to the carboxylate head group. The fraction of free sodium appears to increase by about 31% from pure SDC to 20% SDC, in agreement with the increased fraction of bound lithium ions.

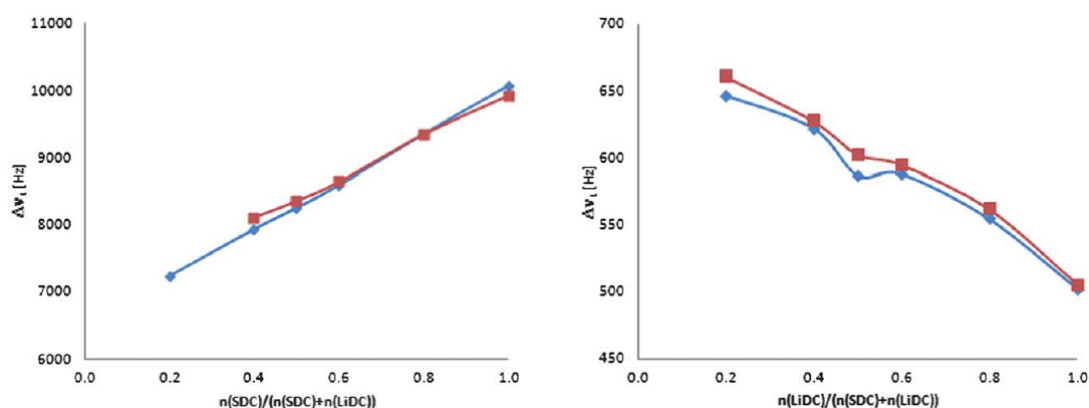


Figure 4.40: Sodium splitting with increasing amount of sodium (left) and lithium splitting with increasing amount of lithium (right) at 300 K and 310 K for 25 wt% SDC/LiDC/octanol in D_2O . \blacklozenge 300 K, \blacksquare 310 K.

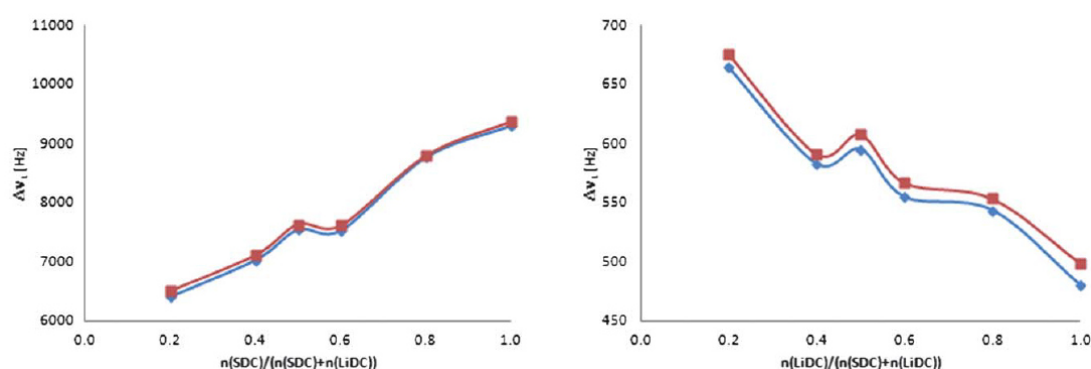


Figure 4.41: Sodium splitting with increasing amount of sodium (left) and lithium splitting with increasing amount of lithium (right) at 300 K and 310 K for 35 wt% SDC/LiDC/octanol in D_2O . \blacklozenge 300 K, \blacksquare 310 K.

The quadrupole splittings of the 45 wt% samples (Fig. 4.42) show the same trend as in the 25 and 35 wt% samples. The sodium splitting is lower than for the 35 wt% samples, while the lithium splitting is still the same. The amount of released sodium ions for this concentration is 24%, whereas the fraction of bound lithium ions apparently increases only by about 11%. However, note that as the concentration of surfactant increases, the temperature dependence of the Δ values increases, along with a decrease in the overall Δ values. The Δ values no longer show a monotonic change. Clearly, as well as the change in Δ values due to the displacement of Na by Li we also have a growth in the fraction of both ions in the bb site. With three sites and a single parameter we are in the fortunate position that almost any interpretation cannot be disproved. Note that irregular behaviour is shown for ca. 1:1 Li/Na mixtures. It appears that the Na ions favour the bb site over the Li ions, but that the Li ions still bind preferentially.

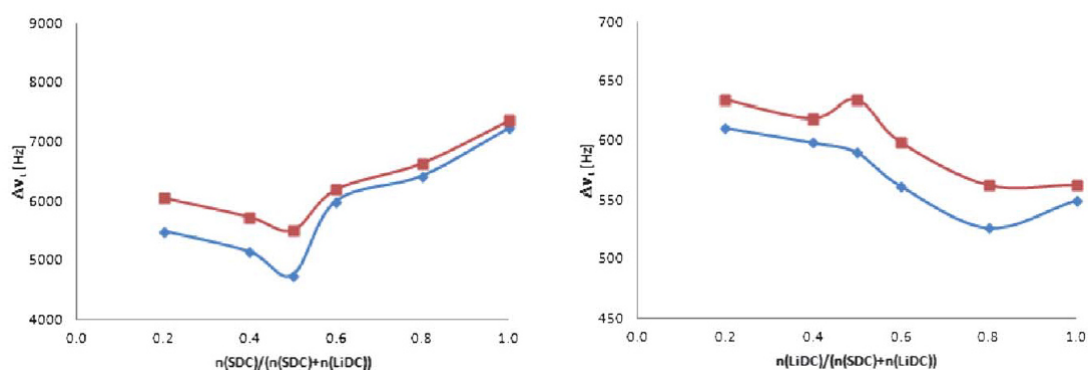


Figure 4.42: Sodium splitting with increasing amount of sodium (left) and lithium splitting with increasing amount of lithium (right) at 300 K and 310 K for 45 wt% SDC/LiDC/octanol in D_2O . \blacklozenge 300 K, \blacksquare 310 K.

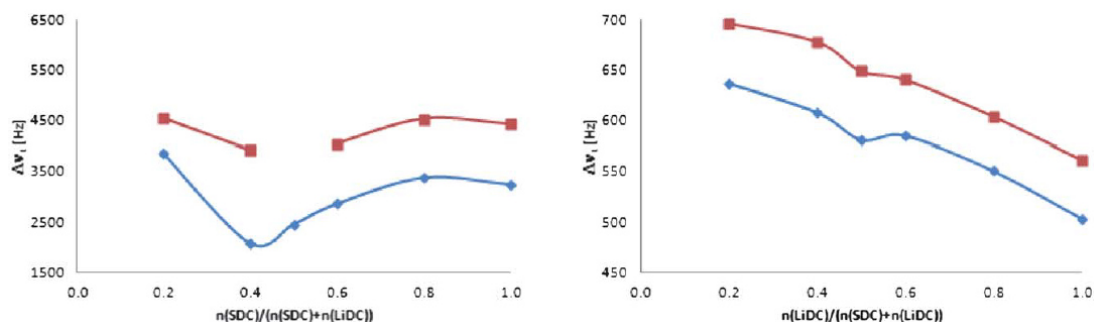


Figure 4.43: Sodium splitting with increasing amount of sodium (left) and lithium splitting with increasing amount of lithium (right) at 300 K and 310 K for 55 wt% SDC/LiDC/octanol in D_2O . \blacklozenge 300 K, \blacksquare 310 K.

This fortunate position continues with the trends of the 55 wt% samples (Fig. 4.43). The sodium splitting is lower than in the more dilute samples and is

4. Results and Discussion

nearly the same for all compositions, except the 40% SDC sample at 300 K. The lithium splitting is the same as the more dilute samples. The splitting decreases with increasing fraction of lithium in the samples. The increase in bound lithium is about 26%.

In summary, all measurements have explicitly shown that lithium binds more strongly to the carboxylate head group than sodium. In addition, the Li ions favour the bs-site over the bb-site.

Ion specificities of sulphate

For this system the lamellar phase concentration range with a ratio of surfactant/octanol of 1:1 was 35–75 wt% SDS/LiDS/octanol in D₂O.

In figure. 4.44 the sodium and the lithium splitting of the 35 wt% samples with an increasing fraction of sodium and lithium respectively is shown. Both splittings remain nearly constant for all compositions. Hence sulphate does not show any ion specificity towards sodium or lithium for this composition.

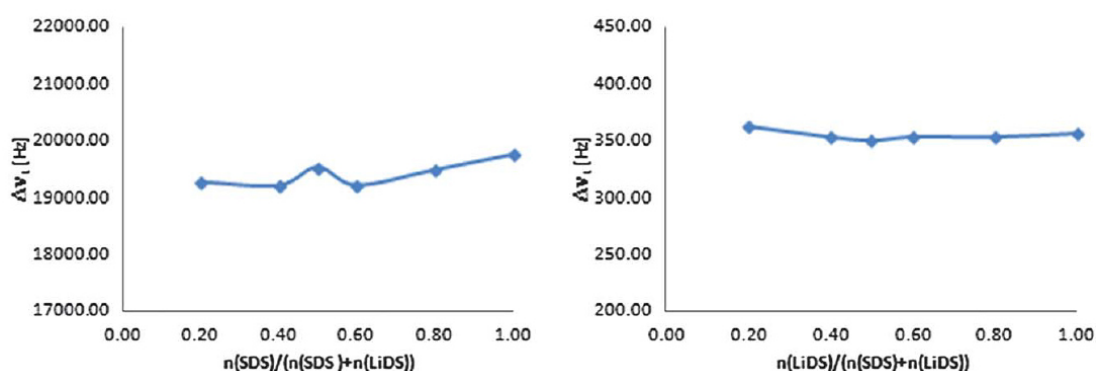


Figure 4.44: Sodium splitting with increasing amount of sodium (left) and lithium splitting with increasing amount of lithium (right) at 300 K for 35 wt% samples.

Similarly, for the 45, 55 and 65 wt% samples (Fig. 4.45-4.47), the Δ values show only small changes with varying amounts of sodium and lithium. The marginal change of the splittings is a hint only of a slight preference of the sulphate head group to sodium. If the three site model is used, the non-monotonic behaviour points to a slight preferential location of Na ions in the bb site. Rather than at 1:1, the most irregular behaviour occurs at ca. 1:4 Li/Na mixtures.

For the 75 wt% SDS/LiDS/octanol in D₂O samples (Fig. 4.48) the sodium splitting decreases with increasing amount of sodium except for pure SDS in octanol and water. In the 80% sodium sample the fraction of bound sodium in

the bb site is 24% higher than in the 20% sodium sample. Admittedly the trend of the lithium splitting is not coincident with the sodium splitting ones. The ion specificity of the sulphate head group towards sodium and lithium is much less pronounced than the ion specificity of the carboxylate head group.

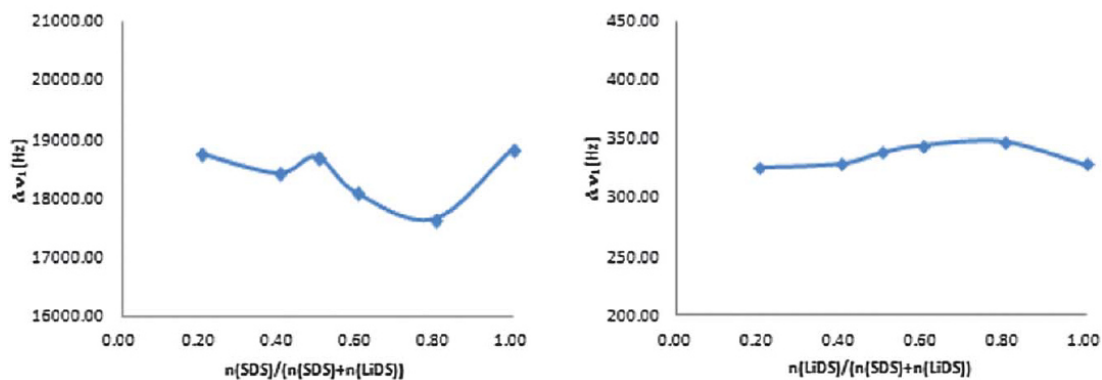


Figure 4.45: Sodium splitting with increasing amount of sodium (left) and lithium splitting with increasing amount of lithium (right) at 300 K for 45 wt% samples.

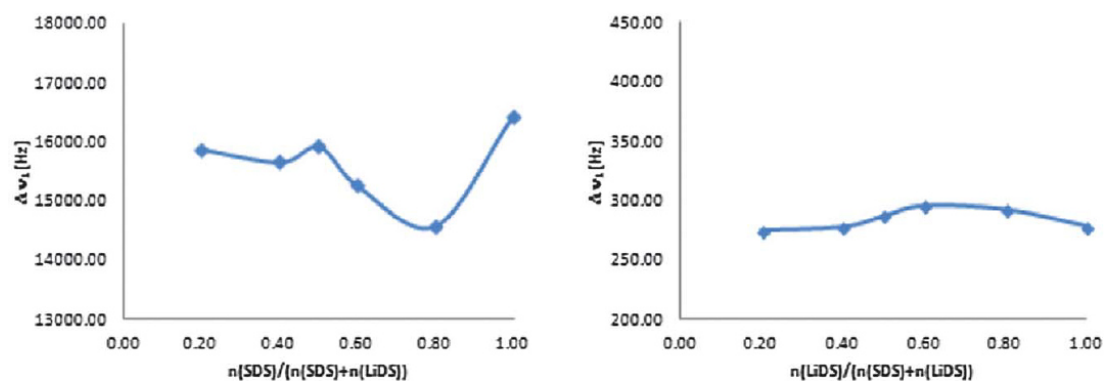


Figure 4.46: Sodium splitting with increasing amount of sodium (left) and lithium splitting with increasing amount of lithium (right) at 300 K for 55 wt% samples.

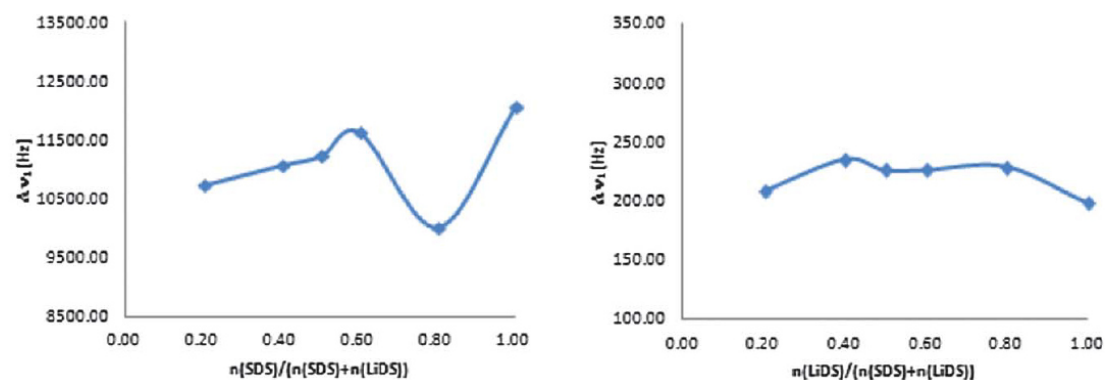


Figure 4.47: Sodium splitting with increasing amount of sodium (left) and lithium splitting with increasing amount of lithium (right) at 300 K for 65 wt% samples.

4. Results and Discussion

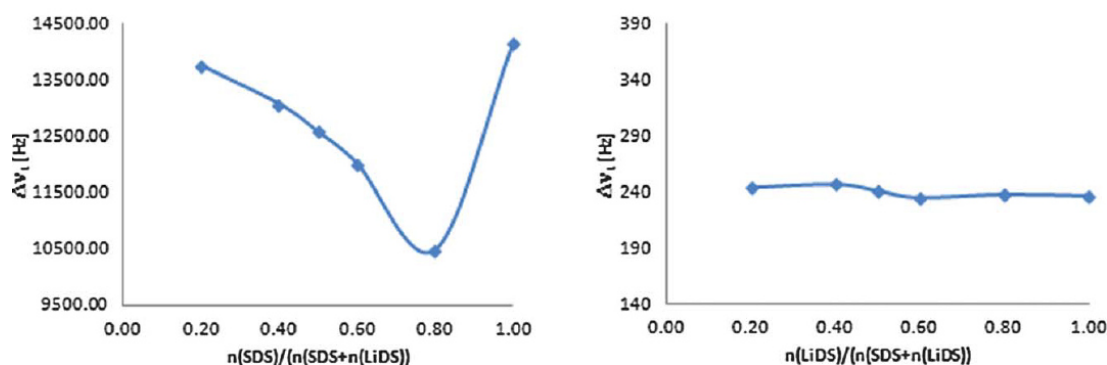


Figure 4.48: Sodium splitting with increasing amount of sodium (left) and lithium splitting with increasing amount of lithium (right) at 300 K for 75 wt% samples.

Discussion

From the results presented in the last section, several conclusions can be drawn.

The quadrupole splitting clearly reflects differences in the local environment of lithium and sodium in liquid crystalline systems made up with carboxylate surfactants and octanol as cosurfactant. The specific ion effects can be interpreted as a preferred propensity of lithium towards carboxylate as compared to sodium. The specificity is more pronounced at smaller absolute surfactant/cosurfactant concentration (35 wt%), whereas the temperature effect is more pronounced at higher surfactant/cosurfactant concentration. In the case of the corresponding sulphate system it turns out that specific ion effects are less pronounced.

For a more detailed interpretation several other factors have to be taken into account. The first is the total ionic strength. Depending on the models and estimations for bound ions, it varies between 0.1 and 0.3 M, which is typically the concentration range for which specific ion effects can be expected.

The second parameter is the area per charge, which is about 108 \AA^2 for the carboxylate systems and about 60 \AA^2 for the sulphate systems. Note that the surfactant/cosurfactant ratio is 1:1 for the sulphate and 1:3 for the carboxylate system. It may be that the higher charge density in the case of the sulphate system cancels out all ion specificity. Such a consequence of high charge density was already observed several times [322, 323]. But it may be also that the behaviour of lithium and sodium in the neighbourhood of

sulphate head groups is not different enough to cause a noticeable difference in the quadrupole splittings. Only further experiments can remove this ambiguity.

The third parameter that has to be taken into account is the available space for the ions and for “bulk” water. Even in the most concentrated systems the thickness of the water layer is at least 1 nm. This is enough to have ions sufficiently far away from the head group so that they can be considered to be unbound. Consequently, there is always an equilibrium possible between bound and unbound ions. In any case, the NMR quadrupole is very sensitive to even small distortions of the local environment around the ions. That means that even a slight displacement of sodium by lithium ions (or vice versa) will be visible in the spectra.

Concerning the amount of counterion condensation onto the negatively charged double layers, the NMR spectra cannot deliver absolute values. However, from classical theories and numerous experiments it can be inferred that about 70 to 80% of the counterions are attached to head groups. According to the present NMR results, there is roughly a replacement of around 25% out of these 70–80% of sodium by lithium close to carboxylic head groups whereas no noticeable change is detectable near sulphate head groups.

Two further points are worth considering. First, the temperature dependence of the quadrupole splittings (measured for carboxylate systems only): obviously a slight raise of temperature of 10 K increases the quadrupole splitting of both ions, whereas the specific ion effects essentially remain unchanged. A plausible explanation could be the assumption that at higher temperatures the ions have a higher tendency to bind at the bs site rather than at the bb site. Of course, these effects are very subtle, but on the other hand, as stated previously, this NMR technique is sensitive enough to subtle effects.

The second point is the negative quadrupole splitting in the case of sodium-carboxylate. As mentioned in the introduction this behaviour can be ascribed to a second binding site of the sodium ions and this site could be deeper within the carboxylate head group. Probably, the average distance of sodium to the carboxylate and sulphate head groups and lithium to the sulphate head groups depends on the presence of other ions either of the same type or of different type and on the concentration of both, cf. figure 4.14. Note that the influence of the ion concentration on the average ion head group distance can

4. Results and Discussion

be of the same order of magnitude as the influence of the competition of lithium and sodium ions.

4.5.2.2 Investigation of ^{137}Cs and ^{87}Rb nuclei

As already mentioned above, mixtures of ionic surfactants with a long chain cosurfactant such as an alcohol form lamellar phases [315, 316]. We have selected dodecyl carboxylate with caesium and rubidium as counterions and octanol as the cosurfactant.

An approach to describe the hydration of ions is the Jones-Dole viscosity B coefficient. It can be calculated from salt solution viscosity η by equation 4.1 with η_0 the viscosity of pure water, A , an electrostatic term, being 1 for moderate salt concentrations and c the salt concentration. B is a direct measure of the strength of ion-water interactions normalized to the strength of water-water interactions.

$$\frac{\eta}{\eta_0} = 1 + Ac^{1/2} + Bc \quad (4.1)$$

The coefficient can be positive or negative. Strongly hydrated ions have positive B coefficients and weakly hydrated ions have negative B coefficients. The point of change in Jones-Dole coefficient sign represents the ideal behaviour at which the interaction water-ion is the same like water-water interaction. The B coefficients of some ions are given in table 4.33 [117, 324]. Consequently, Rb^+ as well as Cs^+ are weakly hydrated whereas the carboxylate head group of fatty acid is strongly hydrated. According to Collins concept the interactions between the head group and the counterions are supposed to be slight. The question answered within this work is, if ion specificity of carboxylate is sufficient to detect a difference in binding behaviour for cations with so similar B coefficients by NMR.

Table 4.33: Jones-Doyle viscosity B coefficients

Cations	B	Anions	B
Ca^{2+}	0.285	CH_3COO^-	0.250
Li^+	0.150	SO_4^{2-}	0.208
Na^+	0.086	Cl^-	-0.007
Rb^+	-0.030	NO_3^-	-0.046

Cs ⁺	-0.045	I ⁻	-0.068
-----------------	--------	----------------	--------

The ¹³⁷Cs and ⁸⁷Rb Δ values were determined as function of surfactant/cosurfactant concentration and for varying ratio Cs/Rb at constant carboxylate/octanol concentration to investigate the binding competition.

Phase structure and NMR spectra

All samples in the concentration range of 15 to 55 wt% D₂O occur lamellar for a ratio surfactant/octanol = 1:3. In figure. 4.24a and 4.24b typical ¹³⁷Cs- and ⁸⁷Rb-NMR spectra can be seen. The number of peaks is given by $2I$. Accordingly, in the ¹³⁷Cs-NMR spectrum (Cs: I = 7/2) seven peaks occur and in the ⁸⁷Rb-NMR spectrum (Rb: I = 3/2) three peaks can be observed. Due to the small quadrupole moment ($Q = -4 \cdot 10^{-31} \text{ m}^2$) of Cs, the signals are narrow [321]. By contrast, the quadrupole moment of Rb is $Q = 0.14 \cdot 10^{-28} \text{ m}^2$, resulting in broader signals [325]. The quadrupole splitting (Δ) is defined as half the distance between the two first neighbouring peaks to the central peak. As can be seen in the figures below, the caesium splitting is clearly smaller than the rubidium splitting (Fig. 4.49). As it is well known for liquid crystalline samples, asymmetric central peaks occur for both ions. This effect is known as chemical shift anisotropy and already mentioned in the section before [321]. Due to the lower splitting of caesium, the anisotropy is more pronounced in the case of ¹³⁷Cs-NMR.

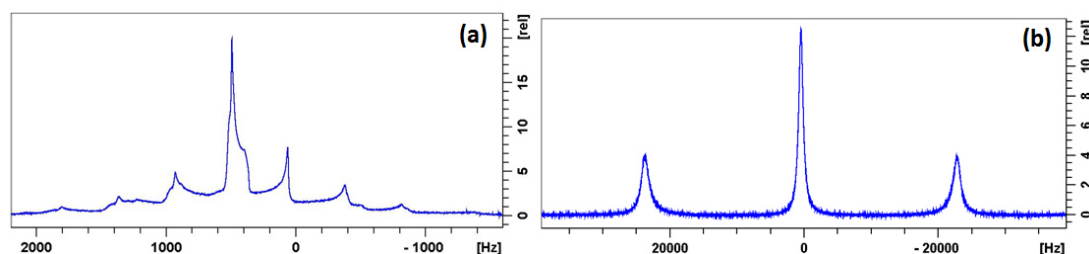


Figure 4.49: (a) ¹³⁷Cs-NMR spectrum of a 85 wt% sample with a composition of CsDC/RbDC = 1/0 at 300 K. The relative intensity of the signals is plotted against the frequency in [Hz]. (b) ⁸⁷Rb-NMR spectrum of a 85 wt% sample with a composition of CsDC/RbDC = 0/1 at 300 K. The relative intensity of the signals is plotted against the frequency [Hz].

Influence of surfactant concentration on the quadrupole splitting

The variations of the caesium and rubidium splitting for the single ion systems, with increasing surfactant and octanol concentration are shown in figure 4.50. The caesium splitting decreases until a concentration of 75 wt%, whereas the rubidium splitting decreases initially and is roughly constant above a concentration of 55 wt% and decreases again for the highest concentration. This non-uniform

4. Results and Discussion

behaviour might be due to the different binding sites at the lamellar interface as can be seen above in figure 2.26. However, the decrease of rubidium splitting at 85 wt% surfactant after increase at 75 wt% is unlikely and can not be explained by different binding sites. It might result from only partially dissolved Rb or from the removal of inner-sphere hydration.

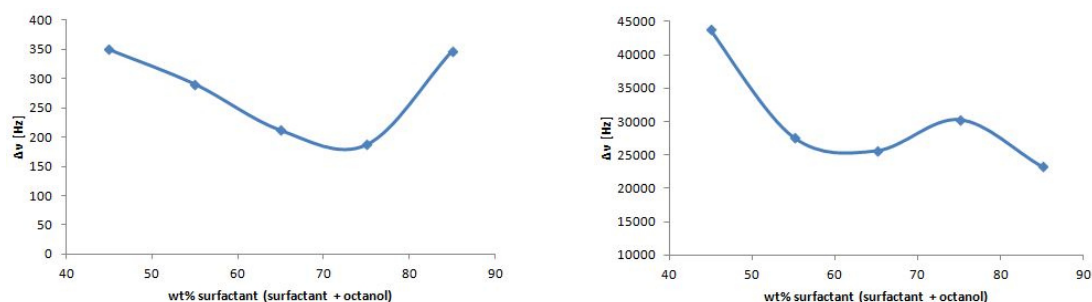


Figure 4.50: Caesium splitting with increasing concentration of surfactant and octanol at 300 K (left) and rubidium splitting with increasing concentration of surfactant and octanol at 300 K (right).

Ion specificity of carboxylate

In figure 4.51 the caesium and rubidium splitting of the 45 wt% samples with an increasing fraction of caesium and rubidium respectively is shown. Caesium splitting remains nearly constant for all composition and rubidium shows only a slight decrease. Hence carboxylate does not show any ion specificity towards caesium or rubidium for this composition.

Similarly, for the 55, 65 and 75 wt% samples (Fig. 4.52-4.54), the Δ values of caesium remain constant. The rubidium splitting is nearly constant for 55 and 75 wt% and shows only small increase for 65 wt%. Consequently, for these compositions carboxylate also doesn't show an ion specificity towards caesium and rubidium.

Except for 85 wt% samples a kink at ratio 1:1 Cs/Rb can be observed for both splitting. This non-monotonic behaviour might point to a special lattice structure for this composition.

Finally, for the 85 wt% samples (Fig. 4.55) the Δ values of caesium decreases with increasing amount of caesium. In contrast, the rubidium splitting increases up to an amount of rubidium of 65 wt% with a slight decline for 55 wt% rubidium and decreases significantly for higher amount of Rb.

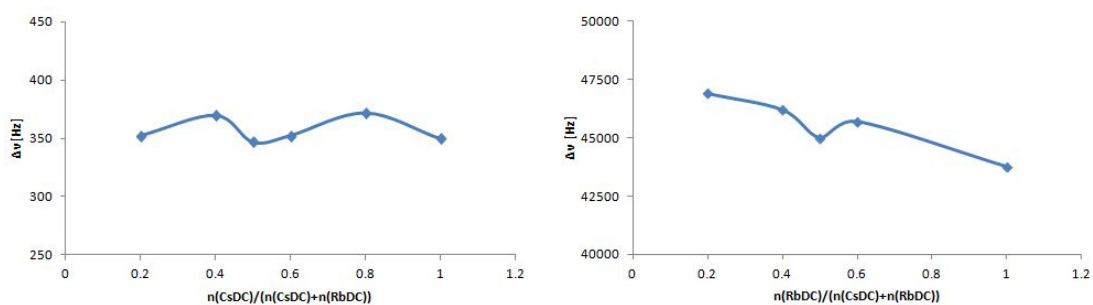


Figure 4.51: Caesium splitting with increasing amount of caesium (left) and rubidium splitting (right) with increasing amount of rubidium for 45 wt% CsDC/RbDC/octanol in D2O at 300 K.

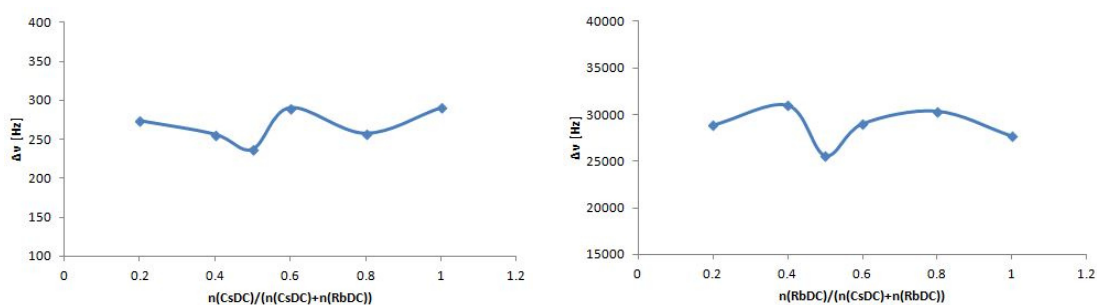


Figure 4.52: Caesium splitting with increasing amount of caesium (left) and rubidium splitting (right) with increasing amount of rubidium for 55 wt% CsDC/RbDC/octanol in D2O at 300 K.

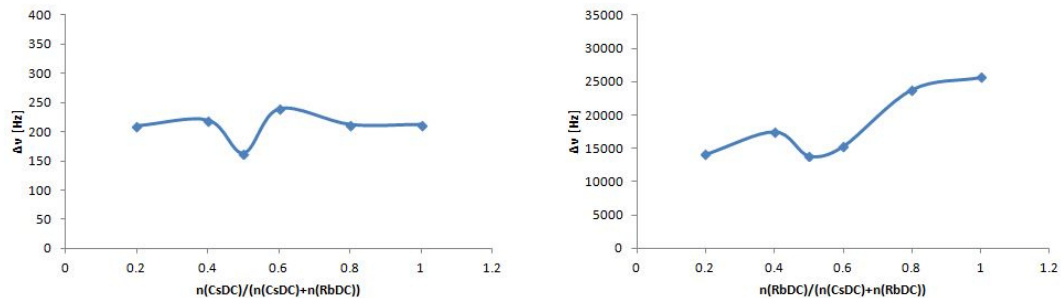


Figure 4.53: Caesium splitting with increasing amount of caesium (left) and rubidium splitting (right) with increasing amount of rubidium for 65 wt% CsDC/RbDC/octanol in D2O at 300 K.

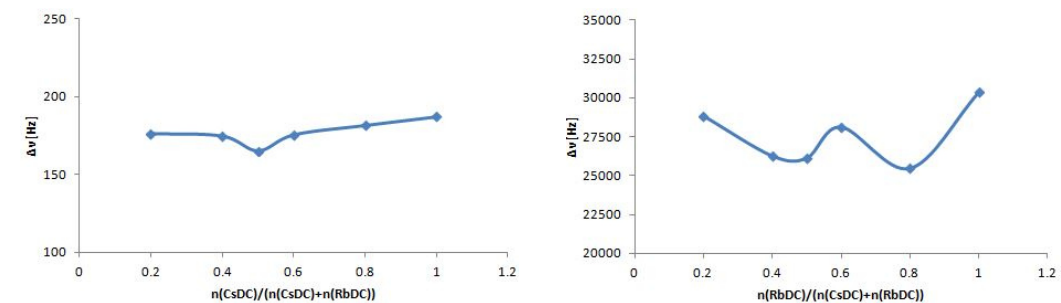


Figure 4.54: Caesium splitting with increasing amount of caesium (left) and rubidium splitting (right) with increasing amount of rubidium for 75 wt% CsDC/RbDC/octanol in D2O at 300 K.

4. Results and Discussion

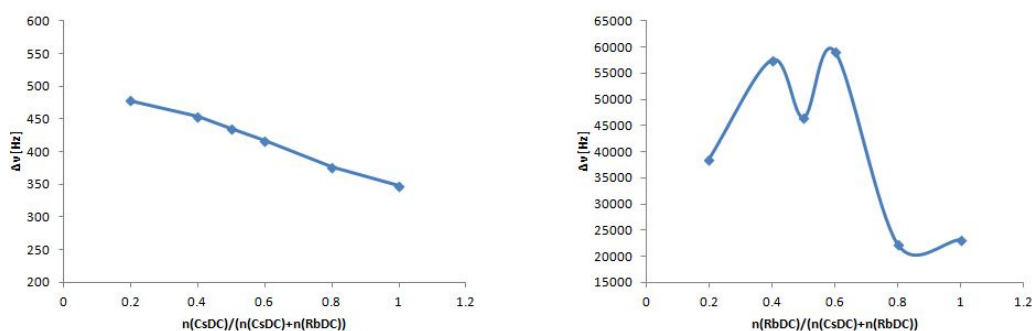


Figure 4.55: Caesium splitting with increasing amount of caesium (left) and rubidium splitting (right) with increasing amount of rubidium for 85 wt% CsDC/RbDC/octanol in D2O at 300 K.

Discussion

Influence of surfactant concentration on the quadrupole splitting

The concept of the Hofmeister series predicts a higher affinity of rubidium to carboxylate in comparison to caesium, but the series does not give any information, how strong this difference might be [183, 326]. Jones-Dole viscosity B coefficients suggests only a very small interaction of both cations with the carboxylate head group. And this is confirmed by our results. The single ion splitting of both cations decreases with increasing concentration of surfactant and octanol up to a certain concentration and increases for higher concentrations. For rubidium splitting an unlikely decrease after increase is observed. Both ions prefer the bb-binding site (negative Δ values) resulting in a decreasing ion splitting. For a very high surfactant concentration the surfactant head groups get very close. Consequently ions are moved to the surfactant head group surface (bs-site; positive Δ values) resulting in an increased splitting. Hence we can speculate that the kink results from the closer packing of the surfactants.

Ion specificity of carboxylate

The caesium and rubidium splitting remain nearly constant for all concentrations and fractions, except of 85 wt%. This is due to the low affinity of carboxylate to caesium and rubidium. The kink observed for all concentrations except 85 wt% samples points to a special lattice structure of bound ions at 1:1 ratio Cs/Rb. But ions are only loosely bound.

For 85 wt% the course of splitting is different. The caesium splitting decreases and the rubidium splitting shows a discontinuous trend. Probably rubidium surfactant

wasn't dissolved completely for this concentration. However, for optically observation these samples occurred also homogenous like all other concentrations.

In summary, the affinity of carboxylate is nearly the same for rubidium and caesium, unlike the ion binding of lithium and sodium considered in a previous paper [208], where preferential binding of lithium was observed. But sodium and lithium having also positive B coefficients like carboxylate are supposed to interact more strongly with carboxylate. Accordingly a precondition for the determination of ion specificities by NMR seems to be a sufficient interaction between anion and cation.

4.5.3 Conclusion

As the ionic strength of the samples is in a concentration range for which typically specific ion effects are suspected and thickness of the water layer is at least 1 nm and accordingly thick enough for coexisting free and bound counter ions the following conclusions can be drawn from the results presented in the last section:

The quadrupole splitting clearly reflects differences in the local environment of cations in liquid crystalline systems made up with carboxylate and sulphate surfactants, respectively and octanol as cosurfactant.

For the carboxylate surfactant head group a preferred propensity of lithium compared to sodium is found which can be interpreted as a higher specificity towards lithium. The lower the concentration the more pronounced is the specificity. For caesium and rubidium no specificity is found. Accordingly, a sufficient interaction is a precondition for ion specificity.

Additionally, from irregular behaviour at 1:1 mixtures Li/Na a preferred lithium binding in bs site and sodium binding in bb site can be concluded.

For the sulphate surfactant head group a less pronounced ion specificity towards lithium and sodium was found, but a slight enhanced one towards sodium. This diminished specificity might result from higher ion charge density in sulphate samples, cancelling out all ion specificities.

Temperature dependent measurements show for carboxylate a change in preferred binding site of sodium and lithium in favour to bs site.

In any case this preliminary study has shown that NMR quadrupole splitting measurements are a valuable technique to investigate even tiny differences in ion-head group interactions as long as the interaction is sufficiently and that this method is therefore suitable for the study of specific ion effects in colloidal systems. It is known that the chloride ion quadrupole splitting for cationic surfactant liquid crystals shows similar behaviour to that described above, hence the method may also be applicable to anions [327]. We hope that more of these experiments will be performed in the future to get a more general and concise picture of these subtle effects, especially concerning the relative importance of ion effects close to different head groups.

Summary

The aim of this work was the investigation and improvement of washing cotton, soiled with triglycerides at room temperature. Therefore the wash efficiency determining interactions were identified and the influence of structures and viscosity of washing agent and temperature on the laundry results determined. To increase systematically the soil release two different strategies were applied. On the one hand we tried to increase the amount of released triglyceride and the other hand we tried to decrease the Krafft temperature of surfactants.

The interaction of triglyceride and surfactant in a binary mixture could result in a decreased melting point or enthalpy. Accordingly, triglyceride liquefaction by surfactants during washing process was supposed. Therefore the influence of surfactants on the phase behavior of triolein and tripalmitin was determined by DSC. The former one is liquid and the latter one is crystalline at room temperature. The investigated surfactants were either anionic or non-ionic. The anionic surfactants were Lutensit A-LBN, a commonly used linear alkyl-benzene sulfonate and choline hexadecylsulphate, a housemade surfactant. The non-ionic surfactants were Lutensol GD70, an alkyl polyglucoside and three different types of Lutensol AO_x, C₁₃C₁₅ alcohols differing in the number of ethoxy groups with $x = 3, 7$ and 20 . It was found that only non-ionic surfactants, Lutensol AO_x, interact with triglyceride. The polymorphism of triglycerides disappears, therefore, the surfactants have an influence on the preferred triglyceride morphology. However, only for very high concentrations of Lutensol AO₃ and Lutensol AO₇ a slight reduction of tripalmitin melting point was determined. Admittedly, the liquefaction of triglyceride with surfactants at room temperature was not reached.

If tripalmitin is not liquefied by surfactants it might get dissolved from cotton by solvents during washing process. Therefore, in a subsequent step the solubilisation of triglycerides by various solvents was investigated. For a systematical selection of potentially suited solvents the R_a value was calculated from Hansen solubility parameters. However, it was found that experimental and calculated data are not in good accordance. Accordingly, solid/liquid equilibrium (SLE) calculations by COSMO-RS were performed giving results which agree in a better way with experimental data. SLE calculations enable a ranking of solvents due to their tripalmitin solubilisation power. The main difference in COSMO-RS and R_a value calculations is the unconsidered crystallization enthalpy of tripalmitin for calculating the R_a -value. The calculated R_a -values of binary mixtures of liquid triolein and solvents are in good agreement with experimental data. Therefore, we assume that Hansen solubility parameters are not suitable for the prediction of

crystalline triglyceride solubilisation. Nevertheless, only small amounts of tripalmitin were dissolved in the tested solvents. The best solvent was chloroform, dissolving 22 wt% tripalmitin. However, this solvent is not applicable in common household laundry. By contrast, more than 50 wt% triolein was dissolved in most of the investigated solvents.

According to the high amount of dissolved triolein in many solvents the dissolution of triolein was supposed as main factor in triglyceride release from cotton. Dissolving triolein from soil leaves a fragile skeleton of crystalline tripalmitin. This is removed mechanically by clashing of clothings in the washing machine. To confirm this assumption washing tests with cotton fibers soiled with mixtures of triolein and tripalmitin with varying ratios were conducted. To determine the washing efficiency, the triglycerides were stained with Sudan black. The fibers were measured at a colorimeter before and after washing. Indeed, except of some outliers, for all tested washing liquors it was shown that soil release increases with increasing fraction of tripalmitin. Additionally, it was shown that increasing the temperature to 40 °C, results in a partial liquefaction of tripalmitin and leads to a declined soil release. However, the reduction of the washing temperature to 10 °C does not result in increased soil release. Quite the contrary, a declined washing result was obtained for all soil compositions. Therefore, further investigations on the temperature effect are necessary.

Due to the important role of triolein dissolution in soil release from cotton fiber, the influence of structuring in washing liquor was investigated. Therefore, washing efficiency of continuous and bicontinuous microemulsions and solution of only surfactant Lutensol AO7 were compared. Best results were found for the solution of only surfactant. The tested bicontinuous microemulsion is a better washing liquor than the comparable continuous one. However, viscosity of the continuous microemulsion was significantly higher than for the bicontinuous one. Therefore, the influence of viscosity on the washing efficiency was investigated.

It was shown that with increasing viscosity the washing efficiency decreases. This declining effect is more pronounced the higher the fraction of oily soil. Accordingly, the diffusion of solvent in cotton fiber and dissolution of triglyceride is decelerated. But to proof this assumption further washing tests using polyester as substrate have to be conducted.

Furthermore, a higher washing efficiency of a 1 wt% solution of Lutensol AO7 than for Spee, a commercial washing agent, was found, independently of Spee concentration.

The improving effect of surfactants in washing liquor on soil release is concluded from a washing test with pure water. The tripalmitin release was less than for surfactant containing washing liquors. Accordingly, the small interactions between surfactants and tripalmitin are sufficient for increased soil release.

However, the Krafft temperature of many surfactants is higher than 25 °C. For the use at washing temperatures below 25 °C the solubility of surfactants has to be enhanced. Therefore we investigated the influence of various osmoprotectants (L-proline, L-carnitine, betaine, ectoine and trehalose), triethylamine and L-lysine on the Krafft temperature of SDS and SDC. Apart from trehalose, all these additives were zwitterionic under the investigated conditions. The Krafft temperature was either increased or decreased by the addition of additives. Except for ectoine, lysine, trehalose, and TMAO, always opposite effects for the both head groups were obtained. For ectoine the Krafft temperature of both surfactants decreased, for lysine the same was observed at low additive concentrations, whereas the Krafft temperature increases for both at high concentrations, and in the case of trehalose the Krafft temperature of both surfactants increases at all concentrations. TMAO has only a slight influence on SDS Krafft temperature but similar to betaine, carnitine und proline a decreasing one. All four additives have an increasing effect on SDC Krafft temperature.

The influence of additives on solubility of surfactants is due to the differing interactions between head group, counterion, additive and water. Salting out of surfactants can be induced by the formation of contact ion pairs or by dehydration of the surfactant head group. In order to get a deeper insight towards the formation of contact ionpairs the ion specificity of sulphate and carboxylate head groups was investigated by NMR. In a first study we investigated the ion specificity of both surfactant head groups to sodium and lithium and in a further one we investigated the ion specificity of carboxylate to caesium and rubidium. We took the quadrupolar splitting into account. For an anisotropic environment of a nucleus with quadrupole moment, quadrupolar splitting is detected by NMR. The magnitude of splitting is related to the dimension of anisotropy of nuclei environment. The vicinity of free, non bound ions appears isotropic, resulting in a quadrupole splitting of zero. Accordingly, quadrupolar splitting gives the fraction of bound ions. It was

shown that with increasing ion concentration the specificity of head groups decreases. Furthermore, it was found that carboxylate has a higher specificity to lithium than sodium and in contrast sulphate shows a slightly increased affinity towards sodium. This preference might be more distinctive for sulphate samples with a low ion concentration. From the investigation of carboxylate specificity to caesium and rubidium can be concluded, that a sufficient interaction between head group and counterion is required to detect ion specificities. Due to the low interaction between carboxylate head group and caesium and rubidium counterions no specificity was detected by NMR.

Zusammenfassung

Ziel dieser Arbeit war es, die Waschergebnisse für das Waschen von Baumwolle, welche mit Triglyceriden verunreinigt ist, bei Raumtemperatur zu verstehen und zu verbessern. Dazu wurden einerseits die für den Wascherfolg entscheidenden Wechselwirkungen identifiziert und andererseits der Einfluss von Strukturierung und Viskosität der Waschlösung und der Temperatur auf das Waschergebnis bestimmt, um ein tieferes Verständnis über die Vorgänge beim Waschen zu erhalten. Zur Steigerung des Waschergebnisses haben wir 2 unterschiedliche Strategien verfolgt, einerseits die Steigerung der Triglyceridablösung und andererseits die Senkung der Kraffttemperatur von Tensiden.

In einer binären Mischung Fett/Tensid kann die Wechselwirkung zu einer Verringerung der Schmelztemperatur oder Schmelzenthalpie führen. Es wurde vermutet, dass feste Triglyceride durch die Wechselwirkung mit Tensiden beim Waschen verflüssigt werden können. Daher wurde im ersten Schritt die Wechselwirkung zwischen Triglyceriden und Tensiden mittels DSC untersucht. Die Auswahl der untersuchten Triglyceride beschränkte sich auf Triolein, als Vertreter der flüssigen Fette und Tripalmitin, welches unter den gegebenen Bedingungen fest vorliegt. Die getesteten Tenside waren entweder anionisch oder nicht ionisch. Als Vertreter der anionischen Tenside wurden Lutensit A-LBN, ein Alkylbenzylsulfonat, das technisch in Waschanwendungen eingesetzt wird und Cholinhexadecylsulfat, ein am Lehrstuhl entwickeltes Tensid getestet. Bei den nichtionischen Tensiden wurden Lutensol GD70, ein Alkylpolyglucosid und drei verschiedene Lutensole AO_x, C₁₃C₁₅ Alkohole, die sich in der Anzahl der EO-Gruppen unterscheiden, getestet. Wobei $x = 3, 7$ oder 20 war. Dabei wurde festgestellt, dass lediglich die nichtionischen Tenside, Lutensol AO_x, mit den Triglyceriden wechselwirken. Diese bewirken, dass die polymorphen Umwandlungen der Triglyceride nicht mehr auftreten, sie nehmen also Einfluss auf die bevorzugte Kristallstruktur der Fette. Allerdings konnte nur für sehr hohe Konzentrationen an Lutensol AO3 und Lutensol AO7 eine Verringerung der Schmelztemperatur von Tripalmitin detektiert werden, die jedoch noch immer deutlich über Raumtemperatur liegt.

Da Tripalmitin nicht verflüssigt werden kann, war ein zweiter Ansatz, dass die Triglyceride mittels Tensid oder Lösungsmittel aus der Baumwolle herausgelöst werden. Um dies zu bestätigen, wurde eine Serie an Lösungsmitteln getestet. Um eine systematische Auswahl der Lösungsmittel zu ermöglichen, wurde versucht, mittels Hansen Löslichkeitsparametern und dem daraus resultierenden R_a Wert geeignete Lösungsmittel vorherzusagen. Allerdings stellte sich dabei heraus, dass die berechneten und experimentellen Daten nur schlecht übereinstimmten. Daher

wurden alternativ SLE (solid/liquid equilibrium) Rechnungen mit COSMO-RS durchgeführt. Die sich daraus ergebenden Rankings stimmten recht gut mit den experimentellen Daten überein. Da der wesentliche Unterschied zwischen den SLE- und R_a -Wert-Berechnungen die Berücksichtigung der Kristallisationsenthalpie in COSMO-RS ist und die R_a Werte gute Vorhersagen für die Löslichkeit von Triolein ermöglichen, konnten wir daraus schließen, dass das Hansen Löslichkeits Konzept nicht geeignet ist für die Berechnung kristalliner Triglyceride. Es stellte sich jedoch heraus, dass Tripalmitin im Gegensatz zu Triolein nur in sehr geringen Mengen in Lösung gebracht werden kann. Die größte Menge (22 wt%) an festem Triglycerid konnte in Chloroform gelöst werden. Dieses Lösungsmittel ist jedoch für Waschanwendungen in privaten Haushalten nicht geeignet.

Aus der Tatsache, dass Triolein in einer Vielzahl an Lösungsmitteln in großen Mengen in Lösung gebracht werden kann, ergab sich die Vermutung, dass der entscheidende Schritt beim Waschen von Triglycerid-Verunreinigungen das Herauslösen der flüssigen Bestandteile ist. Sobald diese entfernt sind, bleibt ein fragiles Gerüst an kristalliner Verunreinigung zurück, das dann durch die Mechanik, die beim Waschen durch das Aneinanderstoßen der Kleidungsstücke auftritt, aufbrechen und abbröseln kann. Um diese Vermutung zu bestätigen, wurden Waschttests an Baumwollstreifen durchgeführt, die mit unterschiedlichen Zusammensetzungen Triolein und Tripalmitin verunreinigt worden sind. Zur Überprüfung des Wascherfolgs wurden die Triglyceridzusammensetzungen mit dem Farbstoff Sudan Black eingefärbt und die Streifen vor und nach dem Waschen am Kolorimeter vermessen. Tatsächlich konnte für alle getesteten Waschlösungen festgestellt werden, dass, abgesehen von einzelnen Ausreißern, mit steigendem Anteil an kristallinem Triglycerid in der Verunreinigung mehr Fett herausgewaschen wurde. Darüber hinaus konnte gezeigt werden, dass durch eine Steigerung der Waschttemperatur auf 40 °C, also bei einem erhöhten Anteil an flüssiger Verschmutzung, die Waschergebnisse schlechter ausfallen. Allerdings konnte durch die Erniedrigung der Waschttemperatur keine Verbesserung der Waschergebnisse erzielt werden. Die Effizienz der Waschlösungen war für alle Schmutzzusammensetzungen verringert. Um diese unerwartete Beobachtung zu bestätigen müssen weitere Temperaturabhängige Waschttest durchgeführt werden.

Da der Wascherfolg maßgeblich durch das Herauslösen der flüssigen Bestandteile aus der Verunreinigung bestimmt wird, wurde der Einfluss von Strukturen in der Waschlösung untersucht. Dazu wurden die Waschergebnisse für kontinuierliche und bikontinuierliche Mikromulsionen und reiner Lutensol AO7 Tensidlösung

verglichen. Dabei stellte sich heraus, dass die höchste Waschwirkung für die reine Tensidlösung erhalten wird. Die getestete bikontinuierliche Mikroemulsion erzielt bessere Ergebnisse als die vergleichbare kontinuierliche Mikroemulsion. Da die Viskosität der kontinuierlichen ME jedoch sehr viel höher ist, als die der bikontinuierlichen, wurde der Einfluss der Viskosität auf die Waschwirkung untersucht.

Es konnte gezeigt werden, dass eine Erhöhung der Viskosität mit einer verringerten Waschwirkung einhergeht. Diese ist auf die verlangsamte Diffusion des LM in der Baumwolle und Ablösung der Triglyceride zurückzuführen. Daher ist der Effekt auch umso stärker ausgeprägt, je höher der Anteil an Triolein in der Verunreinigung ist. Um diese Annahme zu bestätigen müssen noch weitere Waschtest mit Polyester als Substrat durchgeführt werden.

Des Weiteren wurde die Waschleistung der reinen Tensidlösung mit der des kommerziell erhältlichen Waschmittels Spee verglichen. Es stellte sich heraus, dass für alle getesteten Speeverdünnungen die reine Tensidlösung mit einer Tensidkonzentration von 1 wt% Tensidlösung besser abschneidet.

Durch das Waschen mit reinem Wasser konnte gezeigt werden, dass die Anwesenheit eines Tensides in der Waschlösung auch im Fall von reinen Tripalmitin Verunreinigungen zu einer Verbesserung des Waschergebnisses führt. Trotz der schwachen Wechselwirkungen hat das Tensid einen positiven Einfluss auf die Schmutzablösung.

Da die Löslichkeitstemperatur vieler Tenside über 25 °C liegt, aber eine ausreichend hohe Löslichkeit bei niedrigeren Temperaturen für das Waschen mit kaltem Wasser erforderlich ist, haben wir den Einfluss von verschiedenen Osmolyten (L-prolin, L-carnitin, Betain, Ectoin und Trehalose), Trimethylaminoxid und L-Lysin auf die Kraffttemperatur von SDS und SDC untersucht. Abgesehen von Trehalose lagen alle Zusätze unter den untersuchten Bedingungen zwitterionisch vor. Dabei stellten wir fest, dass der Zusatz an Additiven die Kraffttemperatur entweder steigert oder senkt. Außer für Ectoin, Lysine, Trehalose und TMAO beobachtet man immer den entgegengesetzten Effekt für die beiden Tenside. Im Falle von Ectoin sinkt die Kraffttemperatur beider Tenside. Das gleiche beobachtet man für die Zugabe geringer Konzentrationen Lysin, wobei die Kraffttemperatur beider bei höheren Lysinzusätzen ansteigt. Die Zugabe von Trehalose steigert die Kraffttemperatur beider unabhängig von der Konzentration.

TMAO hat nur einen sehr geringen Einfluss auf die Kraffttemperatur von SDS. Genau wie TMAO, nur stärker ausgeprägt, führen Betain, Carnitin und Prolin zu einer Reduktion der Kraffttemperatur von SDS. Alle vier Additive induzieren folglich eine Steigerung der Kraffttemperatur von SDS.

Weshalb der Zusatz von Additiven zu ionischen Tensiden einen Einfluss auf deren Löslichkeit hat, kann durch die unterschiedlich starken Wechselwirkungen zwischen Kopfgruppe, Gegenionen, Additiv und Wasser erklärt werden. Eine Reduktion der Löslichkeit des Tensides kann z.B. durch die Bildung von Kontaktionenpaaren oder die Dehydrierung der Tensidkopfgruppe erreicht werden. Um mehr über die Bildung von Kontaktionenpaaren zu erfahren, untersuchten wir mittels NMR die Ionenspezifität von Sulfat- und Carboxylat-Kopfgruppen. In einer ersten Studie untersuchten wir die Ionenspezifität der beiden Kopfgruppen gegenüber Natrium und Lithium und in einer weiteren Studie die Spezifität von Carboxylat gegenüber Cäsium und Rubidium. Die dabei berücksichtigte Messgröße war das Quadrupol Splitting. Für eine anisotrope Umgebung eines Kerns, der ein Quadrupolmoment besitzt, kann ein Quadrupol Splitting detektiert werden, welches ein Maß für die Anisotropie der Kernumgebung ist. Da für ungebundene Ionen, im Gegensatz zu gebundenen Ionen, die Umgebung isotrop erscheint, kann mittels Quadrupol Splitting auf den Anteil an gebundenen Ionen rückgeschlossen werden. In dieser Arbeit wurde gezeigt, dass eine hohe Ionenkonzentration zu einer verringerten Ionenspezifität führt. Darüber hinaus konnte gezeigt werden, dass Carboxylat spezifischer Lithium statt Natrium bindet und dass im Gegensatz dazu Sulfat eine leicht erhöhte Spezifität gegenüber Natrium zeigt. Allerdings war die Ionenkonzentration der Proben vermutlich zu hoch, um eine stärkere Spezifität zu beobachten. Des Weiteren wurde gezeigt, dass ein Mindestmaß an Wechselwirkung zwischen Kopfgruppe und Gegenion erforderlich ist, um eine Spezifität zu detektieren. Da Carboxylat weder mit Cäsium noch mit Rubidium besonders stark wechselwirkt konnte bei den NMR Messungen auch keine Spezifität gegenüber eines der beiden Ionen beobachtet werden.

Bibliography

1. Wagner, G., *Waschmittel-Chemie, Umwelt, Nachhaltigkeit*. 2005, Weinheim: Wiley-VCH.
2. Schmitz, *Wäsche waschen hat Geschichte*, 2011, PR-Blickpunkt: <http://www.pr-blickpunkt.de/dienstleistungen/artikel/waesche-waschen-hat-geschichte>.
3. CoKG, H.A.: <http://www.henkel.de/nachhaltigkeit/waesche-waschen-33279.htm>.
4. Scheuer, R. and H. Lucas, *Von Anionischen Tensiden bis Zeolithe*. MNU Primar, 2009. 1(1): p. 29-34.
5. *Gesetz über Detergentien in Wasch- und Reinigungsmitteln*, 1961. p. 1653-1654.
6. *Molekulare Enzymtechnologie: umweltfreundliche Biotenside*, 2010, Forum für Wissenschaft, Industrie und Wirtschaft: http://www.innovations-report.de/html/berichte/biowissenschaften_chemie/molekulare_enzymtechnologie_umweltfreundliche_150598.html.
7. Team, m.C., I.f.E.u.U. gGmbH, and F. Bremen, *Marktanalyse nachwachsende Rohstoffe*, 2006, Fachagentur nachwachsender Rohstoffe e.V.: http://www.fnr-server.de/ftp/pdf/literatur/pdf_254marktstudie_2006.pdf.
8. Venkatesh, G.M., et al., *A Study of the Soiling of Textiles and Development of Anti-Soiling and Soil Release Finishes: A Review*. Textile Research Journal, 1974. 44(5): p. 352-362.
9. Breen, N.E., D.J. Durnam, and S.K. Oberndorf, *Residual Oily Soil Distribution on Polyester/Cotton Fabric After Laundering with Selected Detergents at Various Wash Temperatures*. Textile Research Journal, 1984. 54: p. 198-204.
10. Carroll, D., *Physical aspects of detergency*. Colloids and Surfaces A: Physicochemical and Engineering Aspects, 1993. 74: p. 131-167.
11. Kissa, E., *Mechanism of Soil Release*. Textile Research Journal, 1981. 51(8): p. 508-513.
12. Chi, Y.-S. and S.K. Oberndorf, *Aging of Oily Soils on Textiles. Chemical Changes upon Oxidation and Interaction with Textile Fibers*. Journal of Surfactants and Detergents, 1998. 1(3): p. 371-380.
13. GmbH, F.C., *Natural and chemical fibers, bleach as a part of daily life*: http://www.fiz-chemie.de/fileadmin/user_upload/PDF_EN/report/report_60_en.pdf.
14. Hearle, J.W.S., *Ullmann's Encyclopedia of Industrial Chemistry* 2007, Weinheim: Wiley-VCH.
15. Krässing, H.A., *Cellulose: Structure, Accesibility and Reactivity, Polymer Monographs*. Vol. 11. 1993, Amsterdam: Gordon & Breach Science Publisher.
16. Rouette, H.-K., *Handbuch Textilveredelung, Band 1: Ausrüstung* 2006, Frankfurt a. Main: Deutscher Fachverlag.
17. Autorenkollektiv, *Faserstofflehre* 1972, Leipzig: VEB Fachbuchverlag
18. Swicofil, *Cotton: Natural Fibres - Synthetic Fibres*: <http://www.swicofil.com/products/001cotton.html>.
19. Hofer, A., *Stoffe 1. Rohstoffe: Fasern, Garne und Effekte*. 2000, Frankfurt a. Main: Deutscher Fachverlag.
20. Oberndorf, S.K. and N.A. Klemash, *Electron Microscopical Analysis. of Oily Soil Penetration into Cotton and Polyester/Cotton Fabrics*. Textile Research Journal, 1982. 52: p. 434-442.

21. Oberndorf, S.K., Y.M.N. Namasté, and D.J. Durnam, *A Microscopical Study of Residual Oily Soil Distribution on Fabrics of Varying Fiber Content*. Textile Research Journal, 1983. 53: p. 375-383.
22. Morton, G.P. and L.B. Thomas, *Interactions of Fiber, Finish, and Wash Conditions in Laundering Cotton-Containing Fabrics*. Textile Research Journal, 1983. 53: p. 165-174.
23. Barker, R.H., *Additives in fibers and fabrics*. Environmental Health Perspectives, 1975. 11: p. 41-45.
24. Bille, H., A. Eckell, and G.A. Schmidt, *Finishing for Durable Press and Soil Release*. Textile Com. Colorist 1, 1969: p. 600-607.
25. Bille, H. and G.A. Schmidt, *Critical Observations on the Possibilities and Limits of Soil Release Finishing*. Melliand Textilber, 1969. 50: p. 1481-1487.
26. Bowers, C.A. and G. Chantrey, *Factors Controlling the Soiling of White Polyester Cotton Fabrics, Part 1: Laboratory Studies*. Textile Research Journal, 1969. 39: p. 1-11.
27. Brown, C.B., *Studies in Detergency, I : The Oily Constituent in Naturally Occurring Domestic Dirt*. Research 1, 1947: p. 46-48.
28. Sanders, H.I. and J.M. Lambert, *An approach to a more realistic cotton detergency test*. Journal of the American Oil Chemists Society, 1950. 27(5): p. 153-159.
29. Fort, T., H.R. Billica, and C.K. Sloan, *Studies of Soiling and Detergency: Part I: Observations of Naturally Soiled Textile Fibers*. Textile Research Journal, 1966. 36(1): p. 7-12.
30. Moyses, V.J., *Finishing processes for synthetic and blended fiber textiles to confer soil release and related effects*. Textilveredlung, 1970. 5: p. 377-385.
31. Rees, W.H., *An account of the general problem with some observations*. Journal of the Textile Institute, 1954. 45: p. 612-631.
32. Utermohlen, W.P., M.E. Ryan, and D.O. Young, *Improvement of cotton cloth in resistance to soiling and in ease of washing*. Textile Research Journal, 1951. 21(7): p. 510-521.
33. Snell, F.D., C.T. Snell, and I. Reich, *The nature of soil to be deterged and its bonding to the surface*. Journal of the American Oil Chemists Society, 1950. 27(2): p. 62-68.
34. Compton, J. and W.J. Hart, *A study of soiling and soil retention in textile fibers*. Textile Research Journal, 1953. 23(3): p. 158-163.
35. Compton, J. and W.J. Hart, *The effect of yarn and fabric structure in soil retention*. Textile Research Journal, 1953. 23(6): p. 418-423.
36. Compton, J. and W.J. Hart, *The theory of soil fiber complex, formation and stability*. Textile Research Journal, 1954. 24(3): p. 263-264.
37. Minor, F.W. and A.M. Schwartz, *Part III: The Behavior of Liquids on Single Textile Fibers*. Textile Research Journal, 1959. 29(12): p. 940-949.
38. Smith, S. and P.O. Sherman, *Textile Characteristics Affecting the Release of Soil during Laundering: Part I: A Review and Theoretical Consideration of the Effects of Fiber Surface Energy and Fabric Construction on Soil Release*. Textile Research Journal, 1959. 39(5): p. 441-449.
39. Zisman, W.A., *Surface Activity. The Physical Chemistry, Technical Applications, and Chemical Constitution of Synthetic Surface-Active Agents*. Journal of the American Chemical Society, 1964. 84(12): p. 2466-2467.
40. Miller, C.A. and K.H. Raney, *Solubilization-emulsification mechanisms of detergency*. Colloids and Surfaces A, 1993. 74(1): p. 169-215.

41. Kissa, E., *Kinetics and Mechanisms of Detergency: Part I: Liquid Hydrophobic (Oily) Soils* Textile Research Journal, 1975. 45(10): p. 736-741.
42. Dillan, K.W., E.D. Goddard, and D.A. McKenzie, *Oily soil removal from a polyester substrate by aqueous nonionic surfactant systems*. Journal of the American Oil Chemists Society, 1979. 56(1): p. 59-70.
43. Bäckström, K. and S. Engström, *Removal of triglycerides from hard surfaces by surfactants: An ellipsometry study*. Journal of the American Oil Chemists Society, 1988. 65(3): p. 412-420.
44. Adam, N.J., *Detergent Action and its Relation to Wetting and Emulsification*. Journal of the Society of Dyers and Colourists, 1937. 53(4): p. 121-129.
45. Kissa, E., *Kinetics of Oily Soil Release* Textile Research Journal, 1971. 41(9): p. 760-767.
46. Kling, W., *Der Waschvorgang als Umnetzung*. Colloid and Polymer Science, 1949. 115(1-3): p. 37-44.
47. Shinoda, K., *Solvent Properties of Surfactant Solutions.*, ed. K. Shinoda 1967, New York: Dekker.
48. Miller, C.A. and K.H. Raney, *Solubilization-emulsification mechanisms of detergency*. Colloids and Surfaces A: Physicochemical and Engineering Aspects, 1993. 74: p. 169-215.
49. Raney, K.H., H.L. Benton, and C.A. Miller, *Optimum detergency conditions with nonionic surfactants: I. Ternary water-surfactant-hydrocarbon systems*. Journal of Colloid and Interface Science, 1987. 117(1): p. 282-290.
50. Solans, C., et al., *Organized Solutions* 1992, New York: Marcel Dekker.
51. Dillan, K.W., E.D. Goddard, and D.A. McKenzie, *Examination of the parameters governing oily soil removal from synthetic substrates*. Journal of the American Oil Chemists Society, 1980. 57(7): p. 230-237.
52. Raney, K.H. and H.L. Benson, *The effect of polar soil components on the phase inversion temperature and optimum detergency conditions*. Journal of the American Oil Chemists Society, 1990. 67(11): p. 722-729.
53. Durham, K., *Surface activity and detergency*, ed. K. Durham 1961, London: Macmillan.
54. Lawrence, A.C.S., *The Mechanism of Detergence*. Nature, 1959. 183: p. 1491-1494.
55. Batra, A., et al., *Removal of Surface Adhered Particles by Surfactants and Fluid Motions*. American Institute of Chemical Engineers, 2001. 47(11): p. 2557-2565.
56. Evans, D.F., *The Colloidal Domain: Where Physics, Chemistry, Biology, and Technology Meet* 1998: WILEY-VCH.
57. Visser, J., *The concept of negative hamaker coefficients. 1. history and present status* Advances in Colloid and Interface Science, 1981. 15(2): p. 157-169.
58. Visser, J., *The adhesion of colloidal polystyrene particles to cellophane as a function of pH and ionic strength*. Journal of Colloid and Interface Science, 1976. 55(3): p. 664-677.
59. Hogg, R., T.W. Healy, and D. Fuerstenau, *Mutual coagulation of colloidal dispersions*. Transactions of the Faraday Society, 1966. 62: p. 1638-1651.
60. Hamaker, H.C., *The London—van der Waals attraction between spherical particles*. Physica, 1937. 4(10): p. 1058-1072.
61. Lange, H., *Über die energetische Wechselwirkung zwischen Textilfasern und Pigmentschmutz beim Waschprozeß (I)*. Colloid and Polymer Science, 1957. 154(2): p. 103-110.

62. Hamilton, R.J. and A. Bhati, *Recent advances in chemistry and technology of fats and oils*.1987, New York: Elsevier Applied Science.
63. Gunstone, F.D., *Vegetable oils in food technology: composition, properties and uses*.2002: Blackell
64. Phan, T.T., J.H. Harwell, and D.A. Sabatini, *Effects of Triglyceride Molecular Structure on Optimum Formulation of Surfactant-Oil-Water Systems*. Journal of Surfactants and Detergents, 2010. 13: p. 189-194.
65. Klaus, A., *Solubility of Triglycerides in Water Using an Extended Surfactant*, in *Natural Science Faculty IV2011*, University of Regensburg: Regensburg.
66. Sato, K., *Solidification and phase transformation behaviour of food fats - a review*. Fett/Lipid, 1999. 101(12): p. 467-474.
67. Demirbas, A., *Biodiesel fuels from vegetable oils via catalytic and non-catalytic supercritical alcohol transesterifications and other methods: a survey*. Energy Conversion and Management, 2003. 44(13): p. 2093-2109.
68. Wang, Y., et al., *Preparation of biodiesel from waste cooking oil via two-step catalyzed process*. Energy Conversion and Management, 2007. 48(1): p. 184-188.
69. Baumann, H., et al., *Natural Fats and Oils—Renewable Raw Materials for the Chemical Industry*. Angewandte Chemie International Edition in English, 1988. 27(1): p. 41-62.
70. Kalustian, P., *Pharmaceutical and cosmetic uses of palm and lauric products*. Journal of the American Oil Chemists Society, 1985. 62(2): p. 431-433.
71. Caliman, F.A. and M. Gavrilescu, *Pharmaceuticals, Personal Care Products and Endocrine Disrupting Agents in the Environment – A Review*. CLEAN – Soil, Air, Water, 2009. 37(4-5): p. 277-303.
72. Akoh, C.C. and D.B. Min, *Food Lipids: Chemistry, Nutrition, and Biotechnology*2002, New York: Marcel Dekker.
73. Aparicio, R. and R. Aparicio-Ruiz, *Authentication of vegetable oils by chromatographic techniques*. Journal of Chromatography A, 2000. 881(1-2): p. 93-104.
74. McClements, D.J., *Food emulsions: principles, practices, and techniques*. 2nd ed2005: CRC Press.
75. Hamilton, R.J., *Structure and general properties of mineral and vegetable oils used as spray adjuvants*. Pesticide Science, 1993. 37(2): p. 141-146.
76. Evans, C.D., et al., *Structure of unsaturated vegetable oil glycerides: Direct calculation from fatty acid composition*. Journal of the American Oil Chemists Society, 1969. 46(8): p. 421-424.
77. Kamal-Eldin, A. and R.J. Andersson, *A multivariate study of the correlation between tocopherol content and fatty acid composition in vegetable oils*. Journal of the American Oil Chemists Society, 1997. 74(4): p. 375-380.
78. Alander, J. and T. Warnheim, *Model microemulsions containing vegetable oils part 1: Nonionic surfactant systems*. Journal of the American Oil Chemists Society, 1989. 66(11): p. 1656-1660.
79. Alander, J. and T. Warnheim, *Model microemulsions containing vegetable oils 2. Ionic surfactant systems*. Journal of the American Oil Chemists Society, 1989. 66(11): p. 1661-1665.
80. Miñana-Perez, M., et al., *Solubilization of polar oils with extended surfactants*. Colloids and Surfaces A: Physicochemical and Engineering Aspects, 1995. 100: p. 217-227.

81. von Corswant, C., S. Engström, and O. Söderman, *Microemulsions Based on Soybean Phosphatidylcholine and Triglycerides. Phase Behavior and Microstructure*. Langmuir, 1997. 13(19): p. 5061-5070.
82. Huang, L., A. Lips, and C.C. Co, *Microemulsification of Triglyceride Sebum and the Role of Interfacial Structure on Bicontinuous Phase Behavior*. Langmuir, 2004. 20(9): p. 3559-3563.
83. Engelskirchen, S., et al., *Triacylglycerol microemulsions stabilized by alkyl ethoxylate surfactants—A basic study: Phase behavior, interfacial tension and microstructure*. Journal of Colloid and Interface Science, 2007. 312(1): p. 114-121.
84. Garti, N. and K. Sato, *Crystallization and Polymorphism of Fats and Fatty Acids* 1988, New York: Marcel Dekker.
85. Larsson, K., *Classification of Glyceride Crystal Forms*. Acta Chemica Scandinavica, 1966. 20: p. 2255-2260.
86. Malkin, T. and M.L. Meara, *An X-ray and thermal examination of the glycerides. Part IV. Symmetrical mixed triglycerides, CH(O-COR')(CH₂-O-COR)₂*. Journal of the Chemical Society, 1939: p. 103-108.
87. Kodalia, D.R., A. Atkinsona, and D.H. Smalla, *Molecular packing in triacyl-sn-glycerols: Influences of acyl chain length and unsaturation*. Journal of Dispersion Science and Technology, 1989. 10(4-5): p. 393-440.
88. Boubekri, K., et al., *Polymorphic transformations in sn-1, 3-distearoyl-2-ricinoleyl-glycerol*. Journal of the American Oil Chemists Society, 1999. 76(8): p. 949-955.
89. Paoletti, R. and D. Kritchevsky, *Advances in Lipid Research*. Vol. 5. 1967, New York: Academic Press.
90. Hale, J.E. and F. Schroeder, *Phase behaviour of triolein and tripalmitin detected by Differential Scanning Calorimetry*. Lipids, 1981. 16(11): p. 805 - 809.
91. Rossell, J.B., *Phase diagrams of triglyceride systems*. Advances in lipid research, 1967. 5: p. 353-408.
92. Holmberg, K., *Handbook of Applied Surface and Colloid Chemistry*, ed. K. Holmberg. Vol. 1. 2002: John Wiley & Sons.
93. Meyers, D., *Surfactant Science and Technology* 2005: John Wiley & Son.
94. Holmberg, K., et al., *Surfactants and Polymers in aqueous solutions*. 2nd ed. ed 2003: John Wiley & Sons.
95. Mollet, H. and A. Grubenmann, *Formulierungstechnik. Emulsionen, Suspensionen, Feste Formen* 2000: Wiley-VCH Verlag GmbH.
96. Parsonage, N.G. and L.A.K. Staveley, *Disorder in Crystals. International series of monographs on chemistry*. Berichte der Bunsengesellschaft, 1978. 84(9): p. 933-934.
97. Vlachy, N., *Formation and stabilization of vesicles in mixed surfactant systems*, in *Institute of Physical and Theoretical Chemistry* 2008, Regensburg: Regensburg. p. 180.
98. Rosen, M.J., *Surfactants and Interfacial Phenomena*. 2nd ed. ed 1989: John Wiley & Sons.
99. Lindman, B. and H. Wennerström, *Micelles*. Topics in Current Chemistry, 1980. 87: p. 1-83.
100. Meguro, K., M. Ueno, and K. Esumi, *Nonionic Surfactants. Physical Chemistry* 1987, New York: Marcel Dekker.

101. Shinoda, K., et al., *Colloidal surfactants. Some physico-chemical properties*. 1963, London: Academic Press.
102. Gunnarsson, G., B. Jönsson, and W. H., *Surfactant association into micelles. An electrostatic approach*. The Journal of Physical Chemistry, 1980. 84(23): p. 3114-3121.
103. Goodwin, J., *Colloids and Interfaces with Surfactants and Polymers*. 2004: John Wiley & Sons.
104. Israelachvili, J.N., D.J. Mitchell, and B.W. Ninham, *Theory of self-assembly of hydrocarbon amphiphiles into micelles and bilayers*. Journal of the Chemical Society, Faraday Transaction 2: Molecular and Chemical Physics, 1976. 72: p. 1525-1568.
105. Israelachvili, J.N., *Intermolecular Surface Forces: With Applications to Colloidal and Biological Systems* 1985: Academic Press.
106. Tanford, C., *Micelle shape and size*. The Journal of Physical Chemistry, 1972. 76(21): p. 3020-3024.
107. Rosevear, F.B., *The microscopy of liquid crystalline neat and middle phases of soaps and synthetic detergents*. Journal of the American Oil Chemists` Society, 1954. 31: p. 628.
108. Rosevear, F.B., *Liquid Crystals: The Mesomorphic Phases of Surfactant Compositions*. Journal of Cosmetic Science 1968. 19(9): p. 581-594.
109. Tiddy, G.J.T., *Surfactant-water liquid crystal phases*. Physics Reports, 1980. 57(1): p. 1-46.
110. Winsor, P.A., *Binary and multicomponent solutions of amphiphilic compounds. Solubilization and the formation, structure, and theoretical significance of liquid crystalline solutions*. Chemical Reviews, 1968. 68(1): p. 1-40.
111. Mitchell, D.J., et al., *Phase behaviour of polyethoxylene surfactants with water. Mesophase structures and partial miscibility (cloud points)*. Journal of the Chemical Society, Faraday Transaction 1: Physical Chemistry in Condensed Phases, 1983. 79(4): p. 975-1000.
112. Eicke, H.F., *Modern Trends of Colloidal Science in Chemistry and Biology* 1985: Birkhauser Verlag.
113. Holmes, M.C., *Intermediate phases of surfactant-water mixtures*. Current Opinion in Colloid & Interface Science, 1998. 3(5): p. 485-492.
114. Shinoda, K., N. Yamaguchi, and A. Carlsson, *Physical meaning of the Krafft point: observation of melting phenomenon of hydrated solid surfactant at the Krafft point*. The Journal of Physical Chemistry, 1989. 93(20): p. 7216-7218.
115. Gu, T. and J. Sjöblom, *Surfactant structure and its relation to the Krafft Point, cloud point and micellization: Some empirical relationships*. Colloids and Surfaces, 1992. 64(1): p. 39-46.
116. Collins, K.D., *Charge density-dependent strength of hydration and biological structure*. Biophysical Journal, 1997. 72(1): p. 65-76.
117. Collins, K.D., *Ions from the Hofmeister series and osmolytes: effects on proteins in solution and in the crystallization process*. . Methods, 2004. 34(3): p. 300-311.
118. Collins, K.D., G.W. Neilson, and J.E. Enderby, *Biophysical Chemistry*, 2007. 128: p. 95-104.
119. Vlachy, N., et al., *Hofmeister series and specific interactions of charged headgroups with aqueous ions*. Advances in Colloid and Interface Science, 2009. 146(1-2): p. 42.

120. Kjellander, R., *Phase separation of non-ionic surfactant solution. A treatment of the micellar interaction and form.* Journal of the Chemical Society, Faraday Transaction 2: Molecular and Chemical Physics, 1982. 78(12): p. 2025-2042.
121. Wörnheim, T., J. Bokström, and Y. Williams, *Lower consolute temperature in a non-aqueous surfactant system.* Colloid and Polymer Science, 1988. 266(6): p. 562-565.
122. Goel, S.K., *Critical Phenomena in the Clouding Behavior of Nonionic Surfactants Induced by Additives.* Journal of Colloid and Interface Science, 1999. 212(2): p. 604-606.
123. Koshy, L., A.H. Saiyad, and A.K. Rakshit, *The effects of various foreign substances on the cloud point of Triton X 100 and Triton X 114.* Colloid and Polymer Science, 1996. 274(6): p. 582-587.
124. Neuberg, C., *Hydrotropische Erscheinungen.* Biochemische Zeitschrift, 1916. 76: p. 107-176.
125. Balasubramanian, D., et al., *Aggregation behavior of hydrotropic compounds in aqueous solution.* The Journal of Physical Chemistry, 1989. 93(9): p. 3865-3870.
126. Srinivas, V., C.S. Sundaram, and D. Balasubramanian, *Molecular structure as a determinant of hydrotropic action: A study of polyhydroxybenzenes.* Indian Journal of Chemistry, 1991. 30B: p. 147-152.
127. McKee, R.H., *Use of hydrotropic solutions in industry.* Industrial & Engineering Chemistry Research, 1946. 38: p. 382-384.
128. Varade, D. and P. Bahadur, *Effect of hydrotropes on the aqueous solution behavior of surfactants.* Journal of Surfactants and Detergents, 2004. 7(3): p. 257-259.
129. Roy, B.K. and S.P. Moulik, *Effect of hydrotropes on solution behaviour of amphiphiles.* Current Science, 2003. 85(8): p. 1148-1155.
130. da Silva, R.C., et al., *Investigations on the mechanism of aqueous solubility increase caused by some hydrotropes.* Thermochemica Acta, 1999. 328(1-2): p. 161-167.
131. Durand, M., et al., *Solubilizing and Hydrotropic Properties of Isosorbide Monoalkyl- and Dimethyl-Ethers.* Journal of Surfactants and Detergents, 2009. 12(4): p. 371-378.
132. Bancroft, W.D., *The theory of emulsification, V.* The Journal of Physical Chemistry, 1912. 17(6): p. 501-519.
133. Schramm, L.L., *Emulsions, Foams, and Suspensions*, ed. L.L. Schramm 2005, Weinheim: Wiley-VCH.
134. Petesev, D., *Emulsions: Structure, Stability and Interactions*, ed. D. Petesev 2004, London: Elsevier.
135. Fingas, M. and B. Fieldhouse, *Formation of water-in-oil emulsions and application to oil spill modelling.* Journal of Hazardous Materials, 2004. 107(1-2): p. 37-50.
136. Ozawa, K., C. Solans, and H. Kunieda, *Spontaneous Formation of Highly Concentrated Oil-in-Water Emulsions.* Journal of Colloid and Interface Science, 1997. 188(2): p. 275-281.
137. Hoar, T.P. and J.H. Schulman, *Transparent Water-in-Oil Dispersions: the Oleopathic Hydro-Micelle.* Nature, 1943. 152: p. 102-103.
138. Schulman, J.H., W. Stoeckenius, and L.M. Prince, *Mechanism of Formation and Structure of Micro Emulsions by Electron Microscopy.* The Journal of Physical Chemistry, 1959. 63(10): p. 1677-1680.

139. Shinoda, K. and H. Kunieda, *Conditions to produce so-called microemulsions: Factors to increase the mutual solubility of oil and water by solubilizer*. Journal of Colloid and Interface Science, 1973. 42(2): p. 381-387.
140. Eicke, H.F., *Surfactants in non polar solvents*. Topics in Current Chemistry, 1980. 87: p. 85-145.
141. Bodet, J.F., et al., *Fluid microstructure transition from globular to bicontinuous in mid-range microemulsion*. The Journal of Physical Chemistry, 1988. 92(7): p. 1898-1902.
142. Jahn, W. and R. Strey, *Microstructure of microemulsions by freeze fracture electron microscopy*. The Journal of Physical Chemistry, 1988. 92(8): p. 2294–2301.
143. Lichterfeld, F., T. Schmeling, and R. Strey, *Microstructure of microemulsions of the system water-n-tetradecane-alkyl polyglycol ether (C12E5)*. The Journal of Physical Chemistry, 1986. 90(22): p. 5762-5766.
144. Chen, S.H., *Small Angle Neutron Scattering Studies of the Structure and Interaction in Micellar and Microemulsion Systems*. Annual Review of Physical Chemistry, 1986. 37(1986): p. 351-399.
145. Salager, J.-L., et al., *Enhancing Solubilization in Microemulsions—State of the Art and Current Trends*. Journal of Surfactants and Detergents, 2005. 8(1): p. 3-21.
146. Miñana-Perez, M., et al., *Solubilization of polar oils with extended surfactants*. Colloids and Surfaces A: Physicochemical and Engineering Aspects, 1995. 100: p. 217-224.
147. Do, L.d., et al., *Environmentally Friendly Vegetable Oil Microemulsions Using Extended Surfactants and Linkers*. Journal of Surfactants and Detergents, 2009. 12(4): p. 91-99.
148. Tanthakit, P., et al., *Palm Oil Removal from Fabric Using Microemulsion-Based Formulations*. Journal of Surfactants and Detergents, 2010. 13(4): p. 485-495.
149. Phan, T.T., et al., *Microemulsion-Based Vegetable Oil Detergency Using an Extended Surfactant*. Journal of Surfactants and Detergents, 2010. 13(3): p. 313-319.
150. Alander, J. and T. Warnheim, *Model microemulsions containing vegetable oils part 1: Nonionic surfactant*. Journal of the American Oil Chemists Society, 1989. 66(11): p. 1656-1660.
151. Alander, J. and T. Wårnheim, *Model microemulsions containing vegetable oils 2. Ionic surfactant systems*. Journal of the American Oil Chemists Society, 1989. 66(11): p. 1661-1665.
152. Joubran, R.F., D.G. Cornell, and P. N., *Microemulsions of triglyceride and non-ionic surfactant — effect of temperature and aqueous phase composition*. Colloids and Surfaces A: Physicochemical and Engineering Aspects, 1993. 80(2-3): p. 153-160.
153. Fanun, M., *Properties of microemulsions with sugar surfactants and peppermint oil*. Colloid and Polymer Science, 2009. 287(8): p. 899-910.
154. von Corswant, C. and O. Söderman, *Effect of Adding Isopropyl Myristate to Microemulsions Based on Soybean Phosphatidylcholine and Triglycerides*. Langmuir, 1998. 14(13): p. 3506-3511.
155. Garti, N., et al., *Some Characteristics of Sugar Ester Nonionic Microemulsions in View of Possible Food Applications*. Journal of Agricultural and Food Chemistry, 2000. 48(9): p. 3945-3956.

156. De Gennes, P.G. and C. Taupin, *Microemulsions and the Flexibility of Oil/Water Interfaces*. The Journal of Physical Chemistry, 1982. 86(13): p. 2294-2304.
157. Israelachvili, J.N., *The science and applications of emulsions — an overview*. Colloids and Surfaces A: Physicochemical and Engineering Aspects, 1994. 91: p. 1-8.
158. Anderson, J.L., et al., *Characterizing Ionic Liquids On the Basis of Multiple Solvation Interactions*. Journal of the American Chemical Society, 2002. 124(47): p. 14247-14254.
159. Scriven, L.E., *Equilibrium bicontinuous structure*. Nature, 1976. 263: p. 123-125.
160. Langevin, D., *Micelles and Microemulsions*. Annual Review of Physical Chemistry, 1992. 43: p. 341-369.
161. Burke, J., *Solubility Parameters: Theory and Application*, T.A.I.o. Conservation, Editor 1984, Book and Paper Group.
162. Hansen, C.M., *Hansen Solubility Parameters. A User`s Handbook*.2000: CRC Press.
163. Hildebrand, J. and R.L. Scott, *The Solubility of Nonelectrolytes*. 3rd ed, ed. Reinhold1950, New York.
164. Patterson, D. and G. Delmas, *New Aspects of Polymer Solution Thermodynamics*. Off. Dig. Fed. Soc. Paint Technol., 1962. 34(450): p. 677-692.
165. Patterson, D.D., *Introduction to Thermodynamics of Polymer Solubility*. Journal of Paint Technology, 1969. 41(536): p. 489-493.
166. Barton, A.F.M., *Handbook of Solubility Parameters and Other Cohesion Parameters*, ed. B. Raton1983, FL: CRC Press.
167. Blanks, R.F. and J.M. Prausnitz, *Thermodynamics of Polymer Solubility in Polar and Nonpolar Systems*. Industrial & Engineering Chemistry Fundamentals 1964. 3(1): p. 1-8.
168. Hansen, C.M., *The Three Dimensional Solubility Parameter-Key to Paint Component Affinities I*. Journal of Paint Technology, 1967. 39(505): p. 104-117.
169. Hansen, C.M., *The Three Dimensional Solubility Parameter-Key to Paint Component Affinities II*. Journal of Paint Technology, 1967. 39(511): p. 505-510.
170. Hansen, C.M. and K. Skaarup, *The Three Dimensional Solubility Parameter-Key to Paint Component Affinities III*. Journal of Paint Technology, 1967. 39(511): p. 511-514.
171. Rengstl, D., *Choline as a Cation for the Design of Low-toxic and Biocompatible Ionic Liquids, Surfactants, and Deep Eutectic Solvents.*, in *Institute of Physical and Theoretical Chemistry*2013, University of Regensburg: Regensburg.
172. Vlachy, N., *Formation and stabilization of vesicles in mixed surfactant systems.*, in *Institute of Physical and theoretical Chemistry*2008, University of Regensburg: Regensburg.
173. Kauzmann, W., *Some factors in the interpretation of protein denaturation*. Advances in Protein Chemistry, 1959. 14: p. 1-63.
174. Kunz, W., *Specific ion effects in colloidal and biological systems*. Current Opinion in Colloid & Interface Science, 2010. 15: p. 34-39.
175. Hofmeister, F., *Zur Lehre von der Wirkung der Salze*. Arch. Exp. Pathol. Pharmakol., 1888. 24: p. 247-260.

176. Kunz, W., *Specific Ion effects*, ed. W. Kunz 2010, Singapore: World Scientific Publishing Co. Pte. Ltd. .
177. Vlachy, N., et al., *Hofmeister series and specific interactions of charged headgroups with aqueous ions*. *Advances in Colloid and Interface Science*, 2009. 146(1-2): p. 42-47.
178. Kunz, W., J. Henle, and B.W. Ninham, 'Zur Lehre von der Wirkung der Salze' (about the science of the effect of salts): *Franz Hofmeister's historical papers*. *Current Opinion in Colloid & Interface Science*, 2004. 9: p. 19-37.
179. Collins, K.D., *Ions from the Hofmeister series and osmolytes: effects on proteins in solution and in the crystallization process*. *Methods*, 2004. 34(3): p. 300-311.
180. Jungwirth, P. and D.J. Tobias, *Specific Ion Effects at the Air/Water Interface*. *Chemical Reviews*, 2006. 106: p. 1259.
181. Bernal, J. and R.H. Fowler, *A Theory of Water and Ionic Solution, with Particular Reference to Hydrogen and Hydroxyl Ions*. *Journal of Chemical Physics*, 1933. 1(8): p. 515-548.
182. Gurney, R.W., *Ionic Processes in Solution* 1953: McGraw-Hill Book Company, Inc.
183. Kunz, W., *Specific ion effects in colloidal and biological systems*. *Current Opinion in Colloid & Interface Science*, 2010. 15(1): p. 34-39.
184. Lyklema, J., *Simple Hofmeister Series*. *Chemical Physics Letters*, 2009. 467(4-6): p. 217-222.
185. *Grundlagen ternärer Phassendiagramme*: http://www.ifw-dresden.de/userfiles/groups/imw_folder/lectures/Physikalische_Werkstoffeigenschaften/c5-ternpd.pdf.
186. Stratavant, j.M., *Biochemical applications of differential scanning calorimetry*. *Annual Review of Physical Chemistry*, 1987. 38: p. 463-488.
187. Barrall, E.M., *Precise determination of melting and boiling points by differential thermal analysis and differential scanning calorimetry*. *Thermochimica Acta*, 1973. 5: p. 377-389.
188. Cammenga, H.K. and M. Epple, *Grundlagen der Thermischen Analysetechniken und ihre Anwendungen in der präparativen Chemie*. *Angewandte Chemie*, 1995. 107: p. 1284-1301.
189. Masberg, S., *Differentialkalorimetrie (DSC) und Differentialthermoanalyse (DTA) bei hohen Drücken.*, in *Fakultät Chemie* 1999, Ruhr-Universität Bochum: Bochum.
190. Sarge, S.M., *Determination of Characteristic Temperatures with the Scanning Calorimeter*. *Thermochimica Acta*, 1991. 187: p. 323-334.
191. Höhne, G.W.H., et al., *THE TEMPERATURE CALIBRATION OF SCANNING CALORIMETERS*. *Thermochimica Acta*, 1990. 160: p. 1-12.
192. Renoncourt, A., *Study of supra-aggregates in cationic surfactant systems*, in *Institute of Physical and Theoretical Chemistry* 2005, University of Regensburg: Regensburg.
193. Dubois, M., et al., *Self-assembly of regular hollow icosahedra in salt-free cationic solutions*. *Nature*, 2001. 411(6838): p. 672-675.
194. Bloch, F., W.W. Hansen, and M. Packard, *Nuclear Induction*. *Physical Review*, 1946. 69(3-4): p. 127-127.
195. Purcell, E.M., H.C. Torrey, and R.V. Pound, *Resonance Absorption by Nuclear Magnetic Moments in a Solid*. *Physical Review*, 1946. 69(1-2): p. 37-38.

196. Nelson, F.A. and H.E. Weaver, *Nuclear Magnetic Resonance Spectroscopy in Superconducting Magnetic Fields* Science, 1964. 146(3641): p. 223-232.
197. Ernst, R.R. and W.A. Anderson, *Application of Fourier Transform Spectroscopy to Magnetic Resonance* Review of Scientific Instruments, 1966. 37(1): p. 93-102.
198. Ernst, R.R., G. Bodenhausen, and A. Wokaun, *Principles of Nuclear Magnetic Resonance in One and Two Dimensions* 1987, Oxford: Clarendon Press.
199. Kessler, H., M. Gehrke, and C. Griesinger, *Two-Dimensional NMR Spectroscopy: Background and Overview of the Experiments [New Analytical Methods (36)]*. Angewandte Chemie International Edition in English, 1988. 27(4): p. 490-536.
200. Kay, L.E., et al., *Four-dimensional heteronuclear triple-resonance NMR spectroscopy of interleukin-1 beta in solution* Science, 1990. 249(4967): p. 411-414.
201. Silverstein, R.M., F.X. Webster, and D.J. Kiemle, *Spectrometric identification of organic compounds*. Seventh Edition ed2005: John Wiley & Sons.
202. Dengler, S., *Synthesis and Characterisation of Sustainable Low Toxic Cationic Surfactants*, in *Naturwissenschaftlichen Fakultät IV* 2010, University of Regensburg: Regensburg.
203. Jacobsen, N.E., *NMR Spectroscopy Explained* 2007, New Jersey: John Wiley & Sons.
204. Webb, G.A., *Nuclear Magnetic Resonance* 2005: The Royal Society of Chemistry.
205. Kessler, H. and G. Gemmecker, *Skriptum zur Vorlesung Organische Chemie IV*, 2000, Institut für Organische Chemie und Biochemie: Technische Universität München.
206. Weast, R.C., *Handbook of Chemistry and Physics* 1974: CRC Press, Inc.
207. Persson, N.O. and B. Lindman, *Deuteron Nuclear Magnetic Resonance in Amphiphilic Liquid Crystals. Alkali Ion Dependent Water and Amphiphile Orientation*. The Journal of Physical Chemistry, 1975. 79(14): p. 1410-1418.
208. Dengler, S., et al., *How specific are ion specificities? A pilot NMR study*. Faraday Discussions, 2012. 160(6): p. 1-13.
209. Wennerstrom, H., G. Lindblom, and B. Lindman, *Theoretical aspects on the NMR of quadrupolar ionic nuclei in micellar solutions and amphiphilic liquid crystals*. Chemica Scripta, 1974. 6(3): p. 97.
210. Lindblom, G., *Ion binding in liquid crystals studied by NMR: III. Sodium-23 quadrupolar effects in a model membrane system*. Acta Chemica Scandinavica, 1971. 25(7): p. 2767.
211. Leigh, I.D., et al., *Structure of Liquid-crystalline Phases formed by Sodium Dodecyl Sulphate and Water as determined by Optical Microscopy, X-ray Diffraction and Nuclear Magnetic Resonance Spectroscopy*. Journal of the Chemical Society, Faraday Transaction 1: Physical Chemistry in Condensed Phases, 1981. 77(12): p. 2867.
212. Cohen, M.H. and F. Reif, *Quadrupole Effects in Nuclear Magnetic Resonance Studies of Solids*. Solid State Physics, 1957. 5: p. 321-438.
213. Lindblom, G., B. Lindman, and G.J.T. Tiddy, *Ion binding studied using quadrupole splittings of sodium-23(1+) ions in lyotropic liquid crystals. The dependence on surfactant type*. Journal of American Chemical Society, 1978. 100(8): p. 2299.

214. Persson, N.-O. and G. Lindblom, *Cesium ion and water interaction in the lamellar phase of the 1-Monooctanoil-water-CsCl system. NMR quadrupole splittings and chemical shift anisotropies*. The Journal of Physical Chemistry, 1979. 83(23): p. 3015-3019.
215. Tiddy, G.J.T., M.F. Walsh, and E. Wyn-Jones, *Ultrasonic relaxation studies of concentrated surfactant solutions and liquid crystals*. Journal of the Chemical Society, Faraday Transactions 1: Physical Chemistry in Condensed Phases, 1982. 78(2): p. 389-401.
216. Lindblom, G., B. Lindman, and G.J.T. Tiddy, *Counter-ion Quadrupole Splittings in Lyotropic Liquid Crystals. Determination of the Sign of the Order Parameter*. Acta Chemica Scandinavica, 1975. A 29(9): p. 876.
217. Bunkall, P.R. and M. Quinn, *Instrumental colour measurement and control*. Journal of the Society of Cosmetic Chemists, 1969. 20: p. 265-281.
218. GmbH, B.-G., *Solid Color*.
https://www.byk.com/fileadmin/BYK/.../color/en/Intro_Solid_Color.pdf.
219. Lab, H., *The Basics of Color Perception and Measurement*, 2001: www.hunterlab.com/pdf/color.pdf.
220. Hoffmann, G., *CIE Lab Color Space*, 2003: <http://www.fho-empden.de/~hoffmann/cielab03022003.pdf>.
221. Foster, M., *A text-book of physiology* ed. L.B. Co1891.
222. Klamt, A., *COSMO-RS From Quantum Chemistry to Fluid Phase Thermodynamics and Drug Design* 2005: Elsevier.
223. Verma, N.R., et al., *(Solid+liquid) equilibria predictions of ionic liquid containing systems using COSMO-RS*. J. Chem. Thermodynamics, 2012. 48: p. 246-253.
224. Prausnitz, J.M., R.N. Lichtenthaler, and E.G. De Azevedo. *Molecular Thermodynamics of Fluid Phase Equilibria* 1986: Prentice-Hall.
225. Eckert, F., *COSMOtherm Users Manual*, 1999, COSMOlogic GmbH & Co KG.
226. Kratky, O., H. Leopold, and H. Stabinger, *Dichtemessungen an Flüssigkeiten und Gasen auf 10⁻⁶ g/cm³ bei 0.6 cm³ Präparatvolumen*. Zeitschrift für Angewandte Physik, 1969. 27: p. 273-277.
227. Macosko, C.W., *Rheology: Principles, Measurements and Applications* 1994, Weinheim: Wiley VCH.
228. Hutter, K., *Fluid- und Thermodynamik* 1995, Berlin: Springer.
229. Eirich, F.R., *Rheology*. Encyclopedia of Physics 1991, New York: Wiley VCH.
230. Schrödle, S., R. Buchner, and W. Kunz, *Automated apparatus for the rapid determination of liquid-liquid and solid-liquid phase transitions*. Fluid Phase Equilibria, 2004. 216: p. 175-182.
231. Fischer, K., *Neues Verfahren zur maßanalytischen Bestimmung des Wassergehaltes von Flüssigkeiten und festen Körpern*. Angewandte Chemie, 1935. 48(26): p. 394-396.
232. Azemar, N., I. Carrera, and C. Solans, *Studies on textile detergency at low temperature*. Journal of Dispersion Science and Technology, 1993. 14(6): p. 645-660.
233. *Eigenschaften der natürlichen Öle und Fette*: <http://digisrv-1.biblio.etc.tu-bs.de/dfq-files/00036923/DWL/00000037.pdf>.
234. Larsson, K., *Classification of glyceride crystal forms*. Acta Chemica Scandinavica, 1966. 20: p. 2255-2260.

235. Aronhime, J., S. Sarig, and N. Garti, *Emulsifiers as additives in fats: Effect on polymorphic transformation and crystal properties of fatty acids and triglycerides*. Food Structure, 1990. 9: p. 2-17.
236. Hagemann, J.W. and J.A. Rothfus, *Polymorphism and transformation energetics of saturated monoacid triglycerides from differential scanning calorimetry and theoretical modeling*. Journal of the American Oil Chemists Society, 1983. 60(6): p. 1123-1131.
237. Hirschberg, H.G., *Handbuch Verfahrenstechnik und Anlagenbau: Chemie, Technik, Wirtschaftlichkeit*, 1999, Springer Verlag
238. Klein, R., et al., *Choline alkylsulfates - New promising green surfactants*. Journal of Colloid and Interface Science, 2012. 392: p. 274-280.
239. Chemicals, D.:
http://msdssearch.dow.com/PublishedLiteratureDOWCOM/dh_0040/0901b80380040398.pdf?filepath=oxysolvents/pdfs/noreg/110-00927.pdf&fromPage=GetDoc
http://msdssearch.dow.com/PublishedLiteratureDOWCOM/dh_0077/0901b8038007742e.pdf?filepath=oxysolvents/pdfs/noreg/110-00929.pdf&fromPage=GetDoc
http://msdssearch.dow.com/PublishedLiteratureDOWCOM/dh_08ae/0901b803808ae5e4.pdf?filepath=oxysolvents/pdfs/noreg/110-00928.pdf&fromPage=GetDoc
http://msdssearch.dow.com/PublishedLiteratureDOWCOM/dh_0077/0901b80380077483.pdf?filepath=oxysolvents/pdfs/noreg/110-00590.pdf&fromPage=GetDoc
http://msdssearch.dow.com/PublishedLiteratureDOWCOM/dh_08bb/0901b803808bb9c3.pdf?filepath=oxysolvents/pdfs/noreg/110-00934.pdf&fromPage=GetDoc
240. Bergenstahl, B. and K. Fontell, *Phase equilibria in the system soybean lecithin/water*. Progress in Colloid&Polymer Science, 1983. 68: p. 48-52.
241. Ziegelitz, R. and L. Popper, *Lecithin-bewährte Funktionalität*, in *bmi aktuell*2005, Backmittelinstitut: Bonn.
242. Yangxin, Y., Z. Jin, and A.E. Bayly, *Development of Surfactants and Builders in Detergent Formulations*. Chinese Journal of Chemical Engineering, 2008. 16(4): p. 517-527.
243. Scheibel, J.J., *The evolution of anionic surfactant technology to meet the requirements of the laundry detergent industry*. Journal of Surfactants and Detergents, 2004. 7(4): p. 319-328.
244. Tai, L.H.T., *Formulating Detergents and Personal Care Products: A complete Guide to Product Development*2000: AOCS Press.
245. Hoydonckx, H.E., et al., *Furfural and Derivates*, in *Ullmanns Encyclopedia of Industrial Chemistry*2012, Wiley-VCH: Weinheim.
246. Lichtenthaler, F.W., *Carbohydrates as Organic Raw Materials*, in *Ullmanns Encyclopedia of Industrial Chemistry*2012, Wiley-VcH: Weinheim.
247. Klein, R., D. Touraud, and W. Kunz, *Choline carboxylate surfactants: biocompatibel and highly soluble in water*. Green Chemistry, 2008. 10: p. 433-435.
248. Laughlin, R.G., *The Aqueous Phase Behavior of Surfactants*1996, San Diego: Academic Press.
249. Preston, W.C., *Some Corellating Principles of Detergent Action*. The Journal of Physical Chemistry, 1948. 52(1): p. 84-97.

250. Zana, R., *Partial Phase Behavior and Micellar Properties of Tetrabutylammonium Salts of Fatty Acids: Unusual Solubility in Water and Formation of Unexpectedly Small Micelles*. Langmuir, 2004. 20(14): p. 5666-5668.
251. Shinoda, K. and H. Kunieda, *Krafft Points, Critical Micelle Concentrations, Surface Tension, and Solubilizing Power of Aqueous Solutions of Fluorinated Surfactants*. The Journal of Physical Chemistry, 1976. 80(22): p. 2468-2470.
252. Lin, B., et al., *Solubility of sodium soaps in aqueous salt solutions*. Journal of Colloid and Interface Science, 2005. 291(2): p. 543-549.
253. Yu, Z.-J., X. T Zhang, and G. Xu, *Physicochemical properties of aqueous mixtures of tetrabutylammonium bromide and anionic surfactants. 3. Effects of surfactant chain length and salinity*. The Journal of Physical Chemistry, 1990. 94(9): p. 3675-3681.
254. Moberg, R., et al., *ESCA studies of phase-transfer catalysts in solution: ion pairing and surface activity*. Journal of the American Chemical Society, 1991. 113(10): p. 3663-3667.
255. Hrobárik, T., L. Vrbka, and P. Jungwirth, *Selected biologically relevant ions at the air/water interface: A comparative molecular dynamics study* Biophysical Chemistry, 2006. 124(3): p. 238-242.
256. Hofmeister, E., Arch. Exp. Pathol. Pharmakol., 1888. 24.
257. Holthauzen, L.M. and D.W. Bolen, *Mixed osmolytes: the degree to which one osmolyte affects the protein stabilizing ability of another*. Protein Science, 2007. 16(2): p. 293-298.
258. Bolen, D.W., *Protein stabilization by naturally occurring osmolytes*. Methods in Molecular Biology, 2001. 168: p. 17-36.
259. Yancey, P.H., et al., *Living with water stress: evolution of osmolyte systems* Science, 1982. 217(4566): p. 1214-1222.
260. Brown, A.D. and J.R. Simpson, *Water Relations of Sugar-tolerant Yeasts: the Role of Intracellular Polyols* Journal of General Microbiology, 1972. 72(3): p. 589-591.
261. Pollard, A. and R.G. Wyn Jones, *Enzyme activities in concentrated solutions of glycinebetaine and other solutes*. Planta, 1979. 144(3): p. 291-298.
262. Borowitzka, L.J. and A.D. Brown, *The salt relations of marine and halophilic species of the unicellular green alga, Dunaliella*. Archives of Microbiology, 1974. 96(1): p. 37-52.
263. Lang, F., *Mechanisms and significance of cell volume regulation*. Journal of the American College of Nutrition, 2007. 26(5 Suppl): p. 613S-623S.
264. Sussich, F., et al., *Reversible dehydration of trehalose and anhydrobiosis: from solution state to an exotic crystal?* Carbohydrate Research, 2001. 334(3): p. 165-176.
265. Crowe, J.H., J.F. Carpenter, and L.M. Crowe, *The role of vitrification in anhydrobiosis*. Annual Reviews of Physiology, 1998. 60: p. 73-103.
266. Baltes, W. and R. Mattisek, *Lebensmittelkonservierung*, in *Lebensmittelchemie* 2011, Springer: Heidelberg.
267. Crowe, J.H., F.A. Hoekstra, and L.M. Crowe, *Anhydrobiosis*. Annual Review of Physiology, 1992. 54: p. 579-599.
268. Crowe, J.H. and L.M. Crowe, *Preservation of mammalian cells—learning nature's tricks*. Nature Biotechnology, 2000. 18(2): p. 145-146.
269. Guo, N., et al., *Trehalose expression confers desiccation tolerance on human cells*. Nature Biotechnology, 2000. 18(2): p. 168-171.

270. Elbein, A.D., et al., *New insights on trehalose: a multifunctional molecule*. Glycobiology, 2003. 13(4): p. 17R-27R.
271. Crowe, J.H., L.M. Crowe, and D. Chapman, *Preservation of Membranes in Anhydrobiotic Organisms: The Role of Trehalose*. Science, 1984. 223(4637): p. 701-703.
272. Crowe, J.H., L.M. Crowe, and D. Chapman, *Preservation of Membranes in Anhydrobiotic Organisms: The Role of Trehalose* Science, 1984. 223: p. 701-703.
273. Breedveld, M., L.P.T.M. Zevenhuizen, and A.J.B. Zehinder, *Osmotically-regulated trehalose accumulation and cyclic β -(1,2)-glucan excretion by *Rhizobium leguminosarum* biovar *trifolii* TA-1*. Archives of Microbiology, 1991. 156(6): p. 501-506.
274. *Nahrungsergänzungsmittelpräparat mit Aminosäuren und Gewürzextrakt*, 2011, PM-International AG (Luxemburg/Luxembourg, LU) Germany.
275. Römpp, H., *Römpp-Chemie-Lexikon*. Chemie-Lexikon, Stuttgart: Thieme.
276. Peterkofsky, B. and S. Udenfriend, *Conversion of Proline to Collagen Hydroxyproline in a Cell-free System from Chick Embryo*. The Journal of Biological Chemistry, 1963. 238(12): p. 3966-3977.
277. Carey, F.A., *Organic Chemistry*, ed. T.M. Companies. Vol. 5. 2001.
278. Galinski, E.A., H.P. Pfeiffer, and H.G. Trüper, *1,4,5,6-Tetrahydro-2-methyl-4-pyrimidinecarboxylic acid: A novel cyclic amino acid from halophilic phototrophic bacteria of the genus *Ectothiorhodospira**. European Journal of Biochemistry, 1985. 149(1): p. 135-139.
279. Severin, J., A. Wohlfarth, and E.A. Galinski, *The predominant role of recently discovered tetrahydropyrimidines for the osmoadaptation of halophilic eubacteria*. Journal of General Microbiology, 1992. 138(8): p. 1629-1638.
280. Lentzen, G. and T. Schwarz, *Extremolytes: natural compounds from extremophiles for versatile applications*. Applied Microbiology and Biotechnology, 2006. 72(4): p. 623-634.
281. Buenger, J. and H. Driller, *Ectoin: An Effective Natural Substance to Prevent UVA-Induced Premature Photoaging*. Skin Pharmacology and Physiology, 2004. 17: p. 232-237.
282. Beyer, N., H. Driller, and J. Buenger, *Ectoin : a innovative, multi-functional active substance for the cosmetic industry*. SÖFW Journal, 2000. 126(12): p. 26-29.
283. Kuhlmann, A.U., *Biosynthese und Transport des kompatiblen Soluten Ectoin in *Bacillus* spp.*, in *Fachbereich Biologie2002*, Philipps-Universität Marburg: Marburg.
284. Motitschke, L., H. Driller, and E. Galinski, *Ectoin and ectoin derivatives as moisturizers in cosmetics*, 2000, Merck Patent GmbH: United States Patent.
285. Lippert, K. and E. Galinski, *Enzyme stabilization by ectoine-type compatible solutes: protection against heating, freezing and drying*. Applied Microbiology and Biotechnology, 1992. 37(1): p. 61-65.
286. Wohlfarth, A., J. Severin, and E.A. Galinski, *The spectrum of compatible solutes in heterotrophic halophilic eubacteria of the family Halomonadaceae*. Journal of general microbiology, 1990. 136(4): p. 705-712.
287. Malin, G. and A. Lapidot, *Induction of synthesis of tetrahydropyrimidine derivatives in *Streptomyces* strains and their effect on *Escherichia coli* in response to osmotic and heat stress*. . Journal of Bacteriology, 1996. 178(2): p. 385-395.

288. Louis, P., H.G. Trüper, and E.A. Galinski, *Survival of Escherichia coli during drying and storage in the presence of compatible solutes*. Applied Microbiology and Biotechnology, 1994. 41(6): p. 684-688.
289. Gousbet, G., et al., *Erwinia chrysanthemi at high osmolarity: influence of osmoprotectants on growth and pectate lyase production* Journal of General Microbiology, 1995. 141(6): p. 1407-1412.
290. Galinski, E.A., *Compatible solutes of halophilic eubacteria: molecular principles, water-solute interactions, stress protection*. Experientia, 1993. 49: p. 487-496.
291. Inbar, L., F. Frolow, and A. Lapidot, *The conformation of new tetrahydropyrimidine derivatives in solution and in the crystal*. European Journal of Biochemistry 1993. 214: p. 897-906.
292. Peters, P., E.A. Galinski, and H.G. Trüper, *The biosynthesis of ectoine*. FEMS Microbiology Letters, 1990. 71(1-2): p. 157-162.
293. Sikorski, Z.E., S. Kostuch, and I. Kolodziejska, *Zur Frage der Proteindenaturierung im gefrorenen Fischfleisch*. Food/Nahrung, 1975. 19(9-10): p. 997-1003.
294. Barton, K., M. Buhr, and J. Ballantyne, *Effects of urea and trimethylamine-N-oxide on fluidity of liposomes and membranes of an elasmobranch*. Journal of the American Physiological Society-Regulatory, Integrative and Comparative Physiology 1999. 276: p. 397-406.
295. : http://www.novamex.de/Lexikon/Weitere/Cholin_Betain.html.
296. Billigmann, P. and S. Siebrecht, *Physiologie des L-Carnitins und seine Bedeutung für Sportler*, ed. G.f.E. e.V.2004, Hannover: Schlütersche Verlagsgesellschaft mbH & CoKG.
297. Fritz, I., *The effects of muscle extracts on the oxidation of palmitic acid by liver slices and homogenates*. Acta Physiologica Scandinavica, 1955. 34(4): p. 367-385.
298. Fritz, I. and K.T.N. Yue, *Long-chain carnitine acyltransferase and the role of acylcarnitine derivatives in the catalytic increase of fatty acid oxidation induced by carnitine* The Journal of Lipid Research, 1963. 4(3): p. 279-288.
299. Bremer, J., *Carnitine in Intermediary Metabolism: The Biosynthesis of Palmitoylcarnitine by Cell Subfractions*. The Journal of Biological Chemistry, 1963. 238(8): p. 2774-2779.
300. Schmengler, U.S., *Effekte der L-Carnitinsupplementierung auf das metabolische Profil adipöser und insulinresistenter Ponys im Verlaufe einer mehrwöchigen Körpergewichtsreduktion*, in *Institut für Tierernährung, Ernährungsschäden und Diätetik der Veterinärmedizinischen Fakultät*2013, Universität Leipzig: Leipzig.
301. Hoppel, C.L. and A.T. Davis, *Inter-tissue relationships in the synthesis and distribution of carnitine*. Biochemical Society Transactions, 1986. 14(4): p. 673-674.
302. Fischer, M., *Experimentelle Untersuchungen zum Carnitin-Metabolismus beim Schwein*, in *Institut für Agrar- und Ernährungswissenschaften*2009, Martin-Luther-Universität Halle-Wittenberg: Halle/saale.
303. Rebouche, C.J. and H. Seim, *Carnitine metabolism and its regulation in microorganisms and mammals*. Annual Review of Nutrition, 1998. 38: p. 39-61.
304. Vaz, F.M. and R.J. Wanders, *Carnitine biosynthesis in mammals*. Biochemical Journal, 2002. 361(3): p. 417-429.

305. Millington, D.S., et al., *The role of tandem mass spectrometry in the diagnosis of fatty acid oxidation disorders*. Progress in clinical and biological research, 1992. 375: p. 339-354.
306. Cherchi, J., et al., *Effects of L-carnitine on exercise tolerance in chronic stable angina: a multicenter, double-blind, randomized, placebo controlled crossover study*. International Journal of Clinical Pharmacology, Therapy and Toxicology, 1985. 23(10): p. 569-572.
307. Tam, K.Y., et al., *The Permeation of Amphoteric Drugs through Artificial Membranes - An in Combo Absorption Model Based on Paracellular and Transmembrane Permeability*. Journal of Medicinal Chemistry, 2010. 53: p. 392-401.
308. Marcus, J., D. Touraud, and W. Kunz, *Formulation and stability of a soap microemulsion and the apparent pKa herein*. Journal of Colloid and Interface Science, 2013. 407: p. 382-389.
309. Galinski, E.A. and K. Lippert, *Novel Compatible Solutes and Their Potential Application as Stabilizers in Enzyme Technology*, in *General and Applied Aspects of Halophilic Microorganisms* 1991, Springer.
310. Klein, R., et al., *Solubilisation of stearic acid by the organic base choline hydroxide*. Colloids and Surfaces A: Physicochemical and Engineering Aspects, 2009. 338(1-3): p. 129-134.
311. Jungwirth, P. and D.J. Tobias, *Specific ion effects at the air/water interface*. Chemical Reviews, 2006. 106: p. 1259-1281.
312. Dang, L.X. and T.M. Chang, *Molecular mechanism of ion binding to the liquid/vapor interface of water*. The Journal of Physical Chemistry B, 2002. 106: p. 235-238.
313. Schwierz, N., D. Horinek, and R.R. Netz, *Reversed Anionic Hofmeister Series: The Interplay of Surface Charge and Surface Polarity*. Langmuir, 2010. 26: p. 7370.
314. Luzzati, V., *X-ray diffraction studies of lipid-water systems*. Biological Membranes, 1968: p. 71.
315. Ekwall, P., L. Mandell, and K. Fontell, *Ternary Systems of Potassium Soap, Alcohol and Water, I Phase Equilibria and Phase Structures*. Journal of Colloid and Interface Science, 1969. 31(4): p. 508.
316. Ekwall, P., L. Mandell, and K. Fontell, *Ternary Systems of Potassium Soaps, Alcohol and Water, II Structure and Composition of the Mesophases*. Journal of Colloid and Interface Science, 1969. 31(4): p. 530.
317. Ekwall, P., *Compositions, properties and structures of liquid crystalline phases in systems of amphiphilic compounds*. Advances in Liquid Crystals, 1975. 1: p. 1.
318. Ekwall, P., L. Mandell, and K. Fontell, *Solubilization in micelles and mesophases and the transition from normal to reversed structures*. Molecular Crystals and Liquid Crystals, 1969. 8: p. 157.
319. Soderman, O., et al., *The Interactions between Monovalent Ions and Phosphatidyl Cholines in Aqueous Bilayers*. European Journal of Chemistry, 1983. 134: p. 309.
320. Everiss, E., G.J.T. Tiddy, and B.A. Wheeler, *Phase Diagram and NMR Study of the Lyotropic Liquid Crystalline Phases Formed by Lithium Perfluoro-Octanoate and Water*. Journal of Chemical Society: Faraday Transaction I, 1976. 72: p. 1747.

-
321. Wennerstrom, H., et al., *Chemical Shift Anisotropies of $^{133}\text{Cs}^+$ Counterions in Lyotropic Liquid Crystals*. Journal of Magnetic Resonance, 1978. 30(1): p. 133.
 322. Komsa-Penkova, R., et al., *Thermal stability of calf skin collagen type I in salt solutions*. Biochimica and Biophysica Acta, 1996. 1297: p. 171.
 323. Kubicova, A., et al., *Overcharging in Biological Systems: Reversal of Electrophoretic Mobility of Aqueous Polyaspartate by Multivalent Cations*. Physical Review Letters, In Press.
 324. Robinson, J.B., J.M. Strottmann, and E. Stellwagen, *Prediction of neutral salt elution profiles for affinity chromatography* Proceedings of the National Academy of Sciences, 1981. 78(4): p. 2287-2291.
 325. Meyer-Berkhout, U., *Betimmung der elektrischen Quadrupolmomente der Kerne Rb^{85} und Rb^{87} durch Messung der Hochfrequenzübergänge im angeregten $^6P_{3/2}$ -Term des Rb-Atoms*. Zeitschrift für Physik, 1955. 141: p. 185-187.
 326. Kunz, W., *Specific ion effects in colloidal and biological systems*. Current Opinion in Colloid & Interface Science, 2010. 15: p. 34-39.
 327. Blackmore, E.S. and G.J.T. Tiddy, *Optical microscopy, multinuclear NMR (^2H , ^{14}N and ^{35}Cl) and X-Ray studies of dodecyl- and hexadecyl-trimethylammonium chloride/water mesophases*. Liquid Crystals, 1990. 8(1): p. 131.

Appendix

List of figures

Chapter 1

Figure 1.1: Schematic drawing of a wash house. The direction of washing is reversed to the water flow direction. 2

Chapter 2

Figure 2.1: Schematic presentation of the cross section through a cotton fibre. 7

Figure 2.2: Contact area and angle between substrate and soil depending on the state of soil matter and the environment. 10

Figure 2.3: Schematic representation of liquid soil release by (a) roll-up mechanism and (b) emulsification. 13

Figure 2.4: Two-step particulate soil removal from fiber in aqueous washing liquid. 14

Figure 2.5: Sphere-plate model representing the geometry on the left side and the trend of the potential energies on the right side. 15

Figure 2.6: Schematic structure of a triglyceride composed of glycerol and three different fatty acids. 17

Figure 2.7: Structure of the most common natural fatty acids. 18

Figure 2.8: Polymorphic structures of triglyceride subcells in the order of increasing melting temperature. 18

Figure 2.9: Double and triple chain length packing of triglycerides. 19

Figure 2.10: Schematic surfactant monomer molecule. 21

Figure 2.11: Schematic representation of the development of concentration dependent physical properties of an amphiphile dissolved in water. 22

Figure 2.12: Schematic illustration of (a) a lamellar liquid crystalline phase and (b) a normal hexagonal liquid crystalline phase. 24

Figure 2.13: Binary phase diagram of a surfactant solution in water in the region of the Krafft temperature. 25

Figure 2.14: Structures of different common hydrotropes. 27

Figure 2.15: Structure of microemulsions as a function of water to oil ratio with the highest fraction of water in L1 and the lowest one in L2. 30

Figure 2.16: Specific conductivity κ of microemulsion as a function of water fraction ϕ_w 31

Figure 2.17: Illustration of the Hansen solubility parameters in the three dimensional solubility parameter space giving a spherical solubility space [95]. 34

Figure 2.18: A typical Hofmeister series.	36
Figure 2.19: Collins concept of matching water affinities.....	37
Figure 2.20: Schematic phase diagram of a ternary system of oil, surfactant/cosurfactant and water at given temperature. The symbols 1ϕ , 2ϕ and 3ϕ indicate regions of one, two and three phases. In the region of one phase typically regions of micelles, various microemulsions and liquid crystals are distinguished.	38
Figure 2.21: Schematic illustration of a DSC device.	40
Figure 2.22: Schematic illustration of a typical endothermic melting peak yielding by DSC measurement.....	40
Figure 2.23: Representation of a spinning proton in a magnetic field of magnitude B_0	41
Figure 2.24: Energy profile of a nuclei with spin $I = \frac{1}{2}$ applied in a magnetic field of magnitude B_0	43
Figure 2.25: Schematic representation of a nuclear magnetic resonance spectrometer.	44
Figure 2.26: Schematic representation of the counter-ion binding at the lamellar surface. Three possible binding-sites are shown: (a) The counter-ion is moving freely in the water layers. (b) The counter-ion is located symmetrically with respect to the amphiphile polar end-group. (c) The counter-ion is located between amphiphile polar head groups.	47
Figure 2.27: Schematic illustration of a tristimulus colorimeter.....	48
Figure 2.28: Schematic illustration of the $L^*a^*b^*$ space.	49
 Chapter 3	
Figure 3.1: Molecular structure of sudan black B.	56
 Chapter 4	
Figure 4.1: Microscopy picture of 100 wt% technical grade TP at 25 °C (left) and 52 °C (right) under polarizing optical microscope.	65
Figure 4.2: (a) Second cycle of DSC measurement of 100 wt% technical grade TP. (b) First cycle of DSC measurement of 100 wt% technical grade TO. (c) Second cycle of DSC measurement of 100 wt% highly pure TO.	66
Figure 4.3: Structure of Lutensit ALB-N. n varies from 9-11.....	68
Figure 4.4: Structure of choline hexadecyl sulphate.	68
Figure 4.5: Structure of Lutensol GD70. n varies from 11-15 and m varies from 1-5.	69

- Figure 4.6:** The influence of the degree of ethoxylation of Lutensol AOx on the melting point of TP. ■: AO0; ●: AO3; ▲: AO7; ▼: AO20. The x-axis shows an increasing surfactant molar fraction..... 70
- Figure 4.7:** DSC curves of 60 wt% TP/40 wt% AO7 (left) and 60 wt% TP/40 wt% AO3 (right). 71
- Figure 4.8:** COSMO $_{therm}$ calculation of the theoretical melting point of TP after the addition of different surfactants. ■: C₁₃-OH; ●: C₁₅-OH; ▲: AO7; ▼: AO20. The x-axis shows an increasing molar fraction of surfactant. 71
- Figure 4.9:** Experimental powder diffractogram of pure TP at 298.15 K (red) and from single crystal data calculated diffractogram (black). 72
- Figure 4.10:** Experimental powder diffractogram of 40 wt% TP/60 wt%AO7 (left) and 40 wt% TP/60wt% AO3 (right) at 298.15 K (red) and from single crystal data calculated diffractogram of pure TP (black). 72
- Figure 4.11:** Ternary phase diagram with water/TO/AO7 at 298.15 K. The area of 1 ϕ gives the region of microemulsion and the area of 2 ϕ represents the region of emulsion. 87
- Figure 4.12:** Ternary phase diagram with water/TO/AO7/AO3/benzyl alcohol at 298.15 K and varying ratio AO7/cosurfactant and AO3/benzyl alcohol. A) AO7/cosurfactant = 1:1 and AO3/benzyl alcohol = 1:2; B) AO7/cosurfactant = 1:2 and AO3/benzyl alcohol = 1:2; C) AO7/cosurfactant = 1:1 and AO3/benzyl alcohol = 1:1. 88
- Figure 4.13:** Ternary phase diagram with water/TO/AO7 at 298.15 K. Ratio AO7/citronellol = 1:2. 88
- Figure 4.12: Ternary phase diagram with water/TO/AO7/AO3/benzyl alcohol at 298.15 K and varying ratio AO7/cosurfactant and AO3/benzyl alcohol. A) AO7/cosurfactant = 1:1 and AO3/benzyl alcohol = 1:2; B) AO7/cosurfactant = 1:2 and AO3/benzyl alcohol = 1:2; C) AO7/cosurfactant = 1:1 and AO3/benzyl alcohol = 1:1..... 88
- Figure 4.14:** At the colorimeter determined $\Delta\Delta E_{ab}$ values for washing tests with washing liquor Lutensol AO7 with varying surfactant concentration and soil composition. ■: 0.5 wt% AO7; ●: 1 wt% AO7; ▲: 5 wt% AO7; ▼: 10 wt% AO7 90
- Figure 4.15:** At the colorimeter determined $\Delta\Delta E_{ab}$ values for washing tests with mixtures AO7/AO3/benzyl alcohol with varying surfactant concentration and soil composition. AO7/cosurfactant = 1:1, AO3/benzyl alcohol = 1:1; ■: 0.5 wt% AO7; ●: 1 wt% AO7; ▲: 5 wt% AO7; ▼: 10 wt% AO7 92

Figure 4.16: At the colorimeter determined $\Delta\Delta E_{ab}$ values for washing tests with mixture AO7/AO3/benzyl alcohol/lecithin with varying soil composition. AO7/cosurfactant = 1:1, AO3/benzyl alcohol = 1:1; 0.1 wt% lecithin.....	93
Figure 4.17: At the colorimeter determined $\Delta\Delta E_{ab}$ values for washing tests with the mixture AO7/ChS = 1/1 with varying soil composition. 0.5 wt% AO7; 0.5 wt% ChS.	95
Figure 4.18: Ternary phase diagram of mixture 2-MTHF/Lutensol AO7/water at 298.15 K. ●: bicontinuous ME with 14.4wt% AO7 and 17.6 wt% 2-MTHF; ■: continuous ME with 14.4 wt% AO7 and 0.6 wt% 2-MTHF; ▲: continuous ME with 5 wt% AO7 and 6.11 wt% 2-MTHF; ◆: continuous ME with 1 wt% AO7 and 10.11 wt% 2-MTHF.....	96
Figure 4.19: At the colorimeter determined $\Delta\Delta E_{ab}$ values for washing tests with mixture AO7/2-MTHF with varying soil composition. 1 wt% AO7; 10.11 wt% 2-MTHF.	97
Figure 4.20: At the colorimeter determined $\Delta\Delta E_{ab}$ values for washing tests with mixture AO7/2-MTHF with varying soil composition. 5 wt% AO7; 6.11 wt% 2-MTHF.	98
Figure 4.21: At the colorimeter determined $\Delta\Delta E_{ab}$ values for washing tests with mixture AO7/2-MTHF with varying soil composition. 14.40 wt% AO7; 17.6 wt% 2-MTHF.	99
Figure 4.22: At the colorimeter determined $\Delta\Delta E_{ab}$ values for washing tests with mixture AO7/2-MTHF with varying soil composition. 14.40 wt% AO7; 0.06 wt% 2-MTHF.	100
Figure 4.23: At the colorimeter determined $\Delta\Delta E_{ab}$ values for washing tests with varying dilutions of Spee and soil composition. ■: undiluted Spee; ●: dilution with 1-5 wt% overall surfactant concentration; ▲: hand washing dilution.....	102
Figure 4.24: At the colorimeter determined $\Delta\Delta E_{ab}$ values for washing tests with water at varying temperatures and soil composition. ■: washing at 40 C; ●: washing at 25 °C.	103
Figure 4.25: At the colorimeter determined $\Delta\Delta E_{ab}$ values for washing tests with water at varying temperatures and soil composition. ■: washing at 40 C; ●: washing at 25 °C.....	104
Figure 4.26: At the colorimeter determined $\Delta\Delta E_{ab}$ values for washing tests with water at varying temperatures and soil composition. ■: washing at 10 C; ●: washing at 25 °C.	105

- Figure 4.27:** At the colorimeter determined $\Delta\Delta E_{ab}$ values for washing tests with water at varying temperatures and soil composition. ■: washing at 10 C; ●: washing at 25 °C. 106
- Figure 4.28:** At the colorimeter determined $\Delta\Delta E_{ab}$ values for washing tests with water at varying temperatures and soil composition. ■: washing at 10 C; ●: washing at 25 °C. 107
- Figure 4.29:** Biosynthetic pathway of the compatible solute ectoine (framed compounds). 1: L-Aspartate-kinase; 2: L-Aspartate- β -semialdehyde dehydrogenase; 3: L-2,4-diaminobutyric acid transaminase (*ectB*), 4: L-2,4-Diaminobutyric acid N- γ -acetyltransferase (*ectA*); 5: L-ectoine synthase (*ectC*); 6: L-Aspartate acetyl transferase; 7: N-Acetyl aspartokinase; 8: N-Acetyl-aspartate- β -semialdehyde dehydrogenase; 9: N-Acetyl-aspartate- β -semialdehyde transaminase. 113
- Figure 4.30:** Schematic biosynthesis of L-carnitine. 115
- Figure 4.31:** Influence of osmoprotectant concentration of trehalose (■), lysine (●), proline (▲), TMAO (▼), betaine (◆), carnitine (□) and ectoine (○) on the solubility temperature of a 1 wt% solution of SDC (left diagram) and of a 1 wt% solution of SDS (right diagram), respectively. 116
- Figure 4.32:** Influence of trehalose concentration on the solubility temperature of a 1 wt% solution of SDC (left diagram) and of a 1 wt% solution of SDS (right diagram), respectively. 116
- Figure 4.33:** Influence of the amino acid concentration of lysine (●) and proline (■) on the solubility temperature of a 1 wt% solution of SDC (left diagram) and of a 1 wt% solution of SDS (right diagram), respectively. 117
- Figure 4.34:** Influence of the ectoine concentration on the solubility temperature of a 1 wt% solution of SDC (left diagram) and of a 1 wt% solution of SDS (right diagram), respectively. 118
- Figure 4.35:** Influence of the methyl amine concentration of TMAO (■), betaine (●) and L-carnitine (▲) on the solubility temperature of a 1 wt% solution of SDC (left diagram) and of a 1 wt% solution of SDS (right diagram), respectively. 118
- Figure 4.36:** A schematic picture of a lamellar phase. 126
- Figure 4.37:** (a) ^{23}Na -NMR spectrum of a 35 wt% sample with a composition of SDC/LiDC = 2/3 at 300 K. The relative intensity of the signals is plotted against the frequency in [Hz]. (b) ^7Li -NMR spectrum of a 35 wt% sample with a composition of SDC/LiDC = 2/3 at 300 K. The relative intensity of the signals is plotted against the frequency [Hz]. 130
- Figure 4.38:** (a) ^{23}Na -NMR spectrum of a 65 wt% sample with a composition of SDS/LiDS = 2/3 at 300 K. The relative intensity of the signals is plotted against the

frequency in [Hz]. (b) ${}^7\text{Li}$ -NMR spectrum of a 35 wt% sample with a composition of SDS/LiDS = 2/3 at 300 K. The relative intensity of the signals is plotted against the frequency [Hz].	130
Figure 4.39: Sodium splitting with increasing concentration of surfactant and octanol (left) and lithium splitting with increasing concentration of surfactant and octanol (right). ● pure SDC at 300 K, ■ pure SDC at 310 K, ▲ pure SDS at 300 K, ○ pure LiDC at 300 K, □ pure LiDC at 310 K, △ pure LiDS at 300 K.	131
Figure 4.40: Sodium splitting with increasing amount of sodium (left) and lithium splitting with increasing amount of lithium (right) at 300 K and 310 K for 25 wt% SDC/LiDC/octanol in D_2O . ◆ 300 K, ■ 310 K.	132
Figure 4.41: Sodium splitting with increasing amount of sodium (left) and lithium splitting with increasing amount of lithium (right) at 300 K and 310 K for 35 wt% SDC/LiDC/octanol in D_2O . ◆ 300 K, ■ 310 K.	132
Figure 4.42: Sodium splitting with increasing amount of sodium (left) and lithium splitting with increasing amount of lithium (right) at 300 K and 310 K for 45 wt% SDC/LiDC/octanol in D_2O . ◆ 300 K, ■ 310 K.	133
Figure 4.43: Sodium splitting with increasing amount of sodium (left) and lithium splitting with increasing amount of lithium (right) at 300 K and 310 K for 55 wt% SDC/LiDC/octanol in D_2O . ◆ 300 K, ■ 310 K.	133
Figure 4.44: Sodium splitting with increasing amount of sodium (left) and lithium splitting with increasing amount of lithium (right) at 300 K for 35 wt% samples.	134
Figure 4.45: Sodium splitting with increasing amount of sodium (left) and lithium splitting with increasing amount of lithium (right) at 300 K for 45 wt% samples.	135
Figure 4.46: Sodium splitting with increasing amount of sodium (left) and lithium splitting with increasing amount of lithium (right) at 300 K for 55 wt% samples.	135
Figure 4.47: Sodium splitting with increasing amount of sodium (left) and lithium splitting with increasing amount of lithium (right) at 300 K for 65 wt% samples.	135
Figure 4.48: Sodium splitting with increasing amount of sodium (left) and lithium splitting with increasing amount of lithium (right) at 300 K for 75 wt% samples.	136
Figure 4.49: (a) ${}^{137}\text{Cs}$ -NMR spectrum of a 85 wt% sample with a composition of CsDC/RbDC = 1/0 at 300 K. The relative intensity of the signals is plotted against the frequency in [Hz]. (b) ${}^{87}\text{Rb}$ -NMR spectrum of a 85 wt% sample with a composition of CsDC/RbDC = 0/1 at 300 K. The relative intensity of the signals is plotted against the frequency [Hz].	139

Figure 4.50: Caesium splitting with increasing concentration of surfactant and octanol at 300 K (left) and rubidium splitting with increasing concentration of surfactant and octanol at 300 K (right). 140

Figure 4.51: Caesium splitting with increasing amount of caesium (left) and rubidium splitting (right) with increasing amount of rubidium for 45 wt% CsDC/RbDC/octanol in D2O at 300 K..... 141

Figure 4.52: Caesium splitting with increasing amount of caesium (left) and rubidium splitting (right) with increasing amount of rubidium for 55 wt% CsDC/RbDC/octanol in D2O at 300 K..... 141

Figure 4.53: Caesium splitting with increasing amount of caesium (left) and rubidium splitting (right) with increasing amount of rubidium for 65 wt% CsDC/RbDC/octanol in D2O at 300 K..... 141

Figure 4.54: Caesium splitting with increasing amount of caesium (left) and rubidium splitting (right) with increasing amount of rubidium for 75 wt% CsDC/RbDC/octanol in D2O at 300 K..... 141

Figure 4.55: Caesium splitting with increasing amount of caesium (left) and rubidium splitting (right) with increasing amount of rubidium for 85 wt% CsDC/RbDC/octanol in D2O at 300 K..... 142

List of tables

Chapter 1

Table 1.1: Average composition of a sud produced by suspending 1 kg wood ash in 10 l water.....	3
--	---

Chapter 2

Table 2.1: Composition of fatty soil secreted from the human body.....	8
Table 2.2: Average composition of soil originated from the environment.....	8
Table 2.3: Classification of surfactants.....	21
Table 2.4: Correlation between packing parameter P and the shape of the formed micelle.....	23
Table 2.5: Correlation of micellar shape and type of formed liquid crystal by increasing the surfactant concentration.....	24
Table 2.6: Nuclear spin quantum number of some nuclei.....	42

Chapter 3

Table 3.1: Operating parameter for measuring the quadrupole nuclei.....	60
--	----

Chapter 4

Table 4.1: Influence of impurities in technical grade TP on the melting/crystallization points and on the melting and crystallization enthalpies... 67	67
Table 4.2: Influence of the impurities in technical grade TO on the melting/crystallization points and on the melting and crystallization enthalpies... 67	67
Table 4.3: Hansen solubility parameters and R_a value for tripalmitin and chloroform calculated from increments.....	75
Table 4.4: Calculated R_a values for mixtures of tripalmitin and classical alcohols and examined solubility limits at room temperature.....	75
Table 4.5: Calculated R_a values for mixtures of tripalmitin and alkanes and examined solubility limits at room temperature.....	76
Table 4.6: Calculated R_a values for mixtures of tripalmitin and dowanols and examined solubility limits at room temperature. The Hansen solubility parameters of the dowanols are taken from the technical data sheet of Dow Chemicals [238]..	77
Table 4.7: Calculated R_a value and molecular weight of various terpene and natural oils, sorted for decreasing R_a value.....	78

Table 4.8: Experimentally determined solubility of tripalmitin in various classical solvents at room temperature, sorted by decreasing R_a value.....	79
Table 4.9: Experimentally determined solubility of triolein in various solvents at room temperature, sorted for decreasing R_a value.....	80
Table 4.10: Results of COSMO $_{therm}$ calculation and experimental determined solubility limit at 298.15 K with decreasing maximum fusion energy ΔG	81
Table 4.11: Determination of the region of one phase for the addition of water to various mixtures TO/surfactant/cosurfactant at 298.15 K.....	86
Table 4.12: Composition of investigated samples containing AO7, AO3 and benzylic alcohol.....	87
Table 4.13: At the colorimeter determined $\Delta\Delta E_{ab}$ values for washing tests with washing liquor water with varying soil composition.....	89
Table 4.14: Concentration and corresponding viscosity of Lutensol AO7 detergents.....	90
Table 4.15: At the colorimeter determined $\Delta\Delta E_{ab}$ values for washing tests with washing liquor Lutensol AO7 with varying surfactant concentration and soil composition.....	90
Table 4.16: Concentration of AO7/AO3/benzyl alcohol mixture and corresponding Lutensol AO7 concentration and viscosity.....	91
Table 4.17: At the colorimeter determined $\Delta\Delta E_{ab}$ values for washing tests with mixtures AO7/AO3/benzyl alcohol with varying surfactant concentration and soil composition. AO7/cosurfactant = 1:1, AO3/benzyl alcohol = 1:1.....	91
Table 4.18: At the colorimeter determined $\Delta\Delta E_{ab}$ values for washing tests with mixtures AO7/AO3/benzyl alcohol/lecithin with varying soil composition. AO7/cosurfactant = 1:1, AO3/benzyl alcohol = 1:1; 0.1 wt% lecithin.....	93
Table 4.19: At the colorimeter determined $\Delta\Delta E_{ab}$ values for washing tests with mixtures AO7/ChS with varying soil composition. 0.5 wt% AO7; 0.5 wt% ChS.....	94
Table 4.20: Composition of mixtures Lutensol AO7/2-MTHF/water and corresponding viscosity.....	96
Table 4.21: At the colorimeter determined $\Delta\Delta E_{ab}$ values for washing tests with mixtures AO7/2-MTHF with varying soil composition. 1 wt% AO7; 10.11 wt% 2-MTHF.....	97
Table 4.22: At the colorimeter determined $\Delta\Delta E_{ab}$ values for washing tests with mixtures AO7/2-MTHF with varying soil composition. 5 wt% AO7; 6.11 wt% 2-MTHF.....	98

Table 4.23: At the colorimeter determined $\Delta\Delta E_{ab}$ values for washing tests with mixtures AO7/2-MTHF with varying soil composition. 14.40 wt% AO7; 17.6 wt% 2-MTHF.	99
Table 4.24: At the colorimeter determined $\Delta\Delta E_{ab}$ values for washing tests with mixtures AO7/2-MTHF with varying soil composition. 14.40 wt% AO7; 0.06 wt% 2-MTHF.	100
Table 4.25: At the colorimeter determined $\Delta\Delta E_{ab}$ values for washing tests with varying dilutions of Spee with cotton fibers soiled with varying TO/TP compositions.	101
Table 4.26: At the colorimeter determined $\Delta\Delta E_{ab}$ values for washing tests with water at varying temperatures with cotton fibers soiled with varying TO/TP compositions.	103
Table 4.27: At the colorimeter determined $\Delta\Delta E_{ab}$ values for washing tests with water at varying temperatures with cotton fibers soiled with varying TO/TP compositions.	104
Table 4.28: At the colorimeter determined $\Delta\Delta E_{ab}$ values for washing tests with water at varying temperatures with cotton fibers soiled with varying TO/TP compositions.	105
Table 4.29: At the colorimeter determined $\Delta\Delta E_{ab}$ values for washing tests with water at varying temperatures with cotton fibers soiled with varying TO/TP compositions.	106
Table 4.30: At the colorimeter determined $\Delta\Delta E_{ab}$ values for washing tests with 1 wt% solution of Lutensol AO7 with and without thickener culminal and not at room temperature with cotton fibers soiled with varying TO/TP compositions.	107
Table 4.31: Ionic strength of the sodium and lithium carboxylate samples for all compositions and all concentrations.	128
Table 4.32: Ionic strength of the caesium and rubidium carboxylate samples for all compositions and all concentrations.	128
Table 4.33: Jones-Doyle viscosity B coefficients.	138

Supplementary

A: Chapter 4

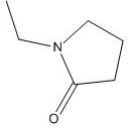
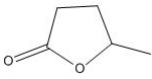
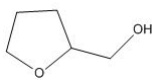
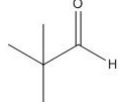
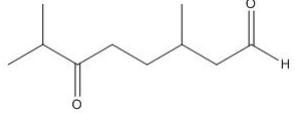
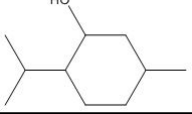
Dowanole

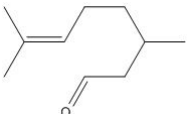
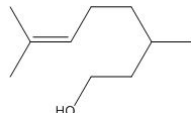
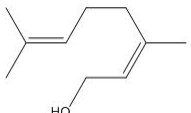
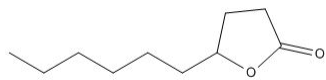
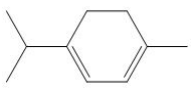
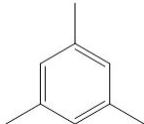
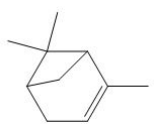
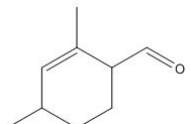
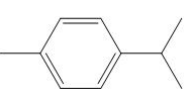
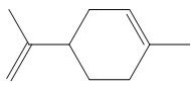
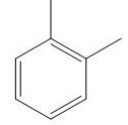
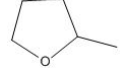
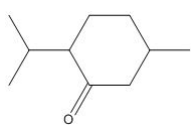
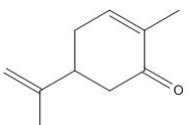
Table A 1: Chemical Structure of Dowanole.

<i>Solvent</i>	<i>Chemical Structure</i>
Dowanol PM (Monopropylenglykolmonomethylether)	$\text{CH}_3\text{-O-CH}_2\text{-CHOH-CH}_3$
Dowanol DPM (Dipropylenglykolmonomethylether)	$\text{CH}_3\text{-O-C}_3\text{H}_6\text{-O-CH}_2\text{-CHOH-CH}_3$
Dowanol TPM (Tripropylenglykolmonomethylether)	$\text{CH}_3\text{-O-C}_3\text{H}_6\text{-O-C}_3\text{H}_6\text{-O-CH}_2\text{-CHOH-CH}_3$
Dowanol DPnP (Dipropylene Glycol n-Propyl Ether)	$\text{C}_3\text{H}_7\text{-O-[CH}_2\text{-CH(CH}_3\text{)-O]}_2\text{-H}$
Dowanol PMA (Propyleneglykolmethylether acetate)	$\text{CH}_3\text{-O-CH}_2\text{-CH(CH}_3\text{)-O-C(O)-CH}_3$

Terpene and natural oils

Table A 2: Chemical Structure of terpene and oils.

<i>Solvent</i>	<i>Chemical Structure</i>
1-Ethyl-2-pyrrolidinone	
γ -Valerolactone	
Tetrahydrofurfuryl alcohol	
Pivaldehyde	
3,7-Dimethyl-6-oxooctanal	
Menthol	

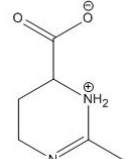
Citronellal	
Citronellol	
Geraniol	
γ -Decanolactone	
α -Pinene	
Mesitylen	
α -Terpinene	
Vertocitral	
p-Cymene	
Limonene	
o-Xylol	
2-Methyl THF	
Menthon	
Carvone	

D-Dihydrocarvone	
Citral	
Ethylpentanoate	
1,8-Cineol	
Ethyl octanoate	
Anethol	
Ethyldecanoate	
Ethyllaurate	

Osmoprotectants

Table A 3: Structure of investigated osmoprotectants.

Osmoprotectant	Structure
Trehalose	
L-Proline	
L-Lysine	
Betaine	
Carnitine	

TMAO	
Ectoine	

List of publications

(1) W. Kunz, E. Maurer, R. Klein, D. Touraud, D. Rengstl, A. Harrar, S. Dengler and O. Zech, Low Toxic Ionic Liquids, Liquid Catanionics, and Ionic Liquid Microemulsions. *Journal of Dispersion Science and Technology*, 2011, **32**, 1694-1699.

(2) S. Dengler, A. Klaus, G. J. Tiddy and W. Kunz, How specific are ion specificities? A pilot NMR study. *Faraday Discussion*, 2013, **160**, 121-133.

(3) S. Dengler, L. Zahnweh, G. J. Tiddy and W. Kunz, Specific Ion Adsorption on Alkyl Carboxylate Surfactant Layers, will be submitted

(4) S. Dengler, V. Fischer, B. von Vacano, R. Klein, and W. Kunz, Can crystalline triglycerides be liquefied by the addition of surfactants or solvents?, submitted to *Journal of Surfactants and Detergents*

(5) S. Dengler and W. Kunz, Influence of additives on the Krafft temperature of sodium dodecyl carboxylate and sodium dodecyl sulphate, will be submitted

(6) S. Dengler, B. von Vacano, R. Klein and W. Kunz, Solubilisation of triglycerides, will be submitted

Eidesstattliche Erklärung

Ich erkläre hiermit an Eides statt, dass ich die vorliegende Arbeit ohne unzulässige Hilfe Dritter und ohne Benutzung anderer als der angegebenen Hilfsmittel angefertigt habe; die aus anderen Quellen direkt übernommenen Daten und Konzepte sind unter Angabe des Literaturzitats gekennzeichnet.

Weitere Personen waren an der inhaltlich-materiellen Herstellung der vorliegenden Arbeit nicht beteiligt. Insbesondere habe ich hierfür nicht die entgeltliche Hilfe eines Promotionsberaters oder anderer Personen in Anspruch genommen. Niemand hat von mir, weder unmittelbar noch mittelbar, geldwerte Leistungen für Arbeiten erhalten, die im Zusammenhang mit dem Inhalt der vorgelegten Dissertation stehen.

Die Arbeit wurde bisher weder im In- noch im Ausland in gleicher oder ähnlicher Form einer anderen Prüfungsbehörde vorgelegt.

Regensburg, _____

Susanne Dengler

Declaration

Herewith I declare that I made this existing work singel handedly. I have used nothing but the stated utilities.

Regensburg, _____

Susanne Dengler